

**MOLECULAR STUDIES OF THE STRUCTURE AND FUNCTION OF
Pseudomonas aeruginosa OprD: AN IMIPENEM SPECIFIC PORIN**

by

HONGJIN HUANG

B.Sc., Sichuan University, Sichuan, China, 1986

M.Sc., Academy of Military Medical Sciences, Beijing, China, 1989

A THESIS SUBMITTED IN PARTIAL FULFILLMENT OF

THE REQUIREMENTS FOR THE DEGREE OF

DOCTOR OF PHILOSOPHY

in

THE FACULTY OF GRADUATE STUDIES

(Department of Microbiology and Immunology)

We accept this thesis as conforming
to the required standard

.....
THE UNIVERSITY OF BRITISH COLUMBIA

May, 1995

© Hongjin Huang, 1995

In presenting this thesis in partial fulfilment of the requirements for an advanced degree at the University of British Columbia, I agree that the Library shall make it freely available for reference and study. I further agree that permission for extensive copying of this thesis for scholarly purposes may be granted by the head of my department or by his or her representatives. It is understood that copying or publication of this thesis for financial gain shall not be allowed without my written permission.

(Signature) _____

Department of MICROBIOLOGY

The University of British Columbia
Vancouver, Canada

Date Sep. 12/85

ABSTRACT

Pseudomonas aeruginosa OprD is a specific porin which facilitates the uptake of basic amino acids and imipenem, a carbapenem antibiotic with high potency against *P. aeruginosa*. To permit further studies of OprD, the *oprD* structural gene was cloned and expressed in *Escherichia coli* on a 2.1-kb *Bam*HI/*Kpn*I fragment. DNA sequencing predicted a 420 amino acid mature OprD protein with a 23 amino acid signal peptide. In addition, a putative *oprD* regulatory gene *opdE* was sequenced, which predicted a hydrophobic protein of 402 amino acids.

A set of *P. aeruginosa* isogenic strains with genetically defined levels of OprD were constructed and utilized to characterize the *in vivo* function of OprD. The results clearly demonstrated that OprD could be utilized by imipenem and meropenem but, even when substantially overexpressed, could not be significantly utilized by other β -lactams, quinolones or aminoglycosides. Regarding its function in uptake of nutrients, OprD selectively facilitated the diffusion of basic amino acids and gluconate under growth-rate limiting conditions. Competition experiments confirmed that imipenem shared common binding sites with basic amino acids in the OprD channel, but not with gluconate or glucose. *In vitro* functional studies using purified OprD provided direct evidence for the presence of a specific binding site(s) for imipenem in the OprD channel, with an I_{50} value of 1.4 μ M.

An OprD topology model was proposed based on sequence alignment with *E.*

coli porin OmpF and structure predictions. Sixteen β -strands were predicted, connected by short turns at the periplasmic side, whereas the eight external loops were of variable length but tended to be much longer. In addition, multiple sequence alignments between OprD and seven representatives from the porin superfamily indicated that OprD was the first specific porin that could be aligned with members of the so-called porin superfamily. PCR-based site directed mutagenesis was performed to separately delete short stretches (4-8) of amino acid residues from each of the predicted external loops. Six out of eight mutants expressed in both *E. coli* and *P. aeruginosa*, maintained substantial resistance to trypsin treatment in the context of outer membranes, and formed functional channels, which supported the general accuracy of the model. The loop 2 deletion mutant only partially reconstituted supersusceptibility to imipenem in an OprD-defective background, and showed much lower affinity to imipenem in the macroscopic conductance inhibition experiment, indicating its involvement in imipenem binding. Deletions in loops 5, 7 or 8 resulted in a channel with enhanced permeability to antibiotics, but which retained the imipenem binding site(s).

A model of the channel architecture of OprD was constructed based on these data, and the mechanism by which imipenem and basic amino acids pass through the OprD channel was discussed.

TABLE OF CONTENTS

ABSTRACT	ii
TABLE OF CONTENTS	iv
LIST OF FIGURES	viii
LIST OF TABLES	x
LIST OF ABBREVIATIONS	xi
ACKNOWLEDGMENTS	xiii
DEDICATION	xiv
INTRODUCTION	1
A. <i>Pseudomonas aeruginosa</i>	1
B. <i>Pseudomonas aeruginosa</i> Outer Membrane	2
1. Outer Membrane Structure.	2
2. Porins: General Porins and Specific Porins	6
3. Antibiotic Uptake Across the Outer Membrane	8
4. Imipenem	10
5. OprD: A Specific Porin for Basic Amino Acids and Imipenem	15
C. Structure Analysis of Porin Proteins	19
1. X-ray Crystallography and Others	19
2. Crystal Structure of General Porin Channels	20
3. Crystal Structure of Specific Porin Channels	23
4. Prediction of Porin Structures: Porin Superfamily	25
D. Model Membrane Studies of Porins	26
E. Aims of This Study	28
MATERIALS AND METHODS	30
A. Strains, Plasmids and Growth Conditions	30
B. Genetic Manipulations	30
1. General DNA Techniques.	30
2. DNA Fragment Isolation	35

3.	DNA Sequencing	35
4.	Transfer of DNA into <i>P. aeruginosa</i>	36
5.	Oligonucleotide Synthesis and Purification	37
C.	Cloning Strategy for the <i>oprD</i> Gene	38
D.	Allele Replacement Mutagenesis	39
1.	Construction of pXH1	39
2.	Selection of the <i>oprD</i> ::Km ^R Ω Mutant	39
E.	Overexpression of the <i>oprD</i> Gene in <i>P. aeruginosa</i>	41
F.	Electrophoresis	41
G.	Growth Experiments	41
H.	Purification of OprD.	43
I.	Immunological Techniques	45
1.	Production and Purification of OprD Antibodies	45
2.	Western-Immunoblotting.	46
J.	Prediction of the Topology Model of OprD	46
1.	Sequence Alignment	46
2.	Structural Characteristics	47
K.	PCR-Based Site Directed Deletion Mutagenesis.	48
1.	Two PCR Strategies.	48
2.	Construction of pMBK19R and pMBE19R.	50
3.	Polymerase Chain Reaction	52
L.	Whole Cell Lysate	52
M.	Trypsinization Studies	56
N.	Black Lipid Bilayer Analysis	56
1.	Single Channel Conductance.	56
2.	Macroscopic Conductance Experiment.	57
3.	Zero Current Membrane Potential	58
O.	Assays	58
1.	Protein Assay	58
2.	Nitrocefin Assay.	59

3. Minimum Inhibitory Concentration (MIC) Determination . . .	59
RESULTS	61
CHAPTER ONE Analysis of Two Gene Regions Involved in the Expression of OprD	61
A. Molecular Cloning of the <i>oprD</i> Gene	61
B. Overexpression of the <i>oprD</i> Gene in <i>E. coli</i> CE1248.	61
C. Nucleotide Sequencing of the <i>oprD</i> Gene.	64
D. Nucleotide Sequencing of the <i>opdE</i> Gene	68
E. Summary	71
CHAPTER TWO Functional Characterization of OprD: <i>In vivo</i> and <i>In vitro</i>	73
A. Introduction	73
B. Construction of a Defined OprD-Defective Mutant H729	74
C. Overexpression of the <i>oprD</i> Gene in <i>P. aeruginosa</i>	75
D. Function of OprD in Antibiotic Uptake.	78
E. Function of OprD in Sugar Transport	80
F. Competition Experiments.	84
G. Purification of OprD.	88
H. Black Lipid Bilayer Analysis	91
I. Summary	94
CHAPTER THREE Structural Characterization of OprD: Membrane Topology Model.	96
A. Introduction	96
B. Prediction of an OprD Topology Model	96
C. PCR-Based Site Directed Deletion Mutagenesis	101
D. Characterization of the Deletion Mutants	104

E. Trypsin Susceptibility of the Deletion Variants	109
F. Revised OprD Model	112
G. Summary	113
CHAPTER FOUR Structure/Function Relationships: Functional	
Alterations of Deletion Mutants	115
A. Introduction	115
B. Effects of Deletion on Imipenem/Meropenem Susceptibilities.	115
C. Effects of Deletion on Other Antibiotic Susceptibilities	118
D. Effects of Deletion on Sugar Transport.	121
E. Purification of the Mutant OprDs	121
F. Effects of Deletion on the Physical Properties of the Channel	124
G. Summary	130
DISCUSSION	131
A. Function of OprD in Antibiotic Uptake.	131
B. Function of OprD in Nutrient Uptake: Is Lysine the Best Substrate?	134
C. Prediction of an OprD Membrane Topology Model	137
D. Molecular Architecture of the OprD Channel	141
E. The Journey of Imipenem Through the OprD Channel	146
F. General Porins and Specific Porins.	148
REFERENCES	151
APPENDIX.	165
A. Revised OprD Model by Multiple Alignments and Amphipathicity Calculations	165

LIST OF FIGURES

Figure 1.	Schematic representation of the outer membrane and peptidoglycan of <i>P. aeruginosa</i>	3
Figure 2.	Structures of thienamycin and imipenem	11
Figure 3.	Structures of some antibiotics and amino acids that penetrate through the OprD channel	18
Figure 4.	Diagram of plasmid pXH1 utilized for allele replacement mutagenesis	40
Figure 5.	Diagram of plasmid pXH2 utilized for the overexpression of the <i>oprD</i> gene	42
Figure 6.	Schematic diagram showing two PCR strategies	49
Figure 7.	Diagram of plasmid pMBK19R.	51
Figure 8.	Diagram of plasmid pMBE19R.	53
Figure 9.	Restriction endonuclease maps of <i>P. aeruginosa</i> PAO1 strain H103 chromosomal DNA derived by Southern hybridization . .	62
Figure 10.	Diagram of plasmid pBK19R.	63
Figure 11.	Overexpression of the <i>oprD</i> gene in <i>E. coli</i>	65
Figure 12.	Nucleotide and the deduced amino acid sequence of the <i>oprD</i> gene	66
Figure 13.	Nucleotide and the deduced amino acid sequence of the <i>opdE</i> gene	69
Figure 14.	Construction of an OprD defective mutant in <i>P. aeruginosa</i> . .	76
Figure 15.	SDS-PAGE demonstrating overexpression and mutagenesis of the <i>oprD</i> gene.	77
Figure 16.	Function of OprD in sugar transport.	83
Figure 17.	Competition between L-lysine and imipenem for the OprD channel	87
Figure 18.	SDS-PAGE of samples from solubilization stages	89
Figure 19.	Purification of OprD	90

Figure 20.	Chart recording of step wise increase of the membrane current formed by 1% oxidized cholesterol in n-decane in the presence of purified proteins	92
Figure 21.	Sequence alignment between OprD and OmpF	98
Figure 22.	Membrane topology model of OprD	99
Figure 23.	Expression of OprD derivatives in the outer membrane of <i>E. coli</i>	106
Figure 24.	Expression of OprD derivatives in the outer membrane of <i>P. aeruginosa</i> OprD-defective strain H729.	108
Figure 25.	Western-immunoblot demonstrating expression of OprD derivatives in <i>P. aeruginosa</i> whole cell lysates	110
Figure 26.	Trypsinization studies of OprD derivatives	111
Figure 27.	Competition between L-lysine and imipenem for OprD Δ L2	119
Figure 28.	Competition between L-lysine and imipenem for OprD Δ L5/7/8	122
Figure 29.	Comparison of heat-modifiabilities between the purified native OprD and mutant OprDs	123
Figure 30.	Comparison of single channel conductance between native and mutant OprDs	125
Figure 31.	Macroscopic conductance inhibition experiments	129
Figure 32.	Schematic representation of the predicted interior architecture of the OprD channel	142
Figure 33.	Multiple sequence alignments between OprD and representatives of porin superfamily.	168
Figure 34.	Revised membrane topology model of OprD	171

LIST OF TABLES

Table I.	Strains	31
Table II.	Plasmids	32
Table III.	PCR-based site specific deletion mutagenesis	54
Table IV.	Influence of OprD expression levels on antibiotic susceptibility of <i>P. aeruginosa</i> strains	79
Table V.	Influence of OprD expression levels on antibiotic susceptibility of <i>E. coli</i> strains	81
Table VI.	Effects of basic amino acids and gluconate on imipenem susceptibilities of <i>P. aeruginosa</i> strains expressing different levels of OprD	86
Table VII.	Deletion mutagenesis of the predicted loops	105
Table VIII.	Effects of deletions on imipenem/meropenem susceptibilities of <i>P. aeruginosa</i> strains	117
Table IX.	Effects of deletions on other antibiotic susceptibilities of <i>P. aeruginosa</i> strains	120
Table X.	Average single-channel conductance of the native and mutant OprD pores in different salt solutions	127
Table XI.	Zero-current membrane potentials	128
Table XII.	Homologies and identities among the porin superfamily	167

LIST OF ABBREVIATIONS

Ap	ampicillin
bp	base pair
Cb	carbenicillin
CFP	cefpirome
Ch	chloramphenicol
CIP	ciprofloxacin
CTX	cefotaxime
DEAE	diethylaminoethyl
EDTA	ethylenediamine tetraacetate
FLER	fleroxacin
FPLC	fast protein liquid chromatography
GM	gentamicin
IMIP	imipenem
IPTG	isopropylthiogalactoside
LBNS	Luria broth, normal salt
LDAO	N, N, dimethyldodecylamine-N-oxide
LPS	lipopolysaccharide
kb	kilobase pair
kD	kilodalton
KDO	2-keto-3-deoxyoctulosonic acid
Km	kanamycin

MERO	meropenem
MOPS	3-N-morpholino propane sulfonic acid
octyl-POE	octyl-polyoxyethylene
OD	optical density
PAGE	polyacrylamide gel electrophoresis
PBPs	penicillin binding proteins
PCR	polymerase chain reaction
PMSF	phenyl methyl sulfonyl fluoride
Pst	phosphate specific transport
rpm	revolutions per minute
SDS	sodium lauryl sulfate
Str	streptomycin
TPCK	N-tosyl-L-phenylalanine chloromethyl ketone

ACKNOWLEDGMENTS

I am most grateful to my supervisor, Bob Hancock, for his excellent supervising, constant support and kindness.

I would like to thank Richard Siehnel for his technical assistance and members of my supervisory committee for their guidance and helpful advices.

I am also deeply grateful to my friends, especially Kathy, Manhong and Hua for their encouragement, friendship and patience during the last several years.

The financial support of Canadian Cystic Fibrosis Foundation is gratefully acknowledged.

DEDICATION

To my beloved Mom and Dad.

INTRODUCTION

A. *Pseudomonas aeruginosa*.

Pseudomonas aeruginosa is an opportunistic human pathogen that causes a variety of infections, usually in immunocompromised hosts such as burn victims and cancer patients, or children with cystic fibrosis (Schimpff et al., 1970). *P. aeruginosa* causes 10-15% of all nosocomial infections, making it second only to *E. coli* as the most frequently hospital-acquired pathogen (Young, 1984). This Gram negative rod also makes several different toxins, some of which may cause shock, while others kill tissue cells or hydrolyse structural tissue proteins such as elastin (Liu, 1974). Given its multifactorial virulence, it is not surprising that *P. aeruginosa* is able to cause a wide variety of diseases such as bacteremia, urinary tract infections, endocarditis and gastrointestinal infections (Pollack, 1990). *P. aeruginosa* is becoming a major clinical problem since it has a high, natural resistance to many commonly used antibiotics, including first and second generation penicillins and cephalosporins, tetracycline, chloramphenicol and vancomycin (Bryan, 1979). It has been shown that the permeability of the *P. aeruginosa* outer membrane to β -lactam antibiotics and also some other simple organic compounds is from twelve (Nicas and Hancock, 1983a) to one hundred fold (Yoshimura and Nikaido, 1982) lower than that of the permeability of *E. coli* outer membrane to the same or similar compounds and clearly this lower permeability of the outer membrane layer plays a major role in the intrinsic antibiotic resistance

of this organism (Nikaido and Hancock, 1986).

B. *Pseudomonas aeruginosa* Outer Membrane

1. Outer Membrane Structure.

The cell envelope of *P. aeruginosa* consists of two membranes separated by a layer of peptidoglycan and a cellular compartment called the periplasm. The innermost, cytoplasmic (inner) membrane is a typical phospholipid bilayer membrane which is studded with a wide variety of polypeptides. The major functions of cytoplasmic membrane proteins are in cellular energization, transport of nutrients and export of toxic byproducts (Cronan et al., 1987). Peptidoglycan is located underneath the outer membrane and is the major determinant of cell shape and osmotic stability (Oliver, 1987). Thus, the periplasm is primarily located between the peptidoglycan and the cytoplasmic membrane. It functions in the processing and traffic of molecules entering or leaving the cell (Oliver, 1987).

The outer membrane is biologically unusual in that, unlike the cytoplasmic membrane, it is an asymmetric bilayer (Fig. 1), in which the inner monolayer is composed of phospholipid, whereas the outer monolayer contains the unique lipid species lipopolysaccharide (LPS) (Lugtenberg and van Alphen, 1983; Nikaido and Nakae, 1979). The basic LPS consists of three regions: (a) the hydrophobic, biologically-active endotoxin lipid A, (b) the rough core and (c) the O-antigen region, which is immunodominant (Rietschel et al., 1984). The lipid A region is typical in

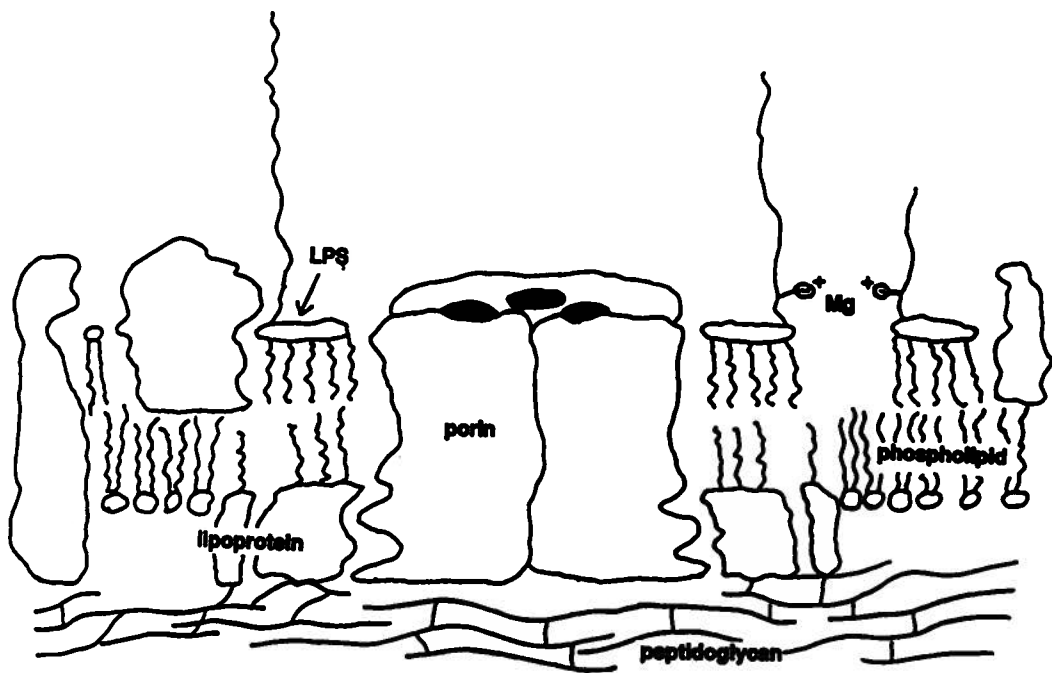


Figure 1: Schematic representation of the outer membrane and peptidoglycan of *P. aeruginosa*.

that a single backbone structure corresponding to glucosaminyl- β -(1-6) glucosamine is substituted with six or seven saturated or hydroxyl fatty acid residues (Karunaratne et al., 1992). This region is antigenically and chemically conserved. The rough core is covalently bound to lipid A. It contains 11 heterogeneous sugar residues, including an unique octose (2-keto-3-deoxyoctulosonic acid [KDO]) as well as glucose, rhamnose and galactosamine residues. In addition, this fraction contains phosphate and alanine. Analysis suggested that there are 11~16 phosphate residues per chain of *P. aeruginosa* LPS core oligosaccharide, which is much higher than that of *Enterobacteriaceae*, such as *Salmonella minnesota*, where only 1 or 2 phosphate residues were present per chain (Drewry et al., 1975; Kropinski et al., 1979). The rough core may be capped by repeating tri- to pentasaccharide units termed the O-antigen. It has been shown that the O-antigen portion of *P. aeruginosa* often contains such sugars as glucose, rhamnose, glucosamine, fucosamine and quinavosamine (Kropinski et al., 1985). This latter repeating saccharide portion is one of the most immunogenic antigens of smooth Gram-negative bacteria and determines the O-serotype of such bacteria (for reviews, see Nikaido and Hancock, 1986; Hancock et al., 1994).

The asymmetric distribution and chemical characteristics of LPS give the outer membrane many of its unique barrier properties. As mentioned above, the presence of a large amount of phosphate in the core region of *P. aeruginosa* LPS results in the strong surface negative charge (Sherbert and Lakshmi, 1973). LPS is anchored in the outer membrane in part, by the fatty acyl chains of its Lipid A

portion (Morrison, 1985). In addition, the non-covalent cross-bridging of adjacent LPS molecules with divalent cations (Mg^{2+} or Ca^{2+}) (Rottem and Leive, 1977), and the hydrophobic interactions between the outer membrane proteins and Lipid A (Nikaido and Vaara, 1985), also contribute to stabilize LPS in the outer membrane. The combination of surface negative charge and divalent cation cross-bridging of LPS makes *P. aeruginosa* and other Gram-negative bacteria resistant to hydrophobic antibiotics, bile salts, detergents, proteases, lipases and lysozyme (Nikaido and Vaara, 1985).

The *P. aeruginosa* outer membrane also contains a few species of "major" proteins. These include the murein lipoproteins, the multifunctional protein OprF and porins (Fig. 1). Two lipoproteins have been identified in *P. aeruginosa*, OprI and OprL, both of them are inserted in the inner phospholipid monolayer and are non-covalently associated with peptidoglycan (Mizuno, 1979; Hancock et al., 1981a). Therefore they are structural proteins that stabilize the architecture of the outer membrane-peptidoglycan complex by seating the outer membrane onto the surface of the peptidoglycan. Multifunctional protein OprF is also strongly but non-covalently associated with peptidoglycan and plays an important role in outer membrane stabilization and cell shape determination (Gotoh et al., 1989; Woodruff and Hancock, 1989). Porins are a group of proteins forming trans-outer-membrane, water-filled channels. In general, porins have monomer molecular weights in the range of 28 kD to 48 kD, are present in membrane as oligomers (usually trimers), are often strongly but non-covalently associated with the underlying peptidoglycan

and with LPS, and have a high content of β -sheet structure. In *P. aeruginosa*, OprB, OprC, OprD, OprE, OprF, OprP and OprO have been identified as porins (for review, see Hancock et al., 1990).

2. Porins: General Porins and Specific Porins.

Porins are generally divided into two classes: non-specific (general) porins and specific porins (Nikaido and Vaara, 1985). General porins form water-filled channels that permit the passive diffusion of hydrophilic molecules below a certain size, and thus are responsible for the non-specific exclusion limit of the outer membrane. Specific porins also produce water-filled channels, which contain stereospecific substrate-binding sites (Hancock, 1987). The diffusion of the specific substrate is accelerated when the solute concentration is low, but it is slowed down when the concentration is high, producing saturation-type kinetics.

General porins take up molecules based on size, electrical charge and hydrophilicity (Nikaido and Vaara, 1985). Though it used to be a controversial issue, OprF is a major non-specific porin in *P. aeruginosa*. Its pore-forming property was confirmed both in model membrane systems (Benz and Hancock, 1981) and in intact cells (Bellido et al., 1992). The channel diameter was estimated to be 20 Å, about twice the width of *E. coli* porin channels, and can allow the passage of saccharides with molecular weights of approximately 3,000 (Nikaido and Hancock, 1986). However, only 400 out of 200,000 OprF molecules per cell are proposed to

form such large channels; the rest appear to form small channels that are predicted to be antibiotic impermeable (Woodruff et al., 1986). Besides OprF, minor outer membrane proteins OprC and OprE are also general porins with small channel size (Yoshihara and Nakae, 1989). The above cited data explains the low outer membrane permeability of *P. aeruginosa* compared to *E. coli* (Angus et al., 1982; Yoshimura and Nikaido, 1982; Nicas and Hancock, 1983a). This, in turn, was proposed to be the major basis for the high intrinsic resistance of *P. aeruginosa* to hydrophilic antibiotics (Nikaido and Hancock, 1986).

To overcome the low permeability and to permit the effective uptake of essential nutrients available at low concentrations in the medium, several specific porins are present in the *P. aeruginosa* outer membrane. OprB, which is induced by growth in the presence of glucose (Hancock and Carey, 1980), forms a channel that prefers D-glucose and D-xylose (Trias et al., 1988). OprD was discovered due to its role in the facilitated uptake of imipenem (Trias and Nikaido, 1990a), a carbapenem which shows excellent activity against *P. aeruginosa*. However, the natural substrate for OprD is not imipenem, but its structural analogues, presumably basic amino acids and small peptides containing those amino acids (Trias and Nikaido, 1990b). OprP is induced by growth under phosphate starvation (0.15 mM or less) conditions (Hancock et al., 1982). Mutational studies demonstrated that OprP is an important component of the high-affinity, phosphate-starvation-inducible, phosphate specific transport (Pst) system of *P. aeruginosa* (Poole and Hancock, 1986). OprP shows 100-fold preference for phosphate over

other anions by virtue of a phosphate binding site with a K_d of 0.3 mM (Hancock and Benz, 1986). In addition, another porin OprO, which is highly homologous to OprP (Siehnel et al., 1992), forms pyrophosphate-specific channels (Hancock et al., 1992).

3. Antibiotic Uptake Across the Outer Membrane.

(a) THE HYDROPHILIC PATHWAY. Hydrophilic antibiotics, including a variety of β -lactam antibiotics, tetracycline and chloramphenicol (Foulds, 1976), can pass across the Gram-negative bacterial outer membrane through the water-filled channels formed by porins. The strongest supporting data has been obtained by comparing porin-deficient mutants with their isogenic wild-type strains. Such mutants have significant increases in MIC for some but not all β -lactams (Hancock and Bell, 1988), as well as 10- to 100-fold-lower rates of β -lactam permeation than their porin-sufficient parent strains (Hancock, 1987). *P. aeruginosa* wild-type cells have a 12-fold lowered permeability to β -lactam antibiotics compared to *E. coli* (Yoshimura and Nikaido, 1982; Nicas and Hancock, 1983a) and a consequent higher resistance to hydrophilic antibiotics (Brown, 1975). Therefore, wild-type *P. aeruginosa* cells behave like porin-deficient mutants despite the high copy number of their major porin OprF (Angus et al., 1982). This is primarily due to the low activity of this porin (only 0.4% of the OprF in the outer membrane forms large pores). Loss of OprF by mutation decreased the outer membrane permeability to the

β -lactam nitrocefin by a further six-fold (Nicas and Hancock, 1983a) but had only a small effect (up to three fold) on sensitivity to many antibiotics (Nicas, 1983; Woodruff and Hancock, 1988).

Certain antibiotics can utilize the channels of specific porins to enhance their uptake since they resemble the specific substrate of the given channel. Diffusion through such specific channels can make a major contribution in *P. aeruginosa*, which has very low outer membrane permeability. One excellent example is imipenem and the related zwitterionic carbapenems. It was shown that OprD produced a diffusion channel with a specific binding site for basic amino acids and their structural analogue imipenem (Trias and Nikaido, 1990). The diffusion of imipenem through this channel followed saturation kinetics (Trias et al., 1989).

(b) THE HYDROPHOBIC PATHWAY. Due to the unusual asymmetric structure and presence of LPS cross-bridged by divalent cations in the outer membrane (see above), most wild-type Gram-negative bacteria (including *P. aeruginosa*) exclude moderately hydrophobic antibiotics that are quite effective against Gram-positive bacteria (Nikaido and Vaara, 1985). These antibiotics include macrolides, novobiocin, the more hydrophobic β -lactams, rifamycin SV and actinomycin D (Nikaido et al., 1983). Permeabilization to hydrophobic antibiotics can be achieved when the structure of the outer membrane bilayer is modified by mutational alterations of LPS components (Nikaido and Vaara, 1985), or by addition of compounds, which remove (e.g. EDTA) or competitively displace (e.g. polycations) divalent cations from their LPS binding sites (Hancock, 1984; Nikaido

and Hancock, 1986).

(c) THE SELF-PROMOTED PATHWAY. The self-promoted pathway has been postulated for the uptake of polycationic antibiotics, like polymyxin and aminoglycosides, across the outer membrane of *P. aeruginosa* (Hancock, 1981; Hancock et al., 1981b; Nicas and Hancock, 1983b). It involves the displacement of divalent cations from LPS by these polycations, thus destroying the LPS cross-bridging and destabilizing the outer membrane (Hancock et al., 1981b; Nicas and Hancock, 1983b). Because this can result in enhancement of uptake of lysozyme, β -lactams and hydrophobic fluorescent dyes across the outer membrane, it was proposed that such interactions promote the uptake of the interacting polycationic antibiotics itself. As further evidence in favour of self-promoted uptake, EDTA, a divalent cation chelator that removes Mg^{2+} from outer membrane sites, causes similar enhancement of uptake of lysozyme and β -lactams (Nicas and Hancock, 1983b) as well as enhanced killing by the polycationic antibiotics (Sykes and Morris, 1975).

4. Imipenem.

Imipenem, or N-formimidoyl thienamycin, is derived from thienamycin, a natural product of the soil organism *Streptomyces cattleya* (Kahan et al., 1979). Thienamycin has unique structural feature (Fig. 2) that distinguishes it from all natural and synthetic β -lactam antibiotics previously described (Albers-Schönberg

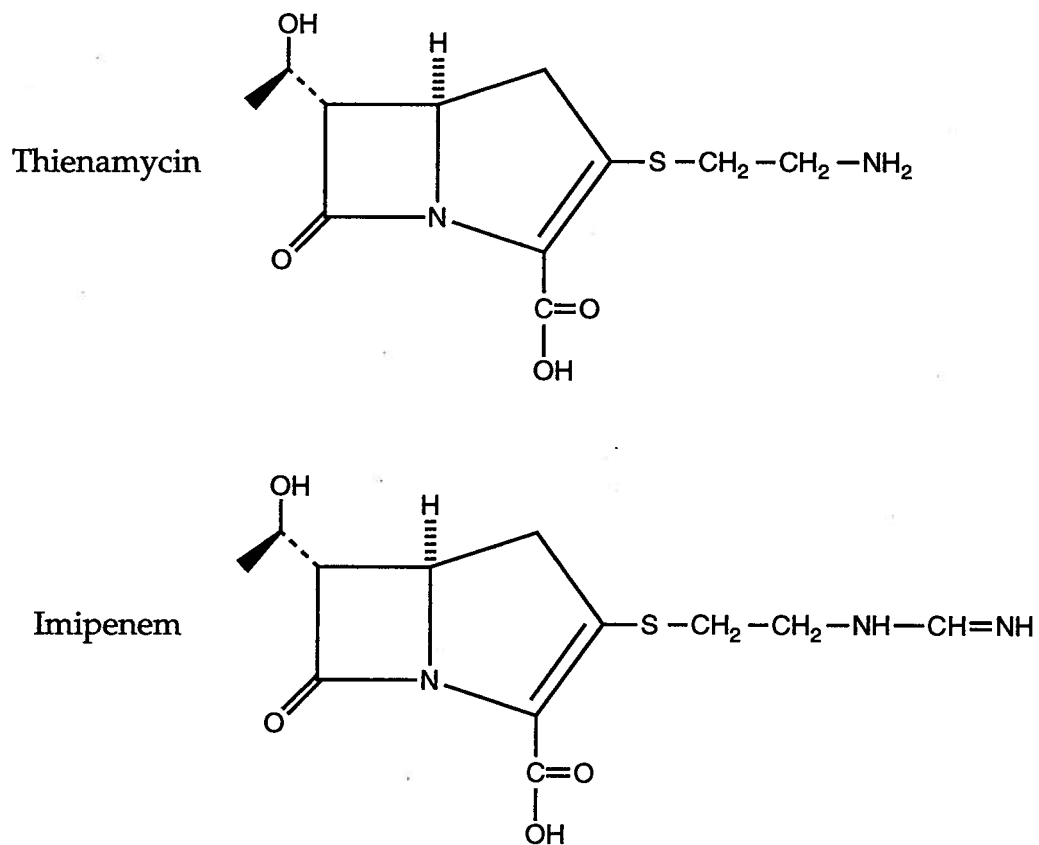


Figure 2: Structures of thienamycin and imipenem.

et al., 1978). It is the first representative of a new class of antibiotics, the carbapenems, *carbapen-* to denote the substitution of carbon for the sulfur molecule of the five-membered ring, and *-em* to signify the double bond in the ring (Fig. 2). The unusual *trans* configuration of the C-6 alkyl side chain and its direct attachment to the β -lactam ring of thienamycin further differentiates this antibiotic from the penicillins and the cephalosporins (Fig. 2), both of which have *cis*-acylamine side chains in the C-6 position. Since thienamycin breaks down spontaneously at high concentrations, synthesis of the amidine derivative N-formimidoyl thienamycin (Leanza et al., 1979) provided a stable, crystalline compound, imipenem (Fig. 2). Imipenem was the first carbapenem antibiotic to be developed for use in humans.

Imipenem is of unique interest because it has an unusually broad spectrum, high potency and no cross-resistance to other β -lactam antibiotics. Significantly, activity against the pathogen *P. aeruginosa* was substantially improved over other β -lactams. Comparative studies (Rolinson et al., 1986) showed that the major advantage of imipenem was its broad spectrum and high potency against isolates exhibiting β -lactamase-mediated resistance to one or more of the penicillins and cephalosporins. Furthermore, imipenem had greater bactericidal activity *in vitro* and greater protective efficacy in experimental infections against diverse pathogenic species (Kropp et al., 1980). Therefore, imipenem is particularly useful in the treatment of pathogens with high intrinsic resistance to many drugs, for example, *P. aeruginosa*, and infections caused by mixtures of bacteria for which a

combination of antibiotics would be normally used. In other cases, however, imipenem did not show superior activity (cf. other β -lactams) (Rolinson et al., 1986), which may be due to the overestimation of the non-specific permeability of imipenem across outer membrane (Bellido and Hancock, personal communication), and the derepression of the chromosomally-encoded β -lactamases (see below). Since imipenem is hydrolysed and thereby inactivated by the renal dipeptidase, dehydropeptidase (Kropp et al., 1982), it is administered in combination with equal amount of cilastatin, a dehydropeptidase inhibitor.

The high potency and unusually broad spectrum of antimicrobial activity of imipenem is due to three aspects. Firstly, it is able to penetrate the outer membrane of many Gram-negative bacteria. Imipenem has a compact structure with a molecular weight of 299 and is zwitterionic, both of which features facilitate its diffusion through the outer membranes of gram-negative bacteria by distinct porin channels (Yoshimura and Nikaido, 1985; Lipman and Neu, 1988). In *P. aeruginosa*, imipenem can overcome the poor outer membrane permeability by penetrating through the specific porin OprD (Trias and Nikaido, 1990a). Secondly, it has high affinity for the critical penicillin binding proteins (PBPs) from a broad range of bacteria. In *E. coli* and *P. aeruginosa*, imipenem showed the highest affinity to PBP-2 and appreciable affinity to most other PBPs (Hashizume et al., 1984). The binding to PBP-1 and PBP-2 is probably the main reason for its bactericidal action, namely rounding of cells at subinhibitory concentrations and lysis at higher concentrations. Thirdly, imipenem is a poor substrate for a broad

range of β -lactamases from Gram-positive and Gram-negative bacteria (Kahan et al., 1983). This stability is due, in part, to the *trans* conformation of the side chain on the 6-position of imipenem (Fig. 2). Finally, imipenem is however, a potent inducer of chromosomal cephalosporinases, a class of β -lactamases that are produced in some aerobic Gram-negative bacteria in the presence of selected β -lactam antibiotics and are capable of hydrolysing many β -lactams. However imipenem is only weakly hydrolysed by these β -lactamases (Livermore and Yang, 1987; Tausk et al., 1985). These properties may account for the general lack of cross-resistance of imipenem with other β -lactam antibiotics.

Correspondingly, resistance to imipenem can be mediated by three ways. Firstly, the constituents of the outer membrane maybe modified to prevent the passage of imipenem. *P. aeruginosa* mutants that are resistant only to imipenem but remain susceptible to most other β -lactams have been isolated both from clinical and laboratory sources. Their resistance is usually due to the decreased or lack of expression of OprD (Büscher, et al., 1987; Lynch et al., 1987; Quinn et al., 1986). Genetic analysis shows that the elimination of OprD results from gene rearrangements in the *oprD* coding region or the upstream promoter region (Yoneyama and Nakae, 1993). Secondly, the structure of PBPs may be altered to reduce the effect of imipenem on the cell wall in, for example, *Streptococcus faecium* (Hellinger and Brewer, 1991). Thirdly, β -lactamases may be expressed which are capable of hydrolysing and thereby inactivating the β -lactam ring of imipenem. *Pseudomonas maltophilia* is known to be uniformly resistant to imipenem. Saino

et al. (1982) demonstrated, in *P. maltophilia*, the presence of an inducible penicillinase, L-1, which is an unusual zinc metalloenzyme that can hydrolyse imipenem. Fortunately, enzymes of this type appear to be extremely rare in other species, although they also have been reported sporadically in *Bacteroids fragilis* (Yotsuji et al., 1983), *Aeromonas hydrophila* (Massidda et al., 1991) and *Serratia marcescens* (Osano et al., 1994). These imipenem-hydrolysing β -lactamases constitute a unique class of Zn^{2+} -containing β -lactamases analogous to the metalloproteases whereas most other β -lactamase are related to serine proteases. In addition, in *P. aeruginosa*, it appears the full expression of resistance to imipenem requires both reduced permeability due to loss of OprD and slow hydrolysis mediated by derepressed chromosomal β -lactamase (Livermore, 1992). In *Enterobacter*, the over-production of group I cephalosporinase and/or the decreased outer membrane permeability due to the deletion of certain porin(s) also conferred imipenem resistance (Lee et al., 1991; Thomson et al., 1993)

5. OprD: A Specific Porin for Imipenem and Basic Amino Acids.

As stated above, imipenem is highly potent against *P. aeruginosa*. However, during clinical therapy of *P. aeruginosa*, imipenem-resistant isolates arise at a significant rate (Quinn et al., 1986), and usually the resistant strains are not cross-resistant to other antibiotics, cannot hydrolyse or modify imipenem and do not show any alterations in the affinity or copy number of penicillin-binding proteins. On the

other hand, they lack an outer membrane protein with apparent molecular weight 46 kD, which has been identified as protein D2 (now called OprD) (Trias et al., 1979; Büscher, et al., 1987; Lynch et al., 1987; Quinn et al., 1986).

OprD is one of the porins in the *P. aeruginosa* outer membrane (Yoshihara and Nakae, 1989). The heat-modifiability property of OprD is like that of *E. coli* OmpA, it runs at a lower molecular weight when solubilized in SDS at low temperature, and at the monomer molecular weight when solubilized in SDS at high temperature. Natively, it is present in the outer membrane as trimers (Yoshihara et al., 1991). OprD forms small diffusion pores, which has been demonstrated in both liposome swelling assays (Yoshihara and Nakae, 1989) and in the black lipid bilayer system (Ishii and Nakae, 1993).

Purified OprD has been found capable of allowing the size-dependent uptake of small hydrophilic molecules, and it was suggested that OprD could permit a general diffusion of monosaccharides, disaccharides and amino acids at a significant rate (Yoshihara and Nakae, 1989; Trias and Nikaido, 1990a; Yoshihara et al., 1991). From this perspective, the channel has been proposed to behave as a general porin. More importantly, the following evidence indicates that OprD is also a specific channel for imipenem, basic amino acids and their structural analogues:

(a) *In vitro* liposome swelling assays demonstrated that the OprD channel allowed the diffusion of imipenem at a rate much higher than expected given its molecular weight, which was the behaviour expected for a specific ligand whose diffusion was facilitated by the given channel (Trias and Nikaido, 1990a).

(b) *In vivo* experiments performed with intact cells carrying a plasmid expressing the gene for L-1 β -lactamase from *P. maltophilia*, showed that the OprD channel was selective for imipenem over other β -lactam antibiotics (Trias and Nikaido, 1990a) .

(c) Regarding other antibiotics, Trias and Nikaido (1990a) suggested carbapenem derivatives, such as Sm-7338, Sch 33755, Sch 33440, meropenem and panipenem (Fukuoka et al., 1993), containing only one basic group at position 2 of the molecule also utilized the OprD channel for the facilitated diffusion. However, it was recently demonstrated that the addition of a second basic group at position 1 or 6 of a carbapenem which already contained a basic group at position 2, abrogated the role of OprD in its activity (Fung-Tomc et al., 1995)

(d) Regarding nutrients, basic amino acids and some small peptides containing these amino acids (Fig. 3) were shown to be competitive inhibitors of the diffusion of imipenem (Trias and Nikaido, 1990b) .

(e) *P. aeruginosa* showed higher susceptibility to imipenem in minimal medium than it did in rich medium such as Mueller-Hinton medium. The susceptibility was decreased by the addition of basic amino acids to the minimal medium, whereas the susceptibility to other antibiotics was not influenced. It was suggested that the decrease in susceptibility to imipenem was related to competition with basic amino acids for permeation through the OprD channel (Fukuoka et al, 1991).

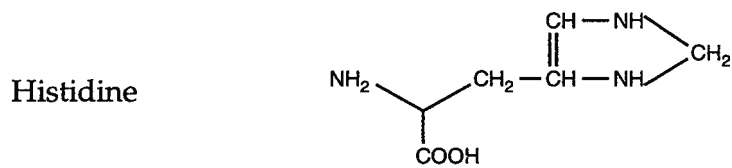
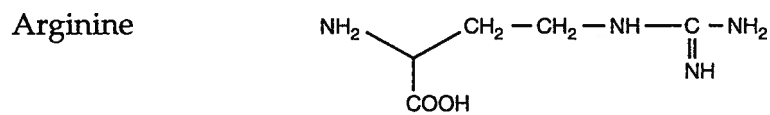
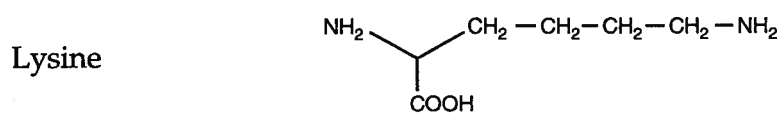
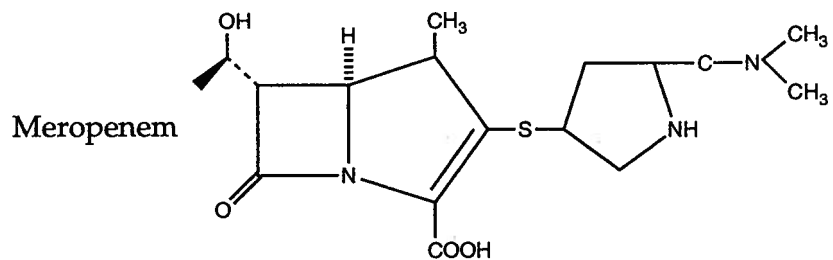
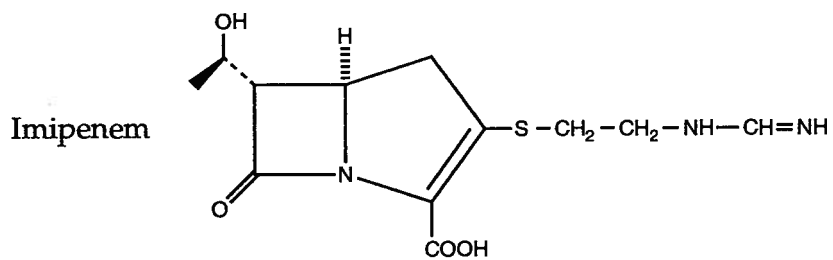


Figure 3: Structures of some antibiotics and amino acids that penetrate through the OprD channel.

C. Structure Analysis of Membrane Proteins.

1. X-ray Crystallography and Others.

Two major approaches have been taken to obtain the structural information on porin proteins. X-ray crystallography solves the structure at the highest possible resolution, i.e. the atomic level. So far, four general porins and one specific porin have been crystallized and analyzed in atomic detail. This has created a milestone in our understanding of porin functions. However, this method has the limitations of being highly technical, requiring specific training and expertise, time consuming, having no guarantee of success, and requiring large amount of highly purified protein. For most porins, in the absence of crystallographic data, structural models have been built using known sequences as the starting point (see details below), followed by using genetic, immunological and biochemical approaches to test and modify the predicted structure. Gene fusion techniques using β -galactosidase, alkaline phosphatase and β -lactamase as reporter enzymes have been successful in studies of the folding of inner-membrane proteins, which contain transmembrane segments composed of hydrophobic residues forming alpha helices (Manoil and Beckwith, 1986). However, since the structure of outer membrane proteins is more rigid by virtue of extensive β -structure, and consequently more dependent on tertiary interactions, the fusion of the reporter enzyme could cause severe perturbations of the native configuration, and fusion junctions may not correspond to loop regions. Therefore, such techniques are not suitable for the study of outer

membrane protein topology. Another technique, linker insertion mutagenesis, involving introduction of a short stretch of amino acids, modifies the proteins in a more subtle way. It has been successfully used to study the topology of several *E. coli* porins including LamB (Boulain et al., 1986), PhoE (Bosch and Tommassen, 1987) and *P. aeruginosa* OprF (Wong et al., 1993).

2. Crystal Structures of General Porin Channels.

The crystal structures of four general porins, including two *E. coli* porins OmpF and PhoE (Cowan et al., 1992), *Rhodobacter capsulatus* porin (Weiss and Schulz, 1992) and *Rhodopseudomonas blastica* porin (Kreusch et al., 1994) have been published. Although they do not share substantial sequence homology, their structures revealed striking similarity.

(a) BARREL TOPOLOGY. All of the general porins form trimers of identical monomers, each monomer consisting of a 16-stranded anti-parallel β -barrel enclosing a pore. The β -strands are amphipathic, in that they are composed of alternating polar and non-polar amino acid residues which are exposed to the aqueous channel and hydrophobic membrane interior respectively. The β -strands are connected by seven short β -hairpin turns at the periplasmic side (smooth end), and by eight long loops exposed at the cell surface (rough end). Six external loops pack together and partially cover the entrance to the barrel. The longest loop L3, contains a short piece of α -helix, folds inside the barrel and constricts the width of

the channel. These loop structures cause the channel to lie off center at an angle of about 16° to the barrel axis. The remaining loops are involved in monomer interactions.

(b) PORE ARCHITECTURE. The shape of the pore varies as it traverses the membrane and it can be divided into three parts: the mouth, constriction zone (eyelet), and exit zone. The pore entrance (the mouth) is narrowed by long loops at the rough end of the barrel to a diameter of 11~19 Å. About half way through the membrane, the cross section decreases to 7×11 Å where the internal loop (L3) and some side chains from barrel walls constrict the size of pore (eyelet). The cross section of the channel increases abruptly to 15×22 Å right after the eyelet since the pore size in this region is simply defined by the barrel walls (exit zone). For OmpF and PhoE, the three pores are separated over a distance of 30 Å which spans the entire passage through the core of the membrane (Cowan et al., 1992). In contrast, the three pores in *R. capsulatus* porin, each with an eyelet determining the solute exclusion limit, run separately over a distance of only 20 Å, and then the three pores merge into one channel at the periplasmic side (Weiss et al., 1991).

(c) EYELET. The eyelet region of OmpF and PhoE is lined on one side by negatively charged residues Asp^{113/106} (OmpF/PhoE numbering), Glu^{117/110}, whereas on the other side it is lined by positively charged residues Lys^{16/16}, Arg^{42/37}, Arg^{82/75} and Arg^{132/126}, giving rise to a strong transverse electrical field. These residues are strictly conserved among eight different porins from enteric bacteria (Jeanteur et al., 1991). Essentially the same arrangement is observed for *R. capsulatus* and *R.*

blastica porins. Several experiments indicate that the eyelet region is important for the selectivity as well as the determination of solute exclusion size for the general porins (Benson et al., 1988; Misra and Benson, 1988; Bauer et al., 1989). The most direct evidence comes from the crystal structure of a mutant OmpF protein (Jeanteur et al., 1994b). With a single mutation Gly-119→Asp in the eyelet region, X-ray structure analysis reveals a locally altered peptide backbone, with the side chain of residue Asp-119 protruding into the channel, causing the original eyelet region to be subdivided into two intercommunicating compartments of 3~4 Å in diameter. The functional consequences of this structural modification included a reduction of the channel conductivity by about one-third, altered ion selectivity and voltage gating, and decrease of permeation rates of various sugars by 2~12 fold.

(d) TRIMER STABILITY. The trimer is stabilized by both hydrophobic and hydrophilic interactions between the monomers. The hydrophobic contacts are made by residues from the barrel walls. Along the trimer axis, large hydrophobic residues pack together to fill up the space completely, leaving no room for water. Away from the trimer axis, the β -sheets of the barrel walls pack in a highly complementary manner, resulting in extensive contact between the monomers. The hydrophilic interactions primarily involve a loop L2, which reaches into the pore of a neighbouring monomer where it participates in extensive hydrogen bonding and a few salt bridges. This loop also fills the gap in the wall of the adjacent monomer left by L3 which folds inside the barrel.

(e) AROMATIC RING. The membrane-facing surface of trimeric porins can

be subdivided into three main areas. Starting from the bottom (periplasmic side), the first zone is characterized by the presence of many aromatic residues, mainly Tyr and Phe. Moving upwards is the expected non-polar region composed mainly of Leu, Val, and Ala. On top is the second aromatic ring at the nonpolar/polar border of the interface between protein and membrane, which functions to anchor the protein in the membrane. The flat aromatic surface is ideal for packing with fatty acyl chains, therefore protecting the porin conformation against adverse membrane fluctuations. For Tyr and Trp, the combined properties of hydrophobicity and the ability to form hydrogen bonds is favourable at the polar/nonpolar interface separating regions with dramatically different dielectric constants.

3. Crystal Structure of Specific Porin Channel.

Very recently, the first crystal structure of a specific porin of *E. coli*, LamB, was solved at 3.1 Å resolution (Schirmer et al., 1995). LamB, originally discovered as the receptor of bacteriophage λ , is also a specific porin for maltose and maltodextrins (Benz et al., 1987; Freundlieb et al., 1988; Gehring et al., 1991), thus it has another name, maltoporin. The X-ray structural analysis of LamB reflects a general similarity to the structure of nonspecific porins. On the other hand, it is more sophisticated to allow for the specific binding and efficient transport of maltose and maltodextrins.

Active maltoporin is a trimer, with each monomer consisting of an 18-

stranded antiparallel β -barrel, instead of the 16-stranded structure of general porins. Each monomer contains an independent channel, and all three monomers of the trimer are required for phage adsorption (Marchal and Hofnung, 1983). Similar to the general porins, the β -strands are connected by short turns at the periplasmic side, whereas the cell surface connections are made by long loops. The third surface loop, L3, is entirely folded into the channel, while L1 and L6 from the same monomer and L2 from a neighbouring monomer fold inside to different extents, forming the constriction zone toward the middle of the channel. The other loops form a sort of umbrella covering the entrance of most of the channel.

As with the general porins, the eyelet region is defined by L3 and a few side chains from the barrel walls, but the lumen at the channel entrance is further constricted by residues from L1 and L6, presumably to increase the selectivity. The pore has a diameter of 5 to 6 Å, considerably smaller than that of OmpF. Charged residues are distributed pairwise in the eyelet region and form an electrostatic field.

The most interesting feature is a series of aromatic residues arranged along a left-handed helical pathway from the inlet to the outlet of the channel. This path (the "greasy slide") guides the diffusion of sugars through stacking interactions. The hydrophobic faces of glycosyl moieties are known to stack with aromatic residues in sugar binding proteins (Spurlino, 1991). Other charged residues in the vicinity of the "greasy slide" interact with the hydroxyl group of the sugars and may account for the stereospecificity of the channel. The positions of all selected

mutations with altered affinities toward maltodextrin (Ferenci and Lee, 1982) cluster at the pore eyelet region.

4. Prediction of Porin Structure: Porin Superfamily.

In the last few years, porin genes from many pathogenic Gram-negative bacteria have been cloned and sequenced. These porins are the focus of many studies because of their potential use as vaccines, or for bacterial typing, and their role in antibiotic resistance. Since their three dimensional structures are usually unknown, prediction of their folding patterns is important for further investigation. As porins are comprised of antiparallel β -strands tranversing the membrane, the first approach to structure prediction was to identify segments causing the polypeptide strands to reverse their direction, i.e., turn prediction. According to Paul and Rosenbush (1985), amino acids can be divided into three groups: turn promoters (N, D, E, G, P, S), turn blockers (A, Q, I, L, M, F, W, Y) and other residues. Turns are then predicted as a segment of three or more residues containing at least one turn promoter and no turn-blockers. Another approach is based on the fact that the transmembrane β -strands are amphipathic (Vogel and Jahnig, 1986), with one face created by every second amino acid being in contact with the hydrophobic core of the membrane, and the other facing the hydrophilic pore lumen. Therefore the β -strands should have high amphipathic values.

The concept of a "porin superfamily" was proposed by Jeanteur et al (1991).

This superfamily consists of over 30 general porins from five distantly related species. Though they do not share significant homology based on overall sequence, their transmembrane segments can be aligned with good homology. Therefore, aligning the porin sequence with those of known structures, provides another approach in the structure prediction. Jeanteur et al. (1994a) first combined turn prediction and amphipathicity calculations with multiple alignments, greatly improving the quality of these predictions. The relevance of this predictive method was confirmed by the crystal structures of OmpF, PhoE and *Rhodobacter capsulatus* porins (Cowan et al., 1992; Weiss and Schulz, 1992). The specific porins LamB and Tsx, however, are not able to align with the porin superfamily. Therefore they form a distant family or families of their own (Jeanteur et al., 1994a)

Multiple alignment and topology prediction are complementary tasks. On the one hand, multiple alignment gives better accuracy to a prediction because, if the sequences are properly aligned, predictions of topological elements will be reinforced by being predicted in all aligned sequences. On the other hand, prediction of topology will help to align sequences because predicted topological elements can be lined up together. In addition, multiple sequence alignments highlight important conserved features of the sequences, thus structural information or biochemical information on one species of porins can be related to more distant porin species.

D. Model Membrane Studies of Porins.

A variety of model systems have been used to investigate the physical properties of porins *in vitro*. The two most-utilized systems are the liposome-swelling assay (Nikaido and Rosenberg, 1981; Hancock, 1986) and black lipid bilayers (Hancock, 1986). These permit one to probe the function of porins in allowing the passage of medium-sized sugars, β -lactams, amino acids and small- to medium- sized ions, respectively. Our laboratory uses the second system in which porins in detergent solution are added to the aqueous salt solution bathing a planar lipid bilayer. Individual porin molecules then spontaneously insert in a time-dependent fashion into the membrane, an event that can be measured as step increases in the conductance between two electrodes placed on either side of the membrane. This method has the rather unique property of having single molecule sensitivity, since amplifying the current through a single channel forming unit, by 10^9 - 10^{10} fold, results in events that can be read out on a chart record. In addition, it is capable of providing an estimate of the channel diameter, a precise measurement of the ion selectivity of a variety of anions and cations, a measurement of the heterogeneity of individual channels, and direct evidence for the presence of substrate binding site(s) in the channel.

This system revealed that general porins have the following properties: porins form water-filled channels, with the size of the channel largely determining the exclusion limit of the outer membrane for hydrophilic compounds; small chemicals pass through the middle of the channel in a manner similar to their diffusion through bulk water; porin channels are usually either cation or anion

selective, ranging from 2 to 30 fold; porin channels are not voltage gated or, in most cases, voltage regulated. For specific porins such as OprP and LamB, it was found they contained substrate binding sites which, when occupied by substrates, block the passage of ions through the channel (Hancock, 1986).

E. Aims of This Study.

OprD, a specific porin for imipenem and basic amino acids, provides an excellent model for studying the mechanisms of antibiotic and nutrient uptake through the specific porins. Even though previous work and other work performed during the investigations described here, suggested that OprD had a specific binding site for imipenem, there still remained many questions. What is the function of OprD in transport of other antibiotics and nutrients? What is the folding pattern of OprD in the outer membrane? Where are the specific binding site(s) located and which residues are responsible for the specific binding? What is the mechanism of facilitated diffusion of imipenem and basic amino acids through the OprD channel? Attempts to solve these questions made the goals of this thesis: (1) to further investigate the substrate selectivity of OprD by using isogenic mutants expressing different levels of OprD; (2) to predict an OprD membrane topology model and verify it by site-directed mutagenesis; (3) to locate the specific binding site(s) for imipenem by studying the functional alterations of the mutants; and (4) to elucidate the molecular architecture of OprD channel in order to understand the

mechanism of imipenem uptake through the channel, which was the ultimate goal of this study.

MATERIALS AND METHODS

A. Strains, Plasmids and Growth Conditions.

All strains used in this study are listed in Table I and all plasmid used are listed in Table II. Strains were routinely grown on Luria Broth (LB) medium (1.0% Tryptone, 0.5% yeast extract, 0.5% NaCl) or LB agar containing, in addition 2% agar. For experiments involving growth on specific carbon sources, *P. aeruginosa* strains were grown on BM2 minimal media (Hancock and Carey, 1979). *P. aeruginosa* strains were also grown on Mueller-Hinton broth. VBMM media is VB (Voger and Bonner, 1956) medium containing 0.3% trisodium citrate as a carbon source and was selective for *P. aeruginosa* since *E. coli* cannot utilize citrate. The formulation for VBMM (per liter) was as follows: Na₃citrate, 3.0g; citric acid, 2.0g; K₂HPO₄ 10.0g; NaNH₄PO₄×4H₂O, 3.5g; adjust (or check) PH 7.0, after autoclaving and cooling add: 0.8 ml of 1M MgSO₄×7H₂O and 0.08 ml of 1M CaCl₂. All media components were obtained from Difco Laboratories, Detroit, Michigan. Antibiotics were used in selective media at the following concentrations, for *E. coli*: ampicillin 75 µg/ml; chloramphenicol 25 µg/ml; kanamycin 35 µg/ml; for *P. aeruginosa*: carbenicillin 500 µg/ml; kanamycin 300 µg/ml; streptomycin 500 µg/ml.

B. Genetic Manipulations.

1. General Techniques.

Table I: Strains.

<u>Strain</u>	Description	Reference/Source
<i>E. coli</i>		
DH5 α	<i>supE44 hsdR17 recA1 endA1 gyrA96 thi-1 relA1</i>	Hanahan, 1983
CE1248	Porin deficient strain: OmpF, OmpC, PhoE	Van der Ley, et al., 1985
S17-1	Mobilizing donor strain in biparental mating	Simon, et al., 1983
<i>P. aeruginosa</i>		
H103	PAO1 prototroph: wild type reference strain	Hancock & Carey, 1979
H636	H103 <i>oprF</i> :: Ω	Woodruff & Hancock, 1988
H673	H103 <i>opdE</i> :: Tn501, imipenem resistant strain	Huang et al., 1992
H729	H103 <i>oprD</i> :: Ω	This study

Table II: Plasmids.

Plasmid	Description	Reference/Source
pTZ18R/19R	general cloning vector, Ap ^R	Pharmacia
pBK18R/19R	pTZ18R/19R with a 2.1-kb <i>Bam</i> HI/ <i>Kpn</i> I fragment encoding the <i>oprD</i> gene	This study
pE37/65	pTZ19R with a 4.0-kb <i>Eco</i> RI fragment encoding the N-terminal portion of the <i>oprD</i> gene	This study
pRK767	low-copy-number shuttle vector	Ditta et al., 1985
pD2-45	pRK767 with a 9.1-kb <i>Bcl</i> I fragment encoding the <i>oprD</i> regulatory gene	Huang et al., 1992
pUCP18/19	pUC18/19-derived broad host range plasmid which can be maintained in both <i>E. coli</i> and <i>P. aeruginosa</i>	Schweizer, 1991
pNOT19	pUC19 with the unique <i>Nde</i> I site changed to a <i>Not</i> I site	Schweizer, 1992
pMOB3	a cassette containing a portable <i>oriT</i> , the <i>sacB</i> gene from <i>Bacillus subtilis</i> and a chloramphenicol-resistance gene allowing positive selection for both <i>oriT</i> and <i>sacB</i> .	Schweizer, 1992
pUC4KAPA	a vector containing a kanamycin resistant (Km ^R) Ω interposon flanked by symmetrical restriction sites	Pharmacia

con't...

Table II: Plasmids (con't)

Plasmid	Description	Reference/Source
pXH1	a plasmid constructed for the allele replacement mutagenesis of the <i>oprD</i> gene	This study
pXH2	pUCP19 with a 2.1-kb <i>Bam</i> <i>HI</i> / <i>Kpn</i> <i>I</i> fragment encoding the <i>oprD</i> gene	This study
pMTZ19R	modified pTZ19R which eliminated the restriction sites <i>Sac</i> <i>II</i> , <i>Pst</i> <i>I</i> , <i>Sph</i> <i>I</i> and <i>Hind</i> <i>III</i> in the multiple cloning site	This study
pMBK19R	pMTZ19R with a 2.1-kb <i>Bam</i> <i>HI</i> / <i>Kpn</i> <i>I</i> fragment encoding the <i>oprD</i> gene	This study
pMBE19R	pMTZ19R with a 1.2-kb <i>Bam</i> <i>HI</i> / <i>Eco</i> <i>RI</i> fragment encoding N-terminal part of the <i>oprD</i> gene	This study
pHE1	pMBK19R with a deletion of 24 bp from the region encoding the predicted loop L1 of OprD	This study
pHE2	pMBK19R with a deletion of 24 bp from the region encoding the predicted loop L2 of OprD	This study
pHE3	pMBK19R with a deletion of 24 bp from the region encoding the predicted loop L3 of OprD	This study

con't...

Table II: Plasmids (con't)

Plasmid	Description	Reference/Source
pHE4	pMBK19R with a deletion of 12 bp from the region encoding the predicted loop L4 of OprD	This study
pHE5	pMBK19R with a deletion of 24 bp from the region encoding the predicted loop L5 of OprD	This study
pHE6	pMBK19R with a deletion of 12 bp from the region encoding the predicted loop L6 of OprD	This study
pHE7	pMBK19R with a deletion of 24 bp from the region encoding the predicted loop L7 of OprD	This study
pHE8	pMBK19R with a deletion of 24 bp from the region encoding the predicted loop L8 of OprD	This study
pHP1~pHP8	pUCP19 containing the corresponding mutant <i>oprD</i> gene with deletions in the region encoding the predicted loops L1~L8	This study

All general DNA techniques such as DNA isolation, agarose gel electrophoresis, radioactive labelling of oligonucleotides, colony blotting, Southern blotting and transformation were performed as described in Sambrook et al. (1989). Other methods included slot lysis gel electrophoresis (Sekar, 1987). DNA restriction and modifying enzymes (Bethesda Research Laboratories (BRL), Burlington, Canada; Boehringer Mannheim, Mannheim, Germany; Pharmacia, Uppsala, Sweden) and Vent DNA polymerase (New England Biolabs, Beverly, MA) were used according to the manufacturer's method.

2. DNA Fragment Isolation.

DNA fragments were isolated by the band interception technique (Winberg and Hammarskjöld, 1980) using DEAE paper and the manufacturer's method (Schleicher and Schuell Inc., Keene, N.H.). In addition, PCR fragments were purified using the QIAEX Gel Extraction Kit (Qiagen Inc., Chatsworth, California) following the manufacturer's protocol.

3. DNA Sequencing.

Plasmid DNA for sequencing was isolated using Qiagen columns (Qiagen Inc., Chatsworth, California) following the manufacturer's protocol. Sequencing reactions were set up according to the manufacturer's method, containing 1 µg of

template DNA, 3.2 pmol of primer and components from an Applied Biosystems Inc. (ABI, Foster City, California) Taq DyeDeoxy Terminator Cycle Sequencing Kit. Sequencing reactions were carried out using an Ericomp thermocycler (96°C for 30 sec, 50°C for 15 sec, 60°C for 4 min; 25 cycles), run on an ABI 370A automated DNA sequencer, and analyzed using ABI 373A Data Collection and Analysis programs for the Macintosh computer.

Two strategies were utilized to obtain the complete sequence from a long fragment. Timed exonuclease III digestions (Erase-a-base, Promega, Madison, WI) were employed to create ordered deletions for both strands of the *oprD* gene. For the strand from *Bam*HI to *Kpn*I (Fig. 10), *Bam*HI generated a 5'-protruding end and the adjacent primer binding site was protected from digestion by the 3'-overhang of the *Sph*I restriction site. For the other strand, *Cla*I and *Kpn*I were used as the 5'-protruding and 3'-overhang restriction site respectively. The reaction was carried out at 30°C, and digestion proceeded at about 210 bp per minute. For each strand, samples were taken at 12 time points at 1 min time intervals. The second strategy was a combination of subcloning and building of oligonucleotide primers which was used to sequence the *oprD* regulatory gene and PCR products.

4. Transfer of DNA into *P. aeruginosa*.

Plasmids were transferred into *P. aeruginosa* by transformation (Olsen et al., 1982). Briefly, cells to be transformed were grown to an OD₅₅₀ of 0.2~0.6 in LBNS.

Cells from 20 ml culture were pelleted and resuspended in 10 ml cold, 0.15 M MgCl₂, placed on ice for 5 min. This step was repeated except that the cells were kept on ice for 20 min. The cells were then pelleted and resuspended in 1 ml ice-cold 0.15 M MgCl₂. For each transformation, 100 ng of DNA was added to 0.2 ml cells and the mixture was placed on ice for 60 min followed by a 3 min heat pulse at 37°C. LBNS (0.5 ml) was added and the mixture was incubated at 37°C for 2.5 h to allow the expression of the plasmid's antibiotic resistance gene. Aliquots (0.1 or 0.25 ml) of cells were plated on selective medium and grown for 24 to 48 h.

Alternatively, biparental mating was also used. Overnight cultures of the plasmid-containing *E. coli* S17-1 strain were grown in LBNS at 30°C with shaking. The recipient strain was grown overnight at 42°C with shaking. Samples (0.1 ml) of both the donor and recipient strains were mixed in 2 ml fresh LBNS and incubated for 10 to 30 min at room temperature. The cell mixture was filtered onto a 0.45 µm membrane. The filter was then plated on a non-selective agar plate and incubated at 30°C overnight. The cells were subsequently washed off the filter with sterile saline, serially diluted, spreaded onto selective plates and incubated at 37°C for up to 48 hours.

5. Oligonucleotide Synthesis and Purification.

Oligonucleotides were synthesized on an ABI (Foster City, California) model 392 DNA/RNA synthesizer according to the manufacturer's protocol. The

synthesized oligonucleotides were incubated at 55°C overnight followed by drying in the Speed Vac Concentrator (Fisher Scientific, Ottawa, ON). The oligonucleotides were resuspended in 1.5 ml of 0.5 M ammonium acetate and further purified on a C₁₈ SEP-PAK cartridge (Millipore, Milford, Massachusetts) as described by Atkinson and Smith (1984). The 0.5 M ammonium acetate solution containing the oligonucleotides was loaded onto a prepared C₁₈ SEP-PAK column, washed with water and eluted with 20% acetonitrile (if the oligonucleotides were less than 40 bases) or 40% acetonitrile (if the oligonucleotides were more than 40 bases). The oligonucleotides were either lyophilized or ethanol precipitated before quantification by A₂₆₀ absorbance.

C. Cloning Strategy for the *oprD* Gene.

OprD was partially purified by Susan Farmer from *P. aeruginosa* PAO1 strain H103 grown in BM2 minimal medium containing succinate as a carbon source and the N-terminal amino acid sequence was determined by Sandy Kielland, (University of Victoria, Canada) to be D A F V S D Q A E A K G F I E D S. Taking into account codon bias in *P. aeruginosa*, a corresponding 48 mer nucleotide oligo pool was deduced. This was then radiolabelled with γ -³²P-ATP and used as a probe in Southern hybridization analysis with *P. aeruginosa* chromosomal DNA that had been singly or pairwise digested with several restriction enzymes: *EcoRI*, *BamHI*, *KpnI*, *ClaI*. The chromosomal restriction map was made and the N-terminus of the

oprD gene was located, while the expression of OprD could be in either of the two directions. Fragments of corresponding sizes were isolated from chromosomal digests and ligated into plasmid pTZ18/19R to construct mini-libraries. The resulting colonies were screened with the same probe described above.

D. Allele Replacement Mutagenesis.

1. Construction of pXH1.

Firstly, a kanamycin-resistance (Km^R) conferring Ω -fragment from pUC4KAPA was isolated as the 1.3-kb *SalI* fragment and cloned into the *XhoI* site on the *oprD* gene, yielding pBK19R:: Ω , which left 0.6-kb and 0.7-kb, respectively of chromosomal DNA sequence on either side of the Km^R cassette. Then the 3.6-kb *BamHI/KpnI* fragment containing the *oprD*:: Ω insert was cloned into the similarly cleaved pNOT19. Subsequently, the MOB3 cassette was isolated as a 5.8-kb *NotI* fragment from pMOB3 and inserted into the unique *NotI* site on pNOT19 with *oprD*:: Ω Km^R to generate plasmid pXH1 (~12-kb) (Fig. 4).

2. Selection of the *oprD*:: $Km^R\Omega$ mutant.

pXH1 was transferred into *P. aeruginosa* by biparental mating. Plasmid cointegrates in which the entire plasmid was inserted into the *P. aeruginosa* chromosome due to homologous recombination were isolated by plating on VBMM

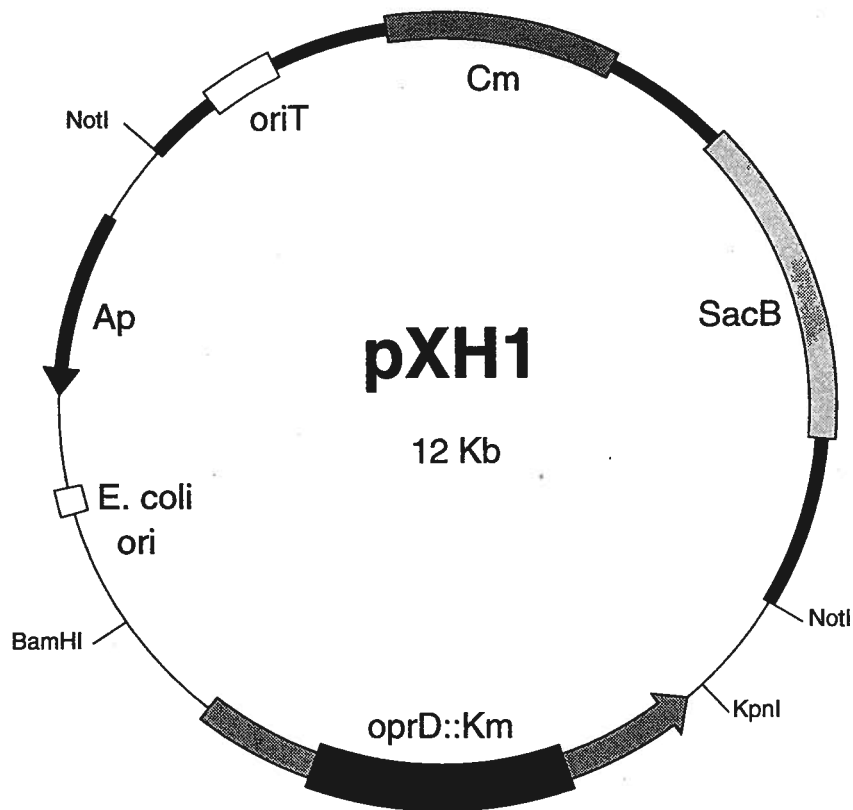


Figure 4: Diagram of plasmid pXH1 utilized for allele replacement mutagenesis.

The lighter shaded arrow between the *Bam*HI and *Kpn*I restriction sites represents the *P. aeruginosa oprD* gene coding region, whereas the black thick bar in the middle represents the 1.3-kb kanamycin-resistance Ω -interposon that was used to interrupt the *oprD* gene. The fragment between the two *Not*I sites is the 5.8-kb MOB3 cassette. The orientations of the *oprD* gene and ampicillin-resistance marker are indicated. Abbreviations: Ap: ampicillin-resistance gene; oriT: origin of transfer; Cm: chloramphenicol resistance gene; SacB: sucrose expression results in susceptibility to sucrose; Km: kanamycin-resistance Ω -interposon; *E. coli* ori: *E. coli* specific origin of replication.

Km Cb plates. Several colonies that were Km^R and Cb^R were then grown on Mueller-Hinton kanamycin plates containing 5% sucrose to select for a recombination event deleting the *sacB* gene and other vector sequences. The mutants were characterized by Southern analysis and the isolation of outer membrane proteins.

E. Overexpression of the *oprD* Gene in *P. aeruginosa*.

To overexpress OprD, the 2.1-kb *Bam*HI/*Kpn*I fragment from pBK19R containing the *oprD* gene was cloned into pUCP19 to form the plasmid pXH2, so that the direction of expression of the *oprD* gene was in the same orientation as the *lac* promoter (Fig. 5). It was then transformed into *E. coli* S17-1 and mobilized back into *P. aeruginosa* H103, H636 and H729.

F. Electrophoresis.

Proteins were separated by electrophoresis through 7%, 11% or 15% SDS-polyacrylamide gels (SDS-PAGE) as previously described (Hancock and Carey, 1979).

G. Growth experiment.

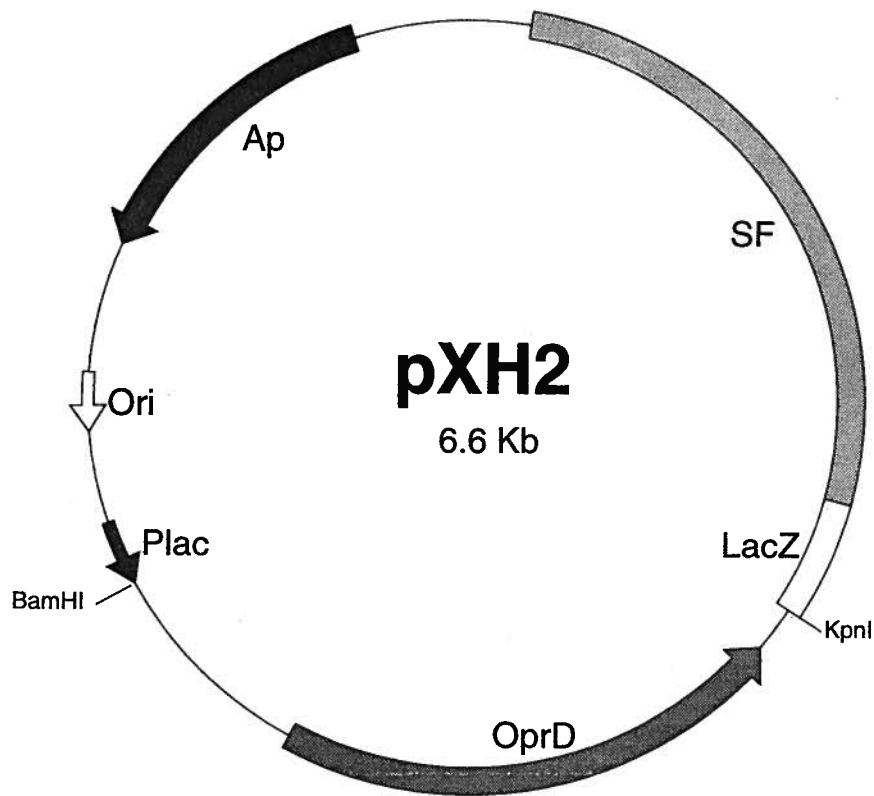


Figure 5: Diagram of plasmid pXH2 utilized for the overexpression of the *oprD* gene.

The dark shaded arrow between the *Bam*HI and *Kpn*I restriction sites represents the *P. aeruginosa* *oprD* gene coding region. The orientations of the ampicillin resistance gene, the *oprD* gene, origin of replication and the *lac* promoter are indicated. The 1.8-kb stabilizing fragment is for the maintenance of the plasmid in *P. aeruginosa*. Abbreviations: Ap: ampicillin resistance gene; SF: stabilizing fragment; Plac: *lac* promoter; Ori: origin of replication for *E. coli*.

For growth experiments, each strain was grown to mid-exponential phase on minimal medium with the specific carbon source, glucose, gluconate or pyruvate. They were then subcultured 1 in 50 into prewarmed fresh media containing the indicated levels of saccharides and grown with shaking at 37°C. Samples (1 ml each) were taken at regular intervals for measurements of optical density at 600 nm. Growth rate was calculated by the equation: $\mu = \ln 2/g$, where μ was growth rate, expressed in hours and, g was doubling (generation) time which was determined from a semi-logarithmic plot of the growth curve.

H. Purification of OprD.

For the purification of OprD from *E. coli*, strain CE1248(pBK19R) was used and cultures were grown at 37°C with 50 µg/ml ampicillin, 0.4% glucose and 1 mM isopropylthiogalactoside (IPTG) to an OD₆₀₀ of 0.8 to 1.0. For the purification of OprD from *P. aeruginosa*, strain H636(pXH2) lacking OprF and overexpressing OprD was used, and cultures were grown at 37°C with 500 µg/ml carbenicillin and 0.4% glucose to an OD₆₀₀ of 0.8 to 1.0. Mutant proteins OprD Δ L2 and OprD Δ L5, were purified from CE1248(pHE2) and CE1248(pHE5) respectively. The whole purification procedure could be divided into the following three steps:

(i) Isolation of outer membranes:

Cultures were harvested and the cell pellet was resuspended in cold 20% sucrose containing 50 µg/ml DNaseI. The cell suspension was passed twice through

a French pressure cell (American Instrument Co., Inc. Silver Spring, MD) at 15,000 psi. After unbroken cells were removed by low-speed centrifugation (3000 rpm, 10 min), the cell lysate was applied to a 2-step sucrose gradient (50% and 70%) and centrifuged in L8-70 Ultracentrifuge (Beckman Instrument, Inc, Fullerton, CA) at 21,000 rpm overnight. The outer membrane band was collected from the interface of the above two sucrose steps and diluted with distilled water, and centrifuged at 45,000 rpm for 1 h to get rid of sucrose.

(ii) Detergent solubilization:

The outer membrane fraction was subjected to a 3-step differential detergent solubilization to concentrate OprD and remove other membrane components. Firstly, the pellet was extracted with 10 mM Tris-HCl (pH8.0), 0.5% octyl-polyethylene (octyl-POE) (Bachem Bioscience Inc., Philadelphia, PA), followed by centrifugation at 45,000 rpm for 1 h. The supernatant was reserved and the pellet was extracted with 10 mM Tris-HCl, 3% Octyl-POE, 0.2 M NaCl followed by centrifugation as above. Finally OprD was largely extracted from the pellet with 10 mM Tris-HCl, 3%Octyl-POE, 0.1 M NaCl and 5 mM EDTA followed by centrifugation, and this supernatant was dialysed against 10 mM Tris-HCl, 5 mM EDTA and 0.08% N, N, dimethyldodecylamine-N-N-oxide (LDAO) (Fluka Chemika, Ronkonkoma, NY).

(iii) Fast Protein Liquid Chromotography (FPLC):

The solubilized protein was loaded onto an FPLC anion exchange column (Mono Q, bed volume=1.0 ml, flow rate=0.5 to 1.0 ml/min) that had been

equilibrated with 10 mM Tris-HCl, 5 mM EDTA and 0.08% LDAO. The protein was eluted by applying a linear gradient of buffer which contained the above ingredients plus 0 to 1.0 M NaCl. After the first run, the fractions which contained the least contaminants were pooled and subjected to a second run with a much flatter salt gradient and a lower elution speed. OprD was eluted in a purified form during this step. The purified OprD was aliquoted and frozen at -70°C.

I. Immunological Techniques.

1. Production and Purification of OprD antibodies.

With the help from Bill Masin and Mike McClymont, anti-OprD polyclonal antibodies were raised in New Zealand White rabbits as described by Poole and Hancock (1986). FPLC-purified (100 µg) OprD was injected subcutaneously on days 0, 14, 28, 42, and 56. A booster shot of 200 µg OprD was given on day 68. For the first injection, OprD was mixed with equal volume of Freund's incomplete adjuvant (Difco, Detroit, MI, USA). Subsequently it was injected in Freund's complete adjuvant. Two weeks after the last injection, the rabbit was bled and the serum was isolated.

The antiserum was purified by absorbing against whole cells of *P. aeruginosa* OprD-defective strain H729 as follows. Cells from 5 ml overnight culture in LBNS were harvested by centrifugation at 7,000 rpm for 10 min and washed twice by resuspension and centrifugation with sterile saline. The cell pellet was resuspended

directly into 1 ml of antiserum and incubated with shaking for 45 min at room temperature. The cells were then pelleted and the antiserum-containing supernatant was absorbed a second time against a fresh batch of washed cells. Whole cell absorption effectively removed most antibodies directed against other outer membrane components and gave reasonably clean backgrounds when used at a 1:2000 dilution in Western-immunoblotting.

2. Western-immunoblotting.

Western-immunoblotting was done as previously described (Mutharia and Hancock, 1983).

J. Prediction of The OprD Topology Model

1. Sequence Alignment.

The first criteria utilized for the modelling was based on sequence alignments of *P. aeruginosa* OprD with *E. coli* OmpF, PhoE and *Rhodobacter* porins. PCGENE program was used to perform the pairwise and multiple alignments, the gap penalty was adjusted to optimize the alignment and minimize gaps in the known transmembrane segments. It is clear that surface loop regions of the porins undergo maximal variation, so the nonhomologous regions and/or small deletions (or insertions) would be preferentially located at the surface loops. Conversely, the transmembrane regions are more conserved. From these

alignments, OprD showed highest homology with *E. coli* OmpF compared to PhoE and *Rhodobacter* porins in the β -strand regions, so the transmembrane segments were primarily predicted according to the consensus between OprD and OmpF sequences.

2. Structural Characteristics.

The primary model was then adjusted to the structural characteristics of porins as confirmed by the known structures.

(a) TURN. The β -strands were connected by short turns at the periplasmic side and turns were mainly identified according to the definition of Paul and Rosenbush (1985). The newly published porin structures have shown that periplasmic loops were very short, involving only a few residues (Cowan et al., 1992; Weiss and Schulz, 1992). As a consequence, the prediction of the periplasmic β -turns also took into account the frequency of residue occurrence within these turns in *E. coli* and *Rhodobacter* porins.

(b) TRANSMEMBRANE STRANDS. Porins have high content (more than 60%) of β -sheet conformation (Kleffel et al., 1985). And the β -strands were typically amphipathic in that they were composed of alternating polar and non-polar amino acids which were exposed to the aqueous porin channel and hydrophobic membrane interior respectively. This requirement was not strict, however, because internal residues could be hydrophobic if they were buried by internal structures.

(c) EXTERNAL LOOPS. The external loops were long and of variable length, they contained many polar residues and were hydrophilic.

(d) CONSERVED RESIDUES. Some residues were conserved among many porin, for example, the existence of a aromatic ring at the water/lipid interface and large excess of negatively charged residues at the level of the LPS headgroup on the outerface of the membrane.

This model was further modified by Dr. Denis Jeanteur, using a computer program to perform multiple alignments with porin superfamily and calculate the amphipathicity of the predicted β -strands (see Appendix).

K. PCR-based Site Specific Deletion Mutagenesis.

1. Two PCR Strategies.

Strategy I, direct extension (Vallette et al, 1989), was applied to those loop-encoding regions with convenient restriction sites adjacent to the nucleotide sequence to be deleted. This procedure required 2 synthetic oligonucleotides as the primers to amplify the nucleotide sequence of interest. Primer 'a' contained the restriction site and the desired deletion. Primer 'b' annealed at another end of the targeted sequence and was oriented in the opposite direction (Fig. 6A).

For those loop-encoding regions without convenient restriction sites located near the sites of mutagenesis, strategy II, overlap extension (Ho et al, 1989), was employed. This method required 2 pairs of primers, an external pair 'a' and 'd'

I. Direct extension.



II. Overlap extension.

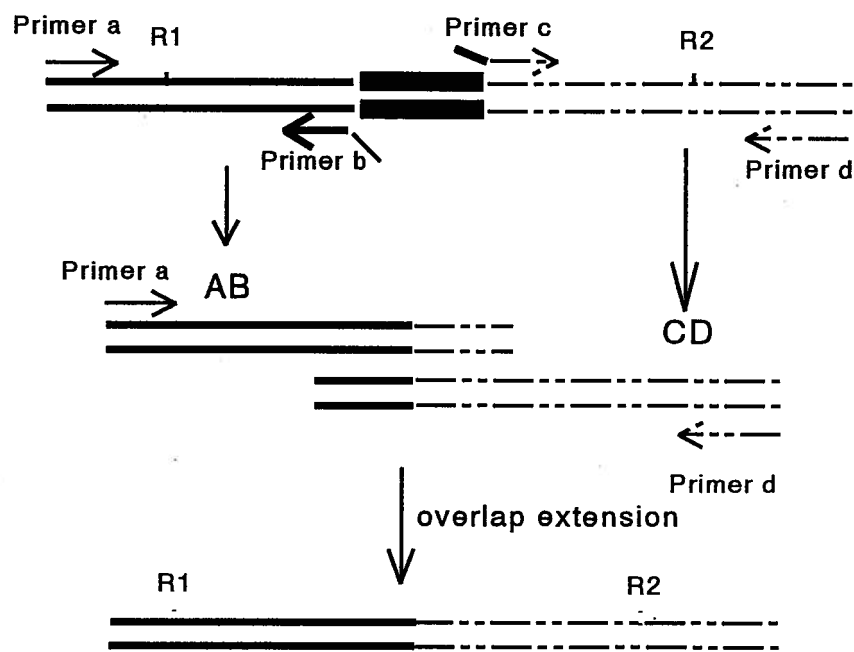


Figure 6: Schematic diagram showing two PCR strategies.

The primer labels presented correspond to those listed in Table III. R1 and R2 were two unique restriction sites flanking the mutated site and they were used for the later cloning procedure. I. Direct extension. The deleted sequence is shown by the broken circle, primer 'a' was the mutagenic oligo which contained restriction site R1 and the deletion. II. Overlap extension. The deleted sequence is shown as the thick bar in the middle, the solid and broken lines are the template sequences on either side of the deletion site. Primers 'b' and 'c' were designed such that their 5' ends were complementary to the template sequence on one side of the deletion and their 3' ends were complementary to the template sequence on the other side of the deletion. The first step PCR products AB and CD thus overlapped at the deletion site.

which hybridized at each end of the target sequence, and an internal complementary pair 'b' and 'c' that hybridized to either side of the desired site of the mutation and contained the desired deletion. The first stage PCR involved separate amplification of the *oprD* gene with primers a/b or c/d, yielded two fragments AB and CD, which overlapped with one another. These PCR products were mixed and the second PCR utilizing primer a/d, involved extension of the overlap and, resulted in the mutant product (Fig. 6B).

To design primers, the PCGENE program was used to minimize the chance of non-specific binding and primer-dimer interactions. For the mutagenic primers, at least 20 nucleotides from each side of the deletion site were included.

2. Construction of pMBK19R and pMBE19R.

Plasmids pMBK19R and pMBE19R were derivatives of pBK19R and constructed as follows. Plasmid pTZ19R was digested by *SalI* and *HindIII* and, the resultant large fragment was blunt ended by Klenow fragment and then self-ligated to form plasmid pMTZ19R. This procedure eliminated the restriction sites *SalI*, *PstI*, *SphI* and *HindIII* in the multiple cloning site. The 2.1-kb *BamHI/KpnI* fragment from pBK19R containing the *oprD* gene was cloned into pMTZ19R to form pMBK19R (Fig. 7), which was used as the template for the mutagenesis of the predicted loops L3 to L8 of OprD. The 1.2-kb *BamHI/EcoRI* fragment from pBK19R containing N-terminal of the *oprD* gene was cloned into pMTZ19R to construct

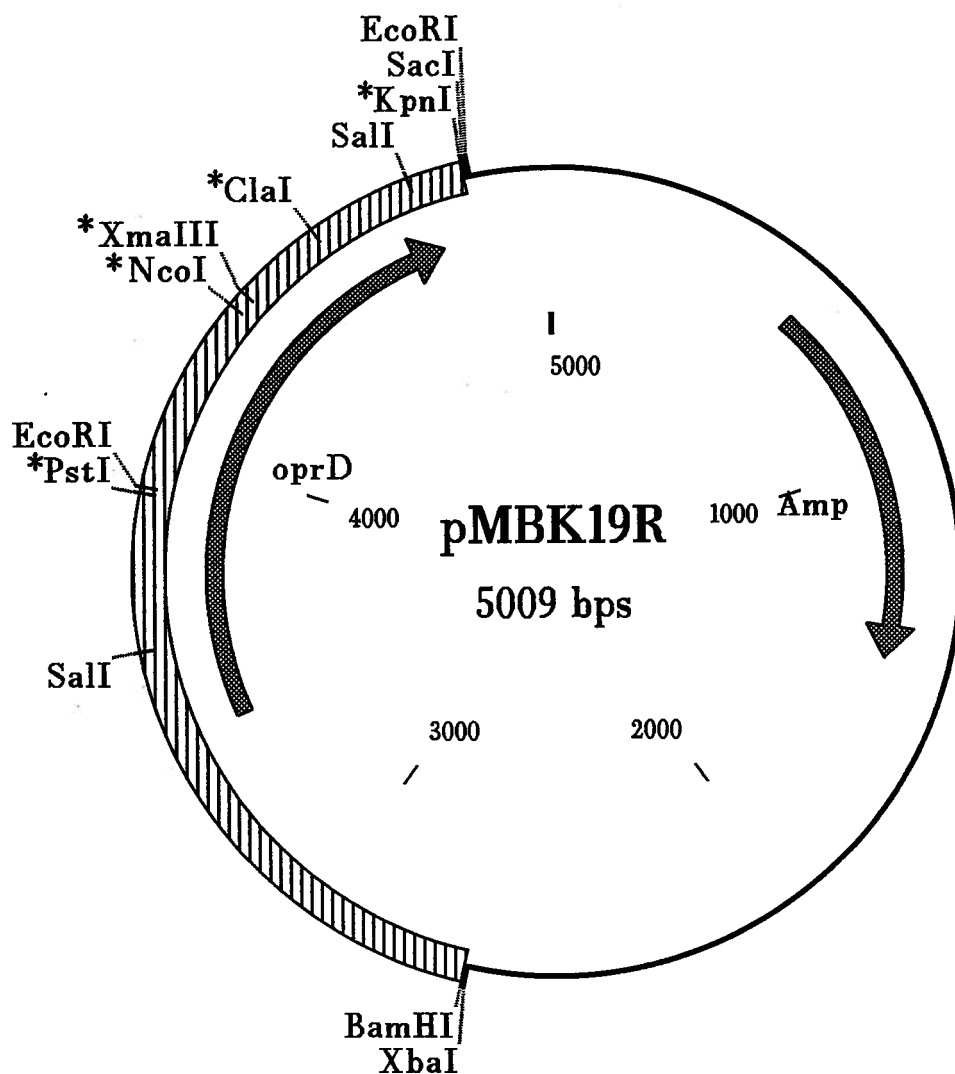


Figure 7: Diagram of plasmid pMBK19R.

The hatched bar represents the 2.1-kb *Bam*HI/*Kpn*I fragment containing the *oprD* gene coding region. The position and orientation of *oprD* and the ampicillin-resistance marker are indicated by the stippled arrows. The restriction sites labelled with asterisks were the unique sites utilized for the PCR-cloning mutagenesis of the predicted loops L3 to L8 (Table III).

pMBE19R (Fig. 8), which was used as the template for the deletion mutagenesis of predicted loops L1 and L2.

3. Polymerase Chain Reaction

The reaction mixture (total volume 50 μ l) contained: 5 μ l of 10 x Vent reaction buffer, 400 μ M each dNTPs, 10 ng DNA template, 1 μ M of each primer, and 2 units of Vent polymerase (New England Biolab, Beverly, MA). The reactions were carried out for 20 cycles using a DNA thermal cycler (Ericomp Inc.). Each cycle included a heat denaturation step at 94 °C (1 min), followed by annealing of the primer at 50-55 °C (2 min) and primer extension at 72 °C (1-1.5 min).

The PCR strategy, oligonucleotide primers, DNA template, and restriction sites used for the mutagenesis of each of the predicted loops are listed in Table III.

L. Whole Cell Lysate.

Cells from a 1.5 ml overnight culture were harvested and resuspended in 100 μ l TE (10 mM Tris-Cl, 1 mM EDTA) containing 1 mM phenyl methyl sulfonyl fluoride (PMSF). The cell suspensions were frozen on dry ice followed by thawing at 37°C for three times. The cell lysate was thoroughly sonicated for 5 min and then centrifuged for 5 min, 5 to 10 μ l of supernatant was heated at 90 °C for 10 min in solubilization-reduction mix (Hancock and Carey, 1979) and run on SDS-PAGE.

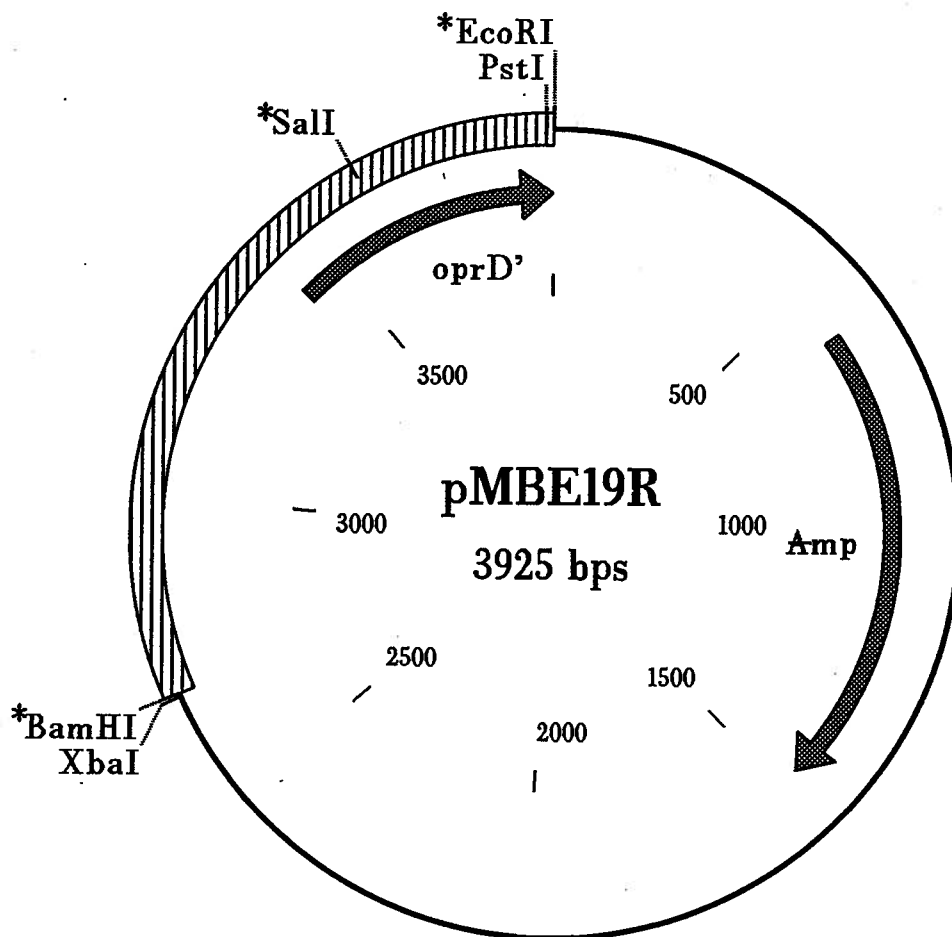


Figure 8: Diagram of plasmid pMBE19R.

The hatched bar represents the 1.2-kb *Bam*HI/*Eco*RI fragment containing the N-terminal coding region of the *oprD* gene. The position and orientation of the incomplete *oprD* gene and the ampicillin-resistance marker are indicated by the stippled arrows. The restriction sites labelled with asterisks were the unique sites utilized for the PCR mutagenesis of the predicted loops L1 and L2 (Table III).

Table III: PCR-based site specific deletion mutagenesis.

Predicted loops	Mutagenesis strategy ^a	Primers for PCR ^b	PCR template	Cloning sites
1	I	1-a: CACACAGGAAACAGCTATGACCATG (reverse primer) 1-b: 930CCAGTGGAC ^c GCGGTCCCCGCTGCCCGT ₉₀₄₋₈₇₉ GTTGCCGGAGCAGCAGGTCGGAG ₈₅₉	pMBE19R	<i>SalI/BamHI</i>
2	II	2-a: 853AGCAGCCTCGACCTGCTGCTCCGC ₈₇₆ 2-b: 1098GCTGTAGTCATCGCGGGCTT ₁₀₇₈₋₁₀₅₃ GCCGGTCCCGGTCTTGTTCGGA ₁₀₃₃ 2-c: 1033TCCGACAAGACCGGCACCCGGC ₁₀₅₃₋₁₀₇₈ AAGCCGGCGGATGACTACAGC ₁₀₉₈ 2-d: CGTTGTAAACGACGGCCAGT (universal primer)	pMBE19R	<i>EcoRI/SalI</i>
3	I	3-a: 1219GGCTTCCAGCTGCAGAGCAGC ₁₂₃₉₋₁₂₆₄ GCAAGCCACITTCACCCGAGGGC ₁₂₈₄ 3-b: 1280TGGGCCAGAGCCGTTGGGGCCGAA ₁₂₅₇	pMBK19R	<i>PstI/NcoI</i>
4	II	4-a: 1189GGCAGCCGCCCTGTTCCCGCAGACCC ₁₂₁₂ 4-b: 1422GAGTTCGGCGCCGTACAGGGA ₁₄₀₂₋₁₃₈₉ ATCGGTGATTGCGTAGCGGGCC ₁₃₆₉ 4-c: 1369GGCCGCTACGCAATCACCGAT ₁₃₈₉₋₁₄₀₂ TCCCTGTACGGCCCGGAAC ₁₄₂₂ 4-d: 3-b	pMBK19R	<i>PstI/NcoI</i>
5	II	5-a: 1372CGCTACGCAATCACCGATAACCTC ₁₃₉₅ 5-b: 1576CCAAGTGGTGTGCTGATGTC ₁₅₄₆₋₁₅₂₁ GTTTGTCCGGTAGATGTTGAA ₁₅₀₁ 5-c: 1501TTCAACATCTACCGCACAAAC ₁₅₂₁₋₁₅₄₆ GACATCAGCAACACCACITGG ₁₅₇₆ 5-d: 3-b	pMBK19R	<i>PstI/NcoI</i>
6	I	6-a: 1645GATTATATCGGCTTCGGCCGC ₁₆₆₅₋₁₆₇₈ GCAGGTGGCGACTCGATTTC ₁₆₉₈ 6-b: 1684GTAGTTCCTATAGCCGACGTTGTT ₁₆₆₁	pMBK19R	<i>XmaIII/ClaI</i>

con't...

Table III: PCR-based site specific deletion mutagenesis (con't).

Predicted loops	Mutagenesis strategy ^a	Primers for PCR ^b	PCR template	Cloning sites
7	I	7-a: <u>1828</u> AAGGACATCGA <u>1848-1873</u> AAGAACTACGGCTACGGCGAG ₁₈₉₃ 7-b: universal primer	pMBK19R	<i>Clal/KpnI</i>
8	II	8-a: <u>1800</u> GACTTTCATGGTCCGTATATCAA ₁₈₂₃ 8-b: <u>2040</u> GATCAGGGCGGAACCTGTTCTG ₁₉₉₅₋₂₀₂₀ GGCACGGTGCCAGGCCTGGCG ₁₉₇₅ 8-c: <u>1975</u> CGCCAGGCCTGGCACCCGTGCC ₁₉₉₅₋₂₀₂₀ CAGAAACGAGTTCCCGCCTGATC ₂₀₄₀ 8-d: universal primer	pMBK19R	<i>Clal/KpnI</i>

- a. Strategy I was direct extension, strategy II was overlap extension.
- b. The labels, a, b, c, d, correspond to the labels in Figure 6. All oligos are listed from 5' to 3' end. Position 1 was the start site of *BamHI* on pBK19R, the number was the nucleotide position on the template. All of the primers with numbers in the middle were the mutagenic primers, where the numbers indicate the corresponding nucleotides from the template that were omitted in the oligonucleotide.
- c. Underlined nucleotides were the restriction sites built into the oligonucleotide.

M. Trypsinization Studies

OprD variants in *P. aeruginosa* outer membrane samples were digested using trypsin (TPCK treated, Sigma) at a concentration of 1 mg/ml, in 10 mM Tris-Cl (PH 8.0) at 37 °C for 1 hour. Untreated samples were incubated in the same conditions except that trypsin was omitted. Proteolysis was stopped by heating at 90 °C for 10 min in solubilization-reduction mix (Hancock and Carey, 1979). The trypsinized samples were run on SDS-PAGE and analyzed by Western-immunoblot with anti-OprD polyclonal antibody.

N. Black Lipid Bilayer analysis.

The techniques and instrument for this procedure were detailed by Benz and Hancock (1981) and Benz et al. (1985). The apparatus included a Teflon chamber divided into two compartments by a Teflon wall that contained a small hole (0.1 mm for single channel conductance experiments; 2 mm for macroscopic conductance experiment). Electrodes dipped into the aqueous solution on both sides of the hole. A membrane was formed across the hole by painting a solution of 1.5% (w/v) oxidized cholesterol in *n*-decane. Bilayer formation was indicated by the membrane turning optically black to incident light.

1. Single Channel Conductance.

For single channel conductance measurements, one electrode was connected to a millivolt voltage source. The other was connected to a Keithley 427 current amplifier to boost the output 10^9 -fold, a Tektronik 5111A storage oscilloscope to monitor the amplified output, and a chart recorder (Huston Instrument). Purified OprD was diluted at least 1000 times in 0.1% Triton-X100 and 5 μ l was added to one side of the chamber. For each experiment, more than 100 events were recorded.

2. Macroscopic Conductance Experiment.

For macroscopic conductance experiments and zero-current potential measurements, one electrode was again connected to a voltage source while the other was connected to a Keithley 610C electrometer. The experiment was initiated by adding 5 to 10 μ l of 1:10 diluted purified OprD to the bathing solution (1.0 M KCl) on either side of the lipid bilayer membrane. The increase in conductance (measured as current increase) was followed until the rate of increase had slowed down considerably. At this time membrane conductance had increased by 2 to 3 orders of magnitude. The bathing solutions in both compartments of the chamber were stirred gently (approx. 60 rev./min) with a magnetic stir bar and aliquots (60 μ l) of imipenem solution (20 μ M) were added carefully to both compartments. Sufficient time (usually 2 min) was allowed for the new current level to be established before addition of the next aliquots.

3. Zero-Current Membrane Potential.

The experiment was initiated exactly as described above for macroscopic conductance experiment using a bathing solution of 0.1 M KCl. After the membrane conductance had increased two orders of magnitude, the applied voltage was turned off and the Keithley 610 electrometer switched to measure voltages. Aliquots (60 μ l) of 3 M KCl solution were added to the compartment on one side of the membrane (the concentrated side) and equal aliquots of 0.1 M KCl solution were added at the same time to the other side. The solutions in the compartments were stirred (approx. 120 rev./min) to allow relatively rapid equilibration. The concentration gradient of KCl across the membrane provided a chemical potential which was the driving force for ion movement. Ions then diffused across the porin channels according to the ion selectivity characteristics of the channel until the voltage caused by preferential one of the ions balanced the chemical potential. At this stage the zero-current potential was measured and fitted to the Goldman-Hodgkin-Katz equation (Benz et al., 1978) to determine the relative permeabilities of anions (P_a) and cations (P_c).

O. Assays.

1. Protein Assay.

Protein concentrations were estimated with a modified Lowry assay

(Sandermann and Stromiger, 1972). A 1 mg/ml solution of bovine serum albumin was used as a standard.

2. Nitrocefin Assay.

Whole cell β -lactamase levels were measured by a nitrocefin assay as previously described by Angus et al. (1982). Briefly, cells of 20 ml cultures were grown to $OD_{600}=0.5\sim 0.8$, harvested and resuspended to the same final OD (1.0) in 10 mM Na-Hepes (PH7.0). 3 ml cell suspension was passed twice through a small French pressure cell at 500 psi. 0.1 ml cell lysate was added to 0.65 ml nitrocefin solution (0.1 mg/ml in Hepes buffer) in a semi-microcuvette, and the kinetics of nitrocefin hydrolysis was monitored at OD_{495} , using a Perkin-Elmer (Lambda 3) dual-beam spectrophotometer coupled to a Perkin-Elmer 561 chart record.

3. Minimum Inhibitory Concentration (MIC) Determination.

To determine the MIC, each strain was grown overnight in Mueller-Hinton medium. Mueller-Hinton or other media agar plates containing serial two-fold dilutions of appropriate antimicrobial agents were inoculated with 10^8 cells in a 10 μ l volume. MICs were determined at least three times and were assessed after 18 h of incubation at 37°C. The MICs were taken as the lowest antibiotic concentration at which cell growth was inhibited. The influence of basic amino acids and

gluconate on imipenem susceptibilities of *P. aeruginosa* strains was determined by using BM2 minimal media containing 20 mM carbon source (glucose or succinate) supplemented with an basic amino acid or glucose or gluconate.

RESULTS

CHAPTER ONE Analysis of Two Gene Regions Involved in the Expression of OprD.

A. Molecular Cloning of the *oprD* Gene.

According to chromosomal restriction mapping, the N-terminus of the *oprD* gene was located between *Bam*HI and *Eco*RI sites, and the expression of OprD could be in either of the 2 directions (Fig. 9B). Since the molecular weight of OprD was 46 kD, the *oprD* gene should be around 1.3-kb. Two fragments were cloned: a 4.0-kb *Eco*RI fragment and a 2.0-kb *Bam*HI/*Kpn*I fragment which should have covered the whole *oprD* gene no matter in which direction the gene was expressed. The 4.0-kb *Eco*RI fragment was cloned into pTZ18R in two orientations, generating plasmids pE37 (correct orientation) and pE65 (inverse orientation), meanwhile, the 2.1-kb *Bam*HI/*Kpn*I fragment was cloned into pTZ18R and PTZ19R, giving rise to pBK18R (inverse orientation) and pBK19R (correct orientation) (Fig. 10) respectively.

B. Overexpression of the *oprD* Gene in *E. coli* CE1248.

Expression studies with the various subclones were performed in *E. coli* CE1248, a mutant which lacks the major *E. coli* porins OmpF, OmpC and PhoE. Plasmids pBK18R, pBK19R, pE37 and pE65 were transformed into *E. coli* CE1248

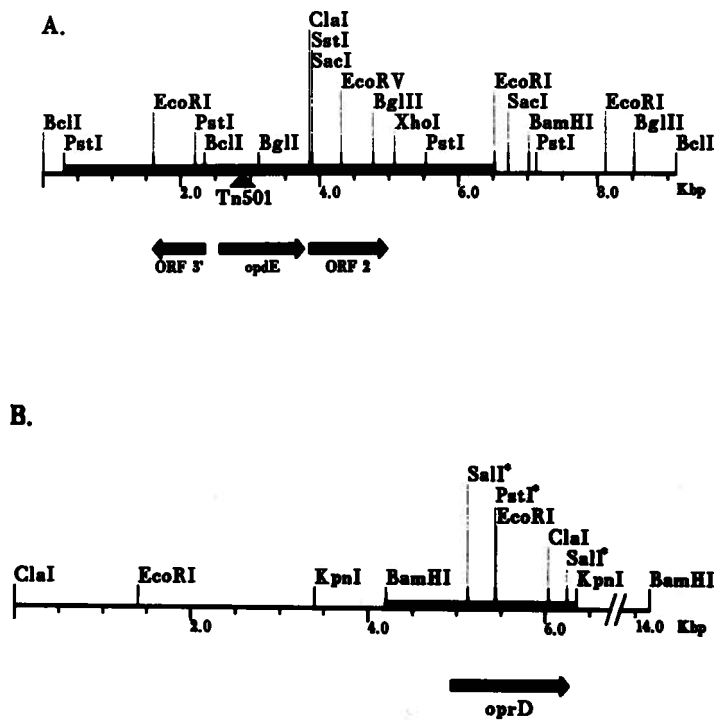


Figure 9: Restriction endonuclease maps of *P. aeruginosa* PAO1 strain H103 chromosomal DNA derived by Southern hybridization.

(A) Map of the region surrounding the insertion site of Tn501 (marked by solid triangle) in strain H673, thick bar indicates DNA cloned in pD2-45. (B) Map of the region surrounding the *oprD* gene, thick bar indicates DNA cloned in pBK19R. Asterisks indicate restriction sites discovered by DNA sequencing only.

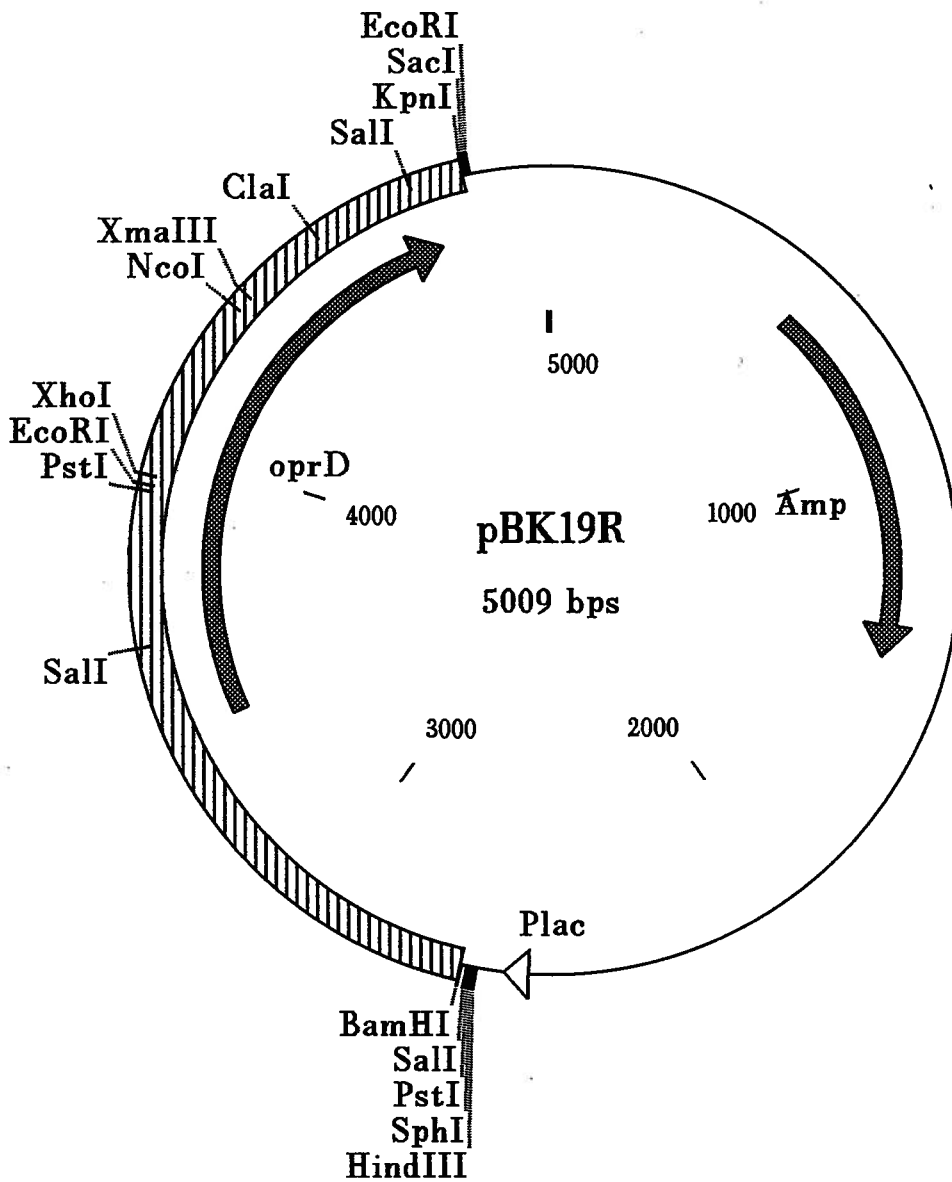


Figure 10: Diagram of pBK19R.

The hatched bar represents the 2.1-kb *Bam*HI/*Kpn*I fragment containing the *oprD* gene coding region. The position and orientation of the *oprD* gene, *lac* promoter and ampicillin-resistance marker are indicated.

and the transformants were grown on LB medium with 1 mM isopropyl- β -D-thiogalactopyranoside (IPTG) to induce the high expression of *lac* promoter adjacent to the insert.

E. coli CE1248(pBK19R) carrying the 2.1-kb *Bam*HI/*Kpn*I fragment cloned in the same orientation as the *lac* promoter revealed expression in *E. coli* of a outer membrane protein migrating with the same mobility as OprD, and the expression level was almost equivalent to that of the *E. coli* major outer membrane protein OmpA (Fig. 11, lanes 5 & 6). When cloned in the reverse orientation to the *lac* promoter in pBK18R, only weak expression was observed (Fig. 11, lane 8), suggesting that the cloned *Bam*HI/*Kpn*I fragment contained an *oprD* gene promoter that could be recognized by *E. coli*, and that OprD was weakly expressed from this promoter. *E. coli* CE1248(pE37) and *E. coli* CE1248(pE65) containing the 4.1-kb *Eco*RI insert did not result in production of a band of equivalent molecular weight to OprD (Fig. 11, lane 9 & 10), proving it did not contain the entire gene.

C. Nucleotide Sequencing of *oprD* Gene.

Both strands of the 2.1-kb *Bam*HI/*Kpn*I fragment containing the *oprD* gene were sequenced. Within this fragment, an open reading frame containing 1,329 nucleotides was obtained (Fig. 12). It encoded a 443 amino acid preprotein. Amino acids 24~40 were identical in sequence to the N-terminal sequence obtained from the purified protein, whereas the first 23 amino acids had the features typical of a

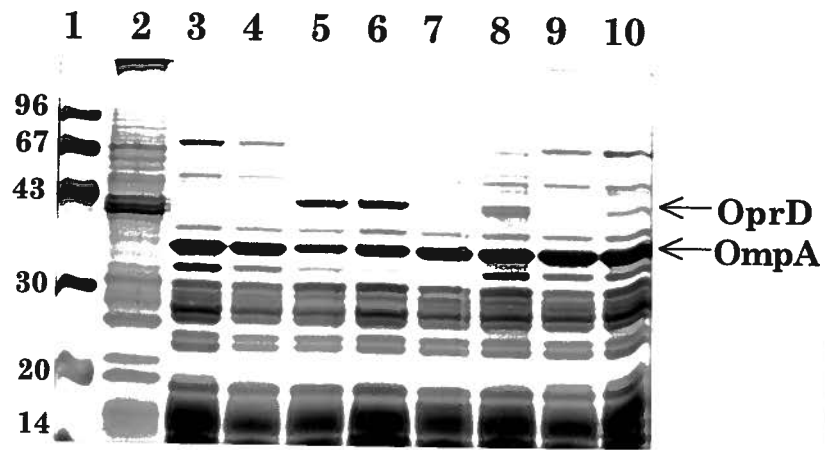


Figure 11: Overexpression of the *oprD* gene in *E. coli*.

SDS-PAGE demonstrating the cloning of DNA fragment influencing the expression of OprD in *E. coli*. Lanes: 1, molecular weight marker; 2, H636; 3, CE1248; 4, CE1248(pTZ19R); 5 & 6, CE1248(pBK19R); 7, CE1248(pTZ18R); 8, CE1248(pBK18R); 9, CE1248(pE37); 10, CE1248(pE65). IPTG was added to all *E. coli* cultures to induce expression from the *lac* promoter.

```

GGATCCAAAGCGAACATACTGACCTCTCCTGTTCCGACCGTCTGTTATGGACAGCTTAGCCCTCCCTCCGGGAAGGGCCCGCGTAAGTCCGCGCAG 99
GATACTTCGCGCCCGGCCAAAGCAAGCCACACATCCGCCCGCCAGCTTGGCGCGCTCTCCAGCCGAACGCCCATAGATGCCGGCCAATGAA 198
TACAGCGCGACGCCGAACATAAGACATGCCGTGGATACAAACGCATTGCCACAGACAACTCGATGGCAACCAACCCTTGAAGCAGACGGATTACAATC 297
AGGTTTCAAAGCATAATTCGTTTGCTTTCAAACAGAATAGCCTCGCTCTCGAAGAGACCAACTGGAATACATAGGCGAAGCCATTTTCCAATTTGTGCA 396
CGGAGTTTGCTTATACCTCTTTTATCACAGTAAGAGGGCCGTACGGAACATGACATTTTTATTACAAGGCCCGCCAATCGGGAAAAGCGACTTGAGA 495
AGCGACCTCAACAAGAGTGACCAACCCCGCAGACATACGTCAATTTTTTCAACTGCGCACCTACGCAGATGCGACATGCGTCATGCAATTTTGCAGACGA 594
CGGTAAGAATCCGTCGCTTCGGAACCTCAACTATCGCCAAGAAACACTGCGTGTATAAGTTAGCGCCGACAAGAAGAACTAGCCGTCAGTCCGCGCAC 693

TGTGATGGCAGAGATAATTTCAAACCAAAGGAGCAATCACAATGAAAGTGATGAAGTGGAGCGCCATTGCACTGGCGGTTTCCGAGGTAGCACTCAG 792
----- M K V M K W S A I A L A V S A G S T Q 19
TTGCGCGTGGCCGACGCATTTCGTGAGCGATCAGGCCGAAGCGAAGGGTTTCATCGAAGACAGCAGCCTCGACCTGCTGCTCCGCAACTACTATTTCAAC 891
F A V A D A F V S D Q A E A K G F I E D S S L D L L L R N Y Y F N 52
CGTGACGGCAAGAGCGGCAGCGGGGACCGCGTGCAGTGGACCAAGGCTTCTCACCACCTATGAATCCGGCTTACCCAAGGCACTGTGGGCTTCGCG 990
R D G K S G S G D R V D W T Q G F L T T Y E S G F T Q G T V G F G 85
GTCGATGCCTTCGGCTACCTGGGCTGAAGCTCGAGCGCACCTCCGACAAGACCGGCACCGGCAACCTGCCGGTGATGAACGACGGCAAGCCGCGCAT 1089
V D A F G Y L G L K L D G T S D K T G T G N L P V M N D G K P R D 118
GACTACAGCCGCGCCGGCGCGCGTGAAGGTGCGCATCTCCAAGACCTGCTGAAGTGGGGCGAGATGCAACCGACCGCCCGGCTTCGCGCGTGGC 1188
D Y S R A G G A V K V R I S K T M L K W G E M Q P T A P V F A A G 151
GGCAGCCGCTGTTCCCGCAGACCGCGACCGGCTTCCAGCTGCAGAGCAGGAATTCGAAGGGCTCGACCTCGAGGCGAGGCCACTTACCCGAGGGAAG 1287
G S R L F P Q T A T G F Q L Q S S E F E G L D L E A G H F T E G K 184
GAGCCGACCACCGTCAAATCGCGTGGCGAAGTCTATGCCACCTACGAGGCGAGACCGCAAGAGCGCGGATTTTCATTGGGGGCGCTACGCAATCACC 1386
E P T T V K S R G E L Y A T Y A G E T A K S A D F I G G R Y A I T 217
GATAACCTCAGCGCTCCCTGTACGGCGCGAAGTCTGAAGACATCTATCGCCAGTATTACCTGAACAGCAACTACCCATCCCCTGGCATCCGACCAA 1485
D N L S A S L Y G A E L E D I Y R Q Y Y L N S N Y T I P L A S D Q 250
TCGCTGGGCTTCGATTTCAACATCTACCGCACAAACGATGAAGGCAAGGCCAAGGCCGCGACATCAGCAACACCCTTGGTCCCTGGCGCGAGCTAC 1584
S L G F D F N I Y R T N D E G K A K A G D I S N T T W S L A A A Y 283
ACTCTGGATGCGCACACTTTCACCTTGGCCTACCAGAAGGTCCATGGCGATCAGCCGTTTATTATATCGGCTTCGGCCGCAACGGCTCTGGCGCAGGT 1683
T L D A H T F T L A Y Q K V H G D Q P F D Y I G F G R N G S G A G 316
GGCGACTCGATTTTCTCGCCAAGTCTGTCCAGTACTCCGACTTCAACGGCCCTGGCGAGAAATCCTGGCAGGCTCGCTACGACCTGAACCTAGCTCC 1782
G D S I F L A N S V Q Y S D F N G P G E K S W Q A R Y D L N L A S 349
TATGGCGTTCGCGGCTGACTTTCATGGTCCGCTATATCAATGGCAAGGACATCGATGGCACAAGATGTCTGACAACAACGTCGGCTATAAGAACTAC 1881
Y G V P G L T F M V R Y I N G K D I D G T K M S D N N V G Y K N Y 382
GGCTACGGCGAGGATGGCAAGCACCCGAAACCAACCTCGAAGCCAAGTACGTGGTCCAGTCCGGTCCGGCCAAGGACCTGTCGTTCCGCATCCGCCAG 1980
G Y G E D G K H H E T N L E A K Y V V Q S G P A K D L S F R I R Q 415
GCCTGGCACCGTGGCAACGCGACCGAGGGCGAAGGGCAGCAGAACGAGTTCCGCCTGATCGTCGACTATCCGCTGTCGATCCTGTAATCGACCGACAGG 2079
A W H R A N A D Q G E G D Q N E F R L I V D Y P L S I L * 443
CAACGAAAAAACCCGGCATCGCGGGTTTTTTCTTCTTGGCGGCAACGCGCTATAAAGGAAGGGCGTAGGTACCGAGCTCGAAT 2164
-----

```

Figure 12: Nucleotide and the deduced amino acid sequence of the *oprD* gene.

The sequence is oriented in the same orientation as the map in Figure 9B and goes from the *Bam*HI site to the rightmost *Kpn*I site. A typical Shine-Dalgarno sequence appears between nucleotides 723-726 while a predicted terminator stem-loop appears between nucleotides 2084-2112 (underlined with a dashed broken line). The accession number in the EMBL data library for this sequence is Z14065.

bacterial signal sequence :

M K V M K W S A I A L A V S A G S T Q F A V A

|→ Polar ←| |→Hydrophobic core ←|

The 420 amino acid sequence of the mature protein predicted certain typical features observed for other outer membrane proteins including an overall negative charge and a typical amphipathicity plot with alternating hydrophobic and hydrophilic stretches (Siehnel et al., 1990)

The GC content of the whole gene was 61%, and at the third codon position, it reached 81.8%, which are features typical of a *P. aeruginosa* gene. The 6 nucleotides AAGGAG which were 8 bp upstream of the starting codon ATG were a typical bacterial Shine-Dalgarno sequence, whereas the 29 nucleotides 16 bp downstream from the stop codon TAA could form a hairpin structure and function as a transcriptional terminator (Fig. 12).

An attempt was made to match the putative OprD sequence to other outer membrane protein sequences obtained from *P. aeruginosa* and to the OmpF and TolC porins from *E. coli*, using the method of Needleman and Wunsch (1970) with a bias parameter of 0 and a gap penalty of 4 with 10 random runs. The alignment scores obtained were 1.4, -0.5, 1.4, 2.6 and 1.1 for *P. aeruginosa* OprF, OprH, OprP and *E. coli* OmpF and TolC, respectively. Although OprD showed the highest homology to OmpF, none of these scores were considered significant above 3 standard deviations.

D. Nucleotide Sequencing of the *opdE* Gene.

In an attempt to mutagenize the *oprD* gene, strain H673 *opdE*::Tn501 was isolated by Howard Meadows in our laboratory. The MIC of imipenem for H673 was 12 µg/ml, whereas the MIC for the parent strain H103 was 1.5 µg/ml, and SDS-PAGE of outer membrane preparations revealed that HM2 was OprD-deficient (data not shown). The region of the chromosome equivalent to that surrounding the transposon insertion site was cloned by Eileen Rawling and Richard Siehnel from the parent strain H103 into vector pRK767, to create plasmid pD2-45 containing a 6-kb *EcoRI/PstI* fragment. When mobilized back into strain H673 by triparental mating by Francis Bellido, pD2-45 was able to complement this strain to imipenem susceptibility (MIC=1.5 µg/ml) and OprD deficiency (data not shown).

It was first assumed that the OprD gene had been cloned. However the sequencing of 3931 base pairs of DNA surrounding the site of transposon insertion failed to reveal a sequence corresponding to the N-terminal amino acid sequence of OprD, and no open reading frame equivalent to an outer membrane protein (i.e. containing a signal sequence) was predicted. In addition, no new protein bands were observed in *E.coli* containing plasmid pD2-45. Furthermore an N-terminal specific oligonucleotide failed to hybridize to plasmid pD2-45 and indeed hybridized with sequences in the *P. aeruginosa* chromosome with an entirely different restriction pattern (Fig. 9).

The DNA sequenced predicted 4 large open reading frames (Fig. 13), 3 of

GAATTCTCTTCGGGGAGCCAGGCGATTCCCAGCCCCGCCAGCGCGCATCCACGATATTCGGCGAGGTGTTGAAAATGAGCTGTCCATCGACACGGAC 99
 F E E E P L W A I G L G A L A A D V I N P S T N F I L Q G D V R V 33
 GTTACAGTGTGCATCTTCCGCTGAAAATCCCAGGCATACAGGCCCGCCGCGACTGCATGCGCATGTTGATGCAGTTGTGGTCGACCAGATCGCGAGG 198
 N V H R D K R Q F D W A Y L G G G S Q M R M N I C N H D V L D R P 66
 ACTCCTGGGCTTCGGATGTGCCCAAAGTAGCCGGGGCCGCGACGCCCATGCGCACTGGCGGCCAATCGGCACGGCGATCATGTCTTGTCTAT 297
 S R P K P H A A F Y A P A A V V A M R V P P G I P V A I M D K D I 99
 GGTGTGCCCCAGGCGTACGCCGGCATCGAACCGGTGCGCCACGATGTCCGAAAAGCCATAGTTGATGTCGAACTCCACCTTGATGTCTGGATATCCAG 396
 T D G L R V G A D F R D A V I D R F G Y N I D F E V K I D P Y E L 132
 CAGCAACGGGGTGAGCCTGGGTAGCAACAGGGTTCGCTGGATGTGATCGCCACAGGTAATGCGAACCGTGCCACTTGGTTGTGCGCGACGCCGACAG 495
 L L P T L R P L L L T R Q I H D G C T I R V T G S P K D R L A S L 165
 CTCGTCCAGTTCGGCTCGATCTCGTGAAGCGATTGCCGATGGCATTCAACAGGCGCTCCCTGCCCGTGGGCGAAAACGCTGCGGGTGGTGGCGGT 594
 E D L E A E I E D F R N G I A N L L R E G A A T P S V S R T T R T 198
 GAGTAAGCGGATCTGCAGGCGCGCTCCAGGCCGCTTATCGACTGGCTCAATGCCACTGCGTCACGCCAGTGGGCGGCGCACGGGTGAAGTTCC 693
 L L R I Q L R A E L G S I S Q S L A S Q T V G L Q A A A R T F T G 231
 CTCGCGGGCGACGGCAACGAAGGACAGGAGGTCGTTGAGGTTACGTTTATCATGATGCGCAATTCTTCCACGGACCATTAATTAGTAGAGCTTATATACC 792
 E R A V A V F S L L D N L N R K I M ---ORF3 251
 ATTAAGAATTGTTAGTAGTAACAGGCCCGCCATACCCGAATTCATTGCAACAATCATCTCCGCTACCGCACCTGACTTCCCTCCCTGCCG 891

ACTCAGCCAGGCGTTTGTACCAGCGGAGCTGATCTCTTCTTTCACTCTTTGGATAAGCCGTTTTTTCATGACAACCCGCGCACTCGATACCCCA 990
 opdE---- M T T R A L D T A 263
 ACGAAAACCTGAACAATCGGGCTCCTGGAGTGGCGTCTGGCATTGCGGTTTGGCGCTTCGCACTGGTCGCGTGGAGTTCCTGCCGTCAGCCTGC 1089
 N E N P E Q S G S W S G V L A I A V C A F A L V A S E F L P V S L 296
 TGACTCCCATCGCAACGACCTGGGAACCTACCGAGGGCATGGCAGGCCAGGGCATCGCCATCTCCGCGCCTTCGCCGTTTTAACAGCCTGTTCA 1188
 L T P I A N D L G T T E G M A G Q G I A I S G A F A V L T S L F I 329
 CATCCGTTGCCGGCAGCCTGAACCGCAAGACGCTGTGCTGGGACTGACGGCGGCAATGGGCATGTCCGGCGCAATCGTCGCGCTCGCGCCAACTATT 1287
 S S V A G S L N R K T L L L G L T A A M G M S G A I V A L A P N Y 362
 TCGTCTACATGCTGGCGCGGCGCTGATCGGCATAGTGATCGGCGGCTTCTGGTCGATGTCGCGCAGCCAGGCCATGCGCCTGGTGCCTGCCAACGACG 1386
 F V Y M L G R A L I G I V I G G F W S M S A A T A M R L V P A N D 395
 TGCCGCGAGCCTGCCCTCGTCAATGGCGGCAACGCTCTGGCGACAGTGGTGGCGCGCGCTGGGCGCCTGGTAGGCACCTCATCGGCTGGCGAG 1485
 V P R A L A L V N G G N A L A T V V A A P L G A W L G T L I G W R 428
 GGGCTTTTCTGCGCTGTGCGCGTAGCCCTGGTGGCACTGGCTGGCAATGGACCACCTGCCCTCCATGCGGGCGCGCGCGTCTCCGCGCCGG 1584
 G A F L C L V P V A L V A L A W Q W T T L P S M R A G A R A P G P 461
 GCAATGTGTTACGGTATTTCGCTGCTCAAGCGTCCGGTGTGATGCTCGGCATGCTCGCCAGCAGCCTGTTCTTCATGGGCGAGTTTTCCCTGTTCA 1683
 G N V F T V F A L L K R P G V M L G M L A S S L F F M G Q F S L F 494
 CCTATGTGCGACCATTCCTGGAGACGGTACCGCGGTACATGGCGCGCATGTTTCGCTGGTACTGCTGGTATCGGTGACGCGGGCTTTATCGGCACCC 1782
 T Y V R P F L E T V T G V H G A H V S L V L L V I G A A G F I G T 527
 TGCTGATCGACCGGTTCTGCAACGGCGCTTCTCCAGACACTGGTCCGATCCCGTTCGCTGATGGCCCTGATCGCCCTGGTACTGACGGTCTTGGCG 1881
 L L I D R V L Q R R F F Q T L V A I P L L M A L I A L V L T V L G 560
 GCTGGCCCGCATCGTTGTCGCTGCTCGGATTGTGGGACTGACCGGTACCTCGGCCCGCTCGGTTGGTGGGCTGGATCGCCAGGGTGTCCAG 1980
 G W P A I V V V L L G L W G L T G T S A P V G W W A W I A R V F P 593
 AGGACGCCGAAGCCGGTGGCGGCTGTTGTCGCGGTGGTCAACTCTCCATTGCCCTGGGCTCCACATTGGGTGGTCTGCTGTTGATCGCACTGGCT 2079
 E D A E A G G G L F V A V V Q L S I A L G S T L G G L L F D R T G 626
 ATCAGGCGACCTTCTTCCAGCGCGCGATGCTGCTGATCGCAGCCTTCTGACCATCTCACCAGCAGCTCGAAAAGCCCCGGCGGTAGACCCCGG 2178
 Y Q A T F F A S A A M L L I A A F L T I L T A R S K A P A G * 656
 GAACGCCCGGACGCGACTTGCCTCGCGCCCCAGGCCAGGTCGTCGAGCCGAATCCCACCACGTCGATCTGATCGATGGAGAAGCCATGGAACCAAGC 2277

ORF2---- M E N A M E T K 666
 ACAGCAATCGAGCTCGCTCTCCAAAGGGTCCCTGAGGGGCGCAGTCTTCCCGGTGCGCTGATGGCTCTCGTGGCTGCCAGACAGTCCGGCGGCAA 2376
 H S N R A R S P K G A L R G A V L A G A L M A L V G C Q T S P A A 699
 CGACTTCGTCAAACACCGGAGGAACCAACATGCAGCTGCAATTGACCCAGGAGTGGGACAAGACCTTCCCTGAGCGCAAAGGTGCAACATCCCAAG 2475
 T T S S N T G G T N M Q L Q L T Q E W D K T F P L S A K V E H P K 732
 TCACCTTCGCCAATCGCTACGGCATCACCTGGCAGCTGACCTGACCTGCCGAAGAACCCTGGCGGCGATCGGCTGCCGGAATCGTGTGCGGCGTC 2574
 V T F A N R Y G I T L A A D L Y L P K N R G G D R L P A I V I G G 765
 CGTTCGGCGGGTCAAGGAGCAGTCTCCGACTGTATGCGCAAACCATGGCCGAACCGGATTGTCACGCTGGCGTTCGACCCATCGTATACCGGTG 2673
 P F G A V K E Q S S G L Y A Q T M A E R G F V T L A F D P S Y T G 798

```

AGAGCGGGGTCAGCCACGCAACGTCGCTTCGCCGGATATCAATACCGAAGACTTCAGCGCGGCGAGTGGATTTTCATCAGTTTGTGCCGGAAGTGAATC 2772
E S G G Q P R N V A S P D I N T E D F S A A V D F I S L L P E V N 831
GCGAGCGCATCGGCGTCATCGGCATCTGCGGCTGGGGTGGCATGGCGCTGAACGCGGTGGCCGTGGACAAGCGCGTCAAGGCGGTGGTACCAGCACCA 2871
R E R I G V I G I C G W G G M A L N A V A V D K R V K A V V T S T 864
TGTACGACATGACGCGGGTCATGTCGAAGGGCTACAACGACAGCGTGACCCTCGAACAGCGCACGGAACGCTGGAACAACCTGGCCAGCAGCGCTGGA 2970
M Y D M T R V M S K G Y N D S V T L E Q R T R T L E Q L G Q Q R W 897
AGGACGCGGAAAGCGGTACCCCGCCTATCAGCCGCCCTACAACGAACCTGAAGGGTGGTGGGACACAGTTCCCTCGTCCGACTACCAGGACTACTACATGA 3069
K D A E S G T P A Y Q P P Y N E L K G G E G Q F L V D Y H D Y Y M 930
CACCCCGTGGCTACCACCCGCGGCAGTCAACTCCGGTAACGCCTGGACGATGACCACGCGCTGTCTGTTTCATGAACATGCCGATCCTCACCTACATCA 3168
T P R G Y H P R A V N S G N A W T M T T P L S F M N M P I L T Y I 963
AGGAGATCTCGCCACGCCGATCCTGTTAATCCACGGCGAAAGGGCCATTACGCTACTTCAGCGAGACCGCTACGCCGCTGCCGACAGGCAAGG 3267
K E I S P R P I L L I H G E R A H S R Y F S E T A Y A A A A E P K 996
AGCTGCTGATCGTTCGGGAGCCAGTCATGTGACCTGTACGACCGGCTGGACAGGATTCTTTTCGATCGGATTGCCGATTCTTCGACGAGCATCTGT 3366
E L L I V P G A S H V D L Y D R L D R I P F D R I A G F F D E H L 1029
AGCGTCGTGCACGCCAGGGCAACAGCGCGGGAGATTGATTCCGNCCTCCCCCGCTCTGTGCGCACCTCTCCGGCTTTTCCGCGCCAGCGAGG 3465
*
TCCCGCTCCGCTCGAGACCTCGCCCTCCCTGGCACCCCTTCAAGCAACCGCCCGCGGTACGATCCCGTCCACCAACCGCGCAATCCCAATGGG 3564

TTGCCATCCTTCAGCGCTTCGGCAGCAACGCGTCCGGTAGTTCTGGTAGCACACCGGGCGCAGGAAACGGTGCATGACCAGGGTGCCACCAGGTA 3663

CCGCGGGCGTCCGAAGTGACCGGGTACGGNCCACCGTGGACCATCGCGTCGCAGACTTCACACCGGTCCGGTAGCCGTTGAGCAGCAGGCGTCTGCC 3762

TTCTGTTCCAGGAGCGGTACCAGGTCGNCGAAGGACGCCAGGTCTTCGCTTCGGCGATCAGGGTCGCGGTGANCTGCCCGTGCAGCCCATGCAGCGCG 3861

CGCTTCAGTTCGGCGTGGTCCGGCACCTCGACGACCACGCTGGCCGGGCGTTGACTTCTTCTGCAG 3929

```

Figure 13: Nucleotide and the deduced amino acid sequence of the *opdE* gene.

The transposon insertion site from H673 is indicated by a solid triangle after nucleotide 1243. The sequence is oriented in the same direction as the map given in Figure 9A, and goes from the leftmost *EcoRI* site to the third *PstI* site. ORF3 was on the complimentary strand and began at base 747, read to the left and proceeded beyond the beginning of this sequence (no stop codon was encountered but was subsequently identified by sequencing beyond the *EcoRI* site by R. Siehnel). The accession number in the EMBL data library for this sequence is Z14065.

which had a codon usage typical of *P. aeruginosa* genes (>80% G+C in position 3 of codons). One of these open reading frames overlapped the region of transposon insertion in *P. aeruginosa* strain H673 and was thus named *opdE* (for putative regulator of OprD expression). This open reading frame was 402 amino acids long with a predicted M_r of 41,592 (Fig. 13). The sequence was quite hydrophobic, with 61.3% non polar amino acids, 29.4% uncharged amino acids and only 34 charged residues. All secondary structure prediction methods used suggested that this protein was an integral membrane protein containing as many as 12 membrane spanning α -helices. Only 85 nucleotides after the end of the *opdE* gene, another large open reading frame (1110 bp, predicted to encode a 370 amino acid protein) was predicted, whereas a third open reading frame of greater than 747 bp (predicted by single stranded sequencing past the *EcoRI* site to be 978 bp in length) was predicted to be encoded by the other strand (Fig. 13). These sequences, called orf2 and orf3, might also be involved in OprD expression since no obvious terminator appears between *opdE* and orf2, suggesting a potential operon structure. A screen of the EMBL Swiss pro database revealed that the protein encoded by the *opdE* gene was homologous to chloramphenicol-resistance proteins from *Streptomyces lividans* and *Rhodococcus fascian*, and the multidrug-resistance protein EmrB from *E. coli*.

E. Summary.

The *oprD* structural gene was cloned as a sequence homologous to an N-terminal specific oligonucleotide probe. The 2.1-kb *Bam*HI/*Kpn*I fragment, cloned in plasmid pBK19R in the same orientation as the *lac* promoter, revealed high expression of OprD in *E. coli* outer membrane. DNA sequencing predicted an open reading frame containing 1,329 bp nucleotides, which encoded a 420 amino acid mature OprD protein with a 23 amino acid signal sequence. The sequence had certain typical features observed for other outer membrane proteins. In addition, a putative *oprD* regulatory gene *opdE* was sequenced, which predicted a hydrophobic protein of M_r 41,592.

CHAPTER TWO Functional Characterization of OprD: *In vivo* and *In vitro*

A. Introduction.

Previous studies suggested that *P. aeruginosa* OprD is a specific porin for basic amino acids and imipenem (Trias and Nikaido, 1990). Regarding its function in the uptake of carbon sources, it was suggested OprD had significant non-specific permeability to monosaccharides and disaccharides (Yoshihara and Nakae, 1989; Yoshihara et al., 1991). From the literature, there was conflicting data about the function of OprD in the uptake of fluoroquinolone antibiotics. It was shown that some, but not all fluoroquinolone-resistant mutants were also cross resistant to imipenem and lacked OprD. For example, Michea-Hamzhepour et al. (1991) demonstrated that decreased fluoroquinolone susceptibility was associated with a decrease or loss of OprD and proposed that OprD can catalyze the facilitated diffusion of fluoroquinolone as it does for imipenem.

Our previous data indicated two gene regions were involved in the expression of the *oprD* gene. One turned out to be the *oprD* structural gene, and the other region (the *opdE* gene) might encode a protein influencing the expression of OprD. In keeping with this hypothesis, the cloned *oprD* gene in *E. coli* was expressed poorly from its own promoter (Fig. 11, lane 8) and the level of OprD observed in the outer membrane of *P. aeruginosa* was influenced by both the growth medium and carbon source (Hancock and Carey, 1980). However, all the strains, including OprD-defective strains, that had been used in prior studies of the *in vivo* function

of OprD, were genetically undefined, and many were from clinical sources. I believe this was the major cause of unclear and controversial results. This chapter describes the construction of a set of isogenic mutants expressing genetically defined levels of OprD, and utilizing them to further investigate the substrate selectivity of OprD *in vivo*.

Regarding the *in vitro* functions of OprD, very limited work has been done to study the physical properties of OprD in the black lipid bilayer system. Ishii and Nakae (1993) measured the single channel conductance of OprD, which was 20 to 30 pS. In addition, they observed larger channels (400 pS). Furthermore, the ion selectivity of the OprD channel was unknown. In addition, no direct evidence had been obtained from black lipid bilayer studies to prove the presence of a specific binding site(s) for imipenem within the OprD channel. This chapter describes the purification of OprD and a thorough analysis of its *in vitro* functions in the black lipid bilayer system.

B. Construction of a Defined OprD Defective Mutant H729.

The improved method of Schweizer (1992) for allele replacement was utilized to replace the wild-type *oprD* gene in strain H103 with an *oprD::Ω* interposon-mutated gene (see Material and Methods). Southern hybridization of chromosomal DNA with a ³²P-labelled *oprD* gene probe confirmed that in strain H729, the *oprD* chromosomal gene was interrupted by a 1.3-kb *SaII* fragment

containing the Km^R-Ω interposon (Fig. 14). In the Southern blot, a 4.5-kb band was present in both the mutant and parent strains (Fig. 14), indicating there was another gene with high homology to the *oprD* gene in *P. aeruginosa*, which might be the *oprE* gene (Yoshinori et al., 1993). Sodium dodecyl sulfate-polyacrylamide gel electrophoresis (SDS-PAGE) of the outer membrane proteins of H729 confirmed the lack of OprD (Fig. 15, lanes 8, 9).

C. Overexpression of the *oprD* Gene in *P. aeruginosa*

To overexpress the *oprD* gene in *P. aeruginosa*, the *oprD* gene was subcloned into plasmid pUCP19 to form plasmid pXH2, so that the direction of expression of the *oprD* gene was in the same orientation as the *lac* promoter (Fig. 5). Plasmid pXH2 was then mobilized back into the *P. aeruginosa* wild type strain H103 and the *oprF*::Ω mutant strain H636. Since *P. aeruginosa* does not have the *lac* repressor gene, IPTG was not added to the medium. SDS-PAGE of the outer membrane proteins demonstrated that in strain H103(pXH2), OprD was expressed to a level almost equivalent of that of *P. aeruginosa* major outer membrane protein OprF (Fig. 15, lane 4), and in H636(pXH2), OprD appeared to be the predominant outer membrane protein (Fig. 15, lane 7).

Plasmid pXH2 was also transferred into the OprD defective strain H729. The results indicated that the loss of OprD could be complemented and that the *oprD* gene was also overexpressed in H729(pXH2) (Fig. 15, lane 10).

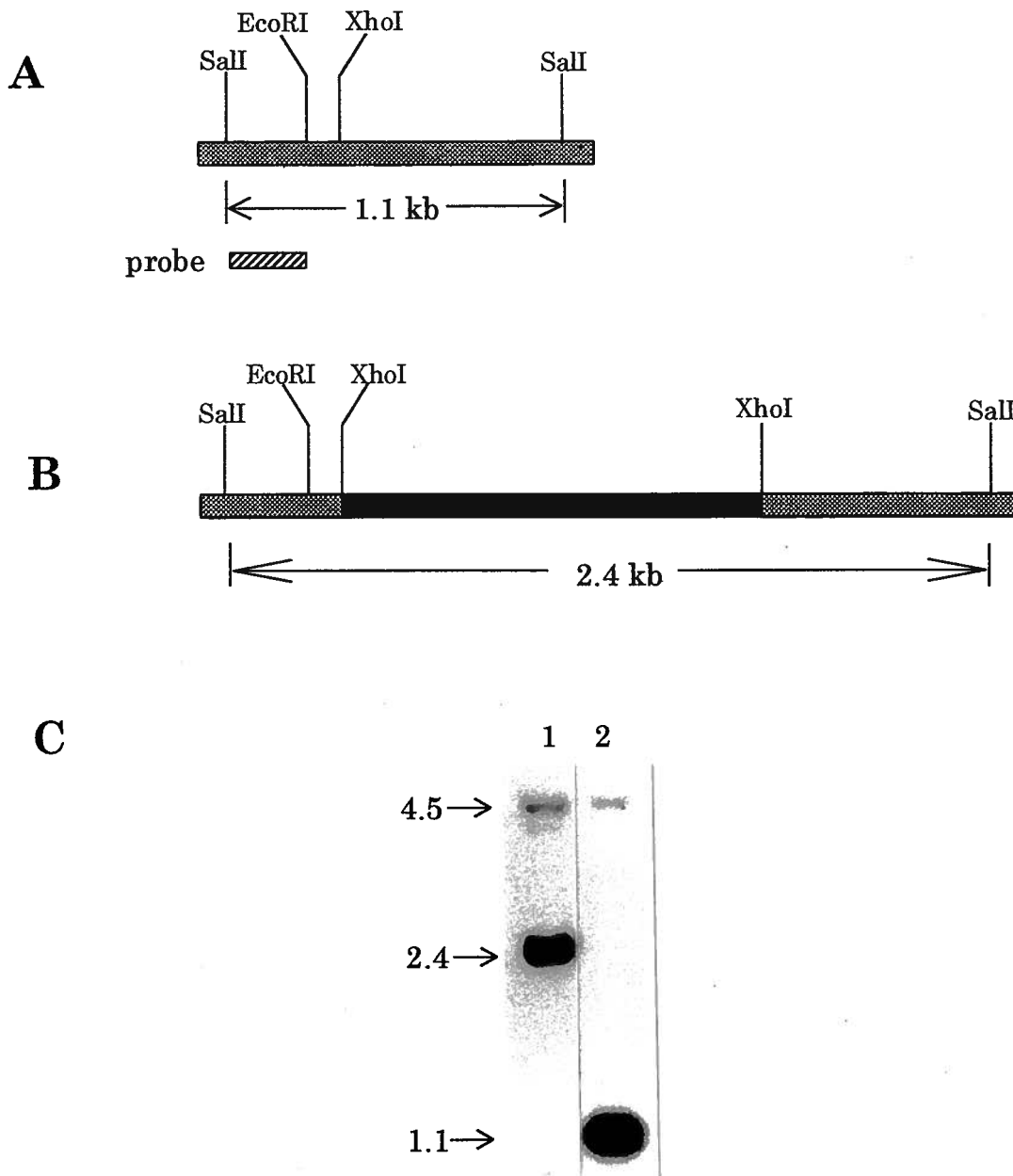


Figure 14: Construction of an *OprD* defective mutant in *P. aeruginosa*.

Genomic Southern hybridization illustrating the interruption of the *oprD* gene (shaded bar) with a kanamycin resistance Ω -interposon (black bar). The physical maps of the wild type (A) and the mutant (B) *oprD* gene region are shown. Genomic DNAs were digested to completion (C) with *SalI* and hybridized to the ^{32}P -labelled 0.3-kb *SalI*-*EcoRI* fragment shown in panel A. Lanes: 1. H729; 2. H103. The molecular sizes of the fragments (in kb) are indicated on the left.

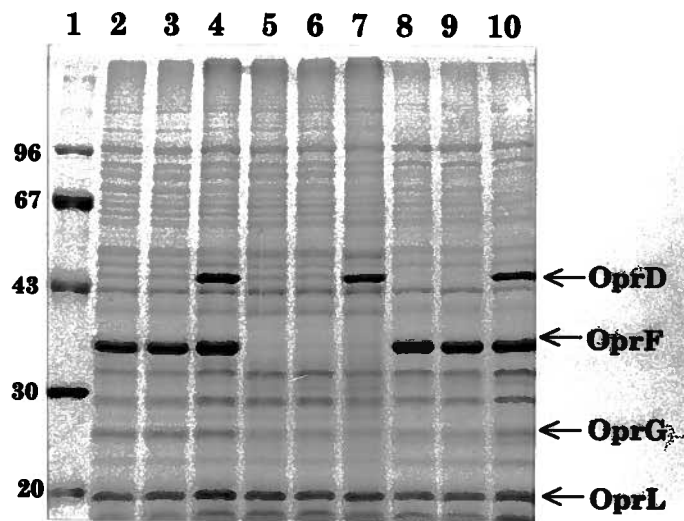


Figure 15: SDS-PAGE demonstrating overexpression and mutagenesis of the *oprD* gene.

The banding position of OprD is indicated by the arrow on the right. Lanes: 1, molecular marker; 2, H103; 3, H103(pUCP19); 4, H103(pXH2); 5, H636; 6, H636(pUCP19); 7, H636(pXH2); 8, H729; 9, H729(pUCP19); 10, H729(pXH2). For each lane, 20 μ g outer membrane proteins were added.

D. Function of OprD in Antibiotic Susceptibility

To reexamine the role of OprD in quinolone uptake and also to confirm, in genetically defined strains, that it was a specific pore for imipenem, MIC determinations were performed by the agar dilution procedure in Mueller-Hinton medium (Table IV). Nine strains which represented different expression levels of the *oprD* and *oprF* gene were utilized. The rationale behind this experiment was that, if OprD could act as channel for certain antibiotics, the overexpression of this porin would increase susceptibility whereas the lack of the porin would decrease susceptibility to these antibiotics; otherwise, the amount of OprD would not influence antibiotic susceptibility.

Two carbapenems were used, imipenem and meropenem, MICs for wild type strain H103 were 4.0 µg/ml and 0.5 µg/ml respectively. The OprD-overexpressing strain H103(pXH2) showed the lowest MICs, 0.5-1.0 µg/ml for imipenem and 0.06-0.12 µg/ml for meropenem, which were 4 to 8-fold lower than that of H103. In contrast, the OprD-defective strain H729 showed the highest MIC, 16 µg/ml for imipenem and 2.0 for meropenem, which were 4-fold higher than that of H103 (Table IV). The overexpression of OprD from plasmid pXH2 in the OprD defective strain H729 restored susceptibility to levels equivalent to those observed in H103(pXH2). In contrast, the loss by mutation of OprF did not influence the MICs to carbapenems, indicating that OprF did not function as a major uptake route for carbapenems (Table IV).

Table IV: Influence of OprD expression levels on antibiotic susceptibility of *P. aeruginosa* strains.

Strains	Relevant properties ^a			MICs (µg/ml) ^b							
	OprD	OprF		IMIP	MERO	CTX	CFP	CIP	FLR	GM	
H103	+	+		4.0	0.50	4.0	1.0	0.12	0.50	2.0	
H103(pUCP19)	+	+		4.0	0.50	8.0	4.0	0.12	0.50	2.0	
H103(pXH2)	+++	+		1.0	0.06	4.0	4.0	0.12	0.50	2.0	
H729	-	+		16.0	2.0	8.0	2.0	0.12	0.05	4.0	
H729(pUCP19)	-	+		16.0	2.0	4.0	4.0	0.12	0.05	2.0	
H729(pXH2)	+++	+		0.5	0.06	8.0	4.0	0.12	0.50	4.0	
H636	+	-		4.0	0.50	8.0	2.0	0.06	0.50	2.0	
H636(pUCP19)	+	-		4.0	0.50	8.0	4.0	0.06	0.50	2.0	
H636(pXH2)	+++	-		1.0	0.12	8.0	4.0	0.06	0.50	2.0	

- Levels of different outer membrane proteins as observed in Figure 15.
- MICs were determined by the agar dilution method on Mueller-Hinton plates. Each MIC was determined three times independently. Abbreviations: IMIP, imipenem; MERO, meropenem; CTX, cefotaxime; CFP, cefpirome; CIP, ciprofloxacin; FLER, fleroxacin; GM, gentamicin.

Other β -lactams (cefotaxime and ceftiofime), quinolones (ciprofloxacin and fleroxacin) and an aminoglycoside (gentamicin), did not show significant differences in MICs, regardless of the expression levels of OprD (Table IV). (N.B. the 2-4 fold increase in susceptibility to cefotaxime and ceftiofime of strains containing the plasmids pUCP19 or pXH2, was due to the plasmid encoded β -lactamase). The additional absence of OprF had little effect on antibiotic resistance. These results indicated that OprD did not significantly facilitate the passage of these antibiotics across the outer membrane.

We also examined the influence of OprD expression on antibiotic susceptibility of *E. coli*. The *oprD* gene was overexpressed to high levels in *E. coli* CE1248(pBK19R), a strain with mutations preventing the production of porins OmpF, OmpC and PhoE. However, even in this background, MICs for the carbapenems were much lower than those for *P. aeruginosa* strains and overexpression of OprD had no effect (Table V), presumably due to the higher intrinsic outer membrane permeability of *E. coli*.

E. Function of OprD in Sugar Transport

Specific porins, with the exception of the sucrose porin of *E. coli* (Schülein et al., 1991), are generally poorly permeable to non-specific substrates. To investigate the role of OprD in sugar transport, a set of isogenic strains: *P. aeruginosa* H729, H103, and H103(pXH2), expressing different levels of OprD were used. Control

Table V: Influence of OprD expression levels on antibiotic susceptibility of *E. coli* strains.

Strains	OprD level	MICs($\mu\text{g/ml}$) ^a			
		IMP	MERO	CTX	CFP
CE1248	-	0.06	0.016	0.16	0.16
CE1248(pTZ19R)	-	0.03	0.016	0.16	0.64
CE1248(pBK19R)	++	0.03	0.016	0.16	0.64

- a. MICs were determined by the agar dilution method on Mueller-Hinton plates. Each MIC was determined three times independently. Abbreviations: IMP, imipenem; MERO, meropenem; CTX, cefotaxime; CFP, ceftiofuran.

experiments demonstrated very similar rates of growth for all three strains on Luria Broth (growth rate 1.26 doublings per hour of all three strains) and Mueller-Hinton broth (growth rate 1.10-1.23 doublings per hour). Therefore, strains were grown in the BM2 minimal medium with either glucose, gluconate or pyruvate as carbon sources, at concentrations varying from 0.5 mM to 10 mM. Growth curves were constructed for each sugar at each concentration and utilized to calculate growth rates. We reasoned that, if OprD could facilitate the transport of a certain sugar, at the growth rate limiting concentrations, different growth rates would be observed depending on the *oprD* gene expression level.

For gluconate, at 0.5 mM concentration, the growth rates of wild type strain H103 and OprD-defective strain H729 were only 60% and 20% respectively, of that of OprD-overexpressing strain H103(pXH1), and these differences were statistically significant ($p < 0.05$ by Student's *t* test) (Fig. 16A). These data were thus consistent with outer membrane permeation being the rate limiting step for growth on gluconate, and further suggested OprD was the major porin involved in gluconate passage across the outer membrane at growth-limiting conditions.

As the initial concentration of gluconate in the medium was increased, the growth rates for H103 and H729 increased, whereas the growth rate of the OprD overexpressing strain H103(pXH2) remained stable. The growth rates of the three strains converged with increasing saccharide concentrations and eventually became not significantly different at 10 mM gluconate. This result indicated that outer membrane permeation through OprD ceased to become rate limiting at high

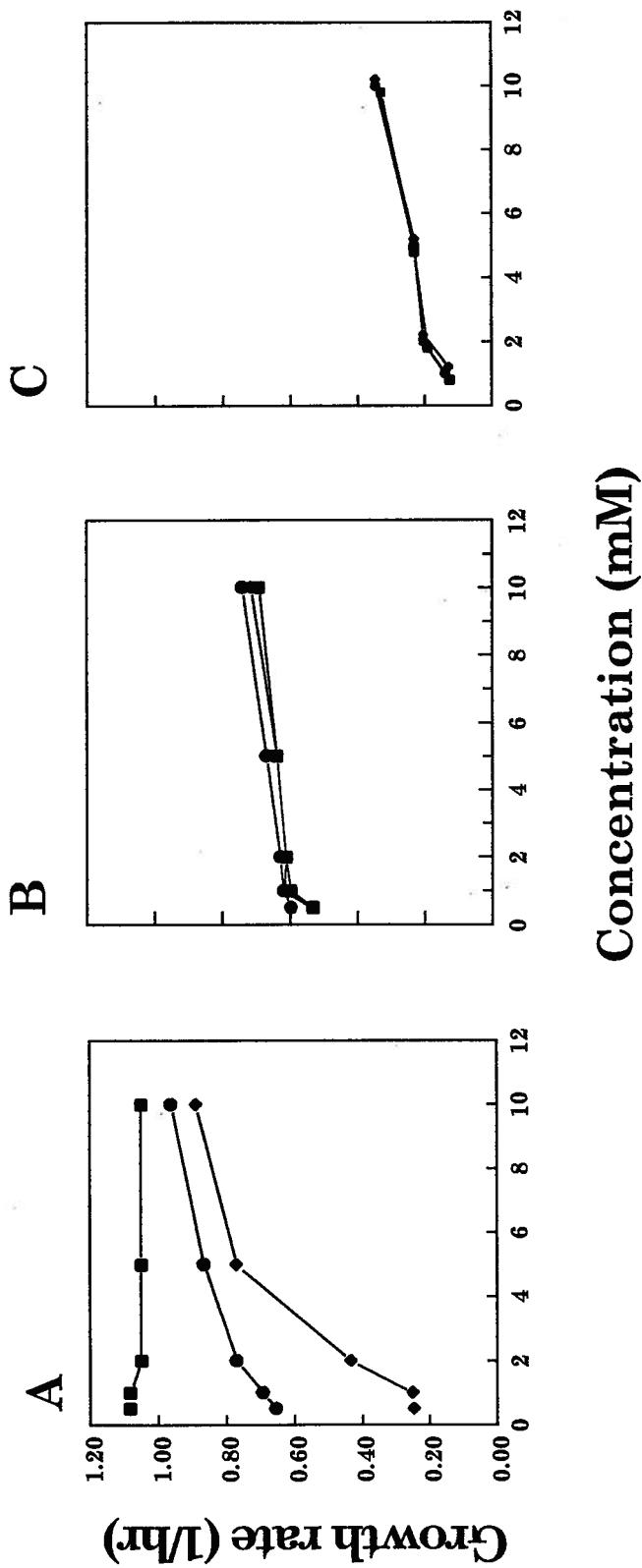


Figure 16: Function of OprD in sugar transport.

Influence of substrate concentrations on the growth rate of H103 (circle), its OprD-overexpressing strain H103(pXH2) (square) and OprD-defective strain H729 (diamond). (A) glucose, (B) gluconate, (C) pyruvate. Data points are the average results from 3 experiments with less than or equal to 10% variation between experiments.

saccharide concentrations, at which other porins could substitute for OprD (Fig. 16A).

To further exclude the possibility that the slow growth rate of the OprD-defective strain H729 had resulted from metabolic disturbances due to the mutation, another carbon source, glucose, was used as a control. At 0.5 mM glucose concentration, the growth rates for H103 and H729 were 110% and 90% that of H103(pXH2), which were not significantly different ($p>0.5$). As the glucose concentration was increased, the growth rates for all three strains increased but remained very close for the three strains (Fig. 16B). The results were reasonable since, as previously demonstrated, in the presence of glucose, *P. aeruginosa* strains induce a specific porin OprB (Hancock and Carey, 1980). The OprB levels in all three strains were found to be the same, and approximately 5 fold lower than the level of OprD in strain H103(pXH2). These results indicated that loss or overexpression of OprD did not affect the normal growth of the cell.

Since growth in pyruvate leads to higher expression levels of OprD in *P. aeruginosa* (Hancock and Carey, 1980), it was questioned whether OprD could also allow the specific passage of pyruvate. The results showed no significant difference in the growth rates of *P. aeruginosa* H103(pXH2), H103 and H729 at pyruvate concentrations from 1 mM to 10 mM (Fig. 16C), indicating that OprD was not able to function as the predominant channel for the transport of pyruvate.

F. Competition Experiments.

Since OprD can facilitate the permeation of basic amino acids (Trias and Nikaido, 1990b) and the above suggested a role in uptake of gluconate and zwitterionic carbapenems, competition experiments were performed as described by Fukuoka et al (1991) to determine if common binding sites were shared by these substrates. The susceptibilities of the isogenic variants to imipenem were determined using BM2 medium supplemented with basic amino acids or gluconate and were compared with the results obtained in unsupplemented BM2 glucose or succinate respectively (Table VI). The MICs for H103 and H103(pXH2) were increased 8-16 fold and 4-8 fold respectively by the addition of 50 mM basic amino acids. However only a 2 fold effect was observed for the OprD-deficient mutant H729. Such a change in MIC is usually considered to be not significant. In addition, the effect of L-lysine concentrations in BM2 glucose medium on the susceptibilities of the isogenic variants to imipenem was determined. Figure 17 showed that the MICs for H103 and H103(pXH2) increased as the concentration of L-lysine increased, until they reached the same level as the OprD-deficient mutant H729. In contrast, the susceptibility of the OprD defective strain H729 was not significantly influenced by the addition of basic amino acids. The results suggested that imipenem and basic amino acids shared a common binding site(s) in OprD channel.

The same competition experiments were also performed with gluconate or glucose at the concentrations of 20 mM, 50 mM, 100 mM and 150 mM (Table VI). In contrast to the results for the basic amino acids, the susceptibilities of H103 and

Table VI: Effects of basic amino acids and gluconate on imipenem susceptibilities of *P. aeruginosa* strains expressing different levels of OprD.

Strains	OprD levels	MICs ($\mu\text{g/ml}$) in different media ^a						
		BM2 ^{b+} 50 mM	BM2 ^b 50 mM	BM2 ^{b+} 50 mM	BM2 ^{b+} 50 mM	BM2 ^o 20-150 mM	BM2 ^{o+} 20-150 mM	
H729	-	8.0	4.0	8.0	8.0	4.0	8.0	4.0
H103	+	4.0	0.5	8.0	8.0	1.0	2.0	1.0
H103(pXH2)	++	1.0	0.25	4.0	4.0	0.5	1.0	0.5

- a. MICs were determined by the agar dilution method. Each MIC was determined three times independently.
- b. Glucose was used as the carbon source in BM2 media.
- c. Succinate was used as the carbon source in BM2 media.

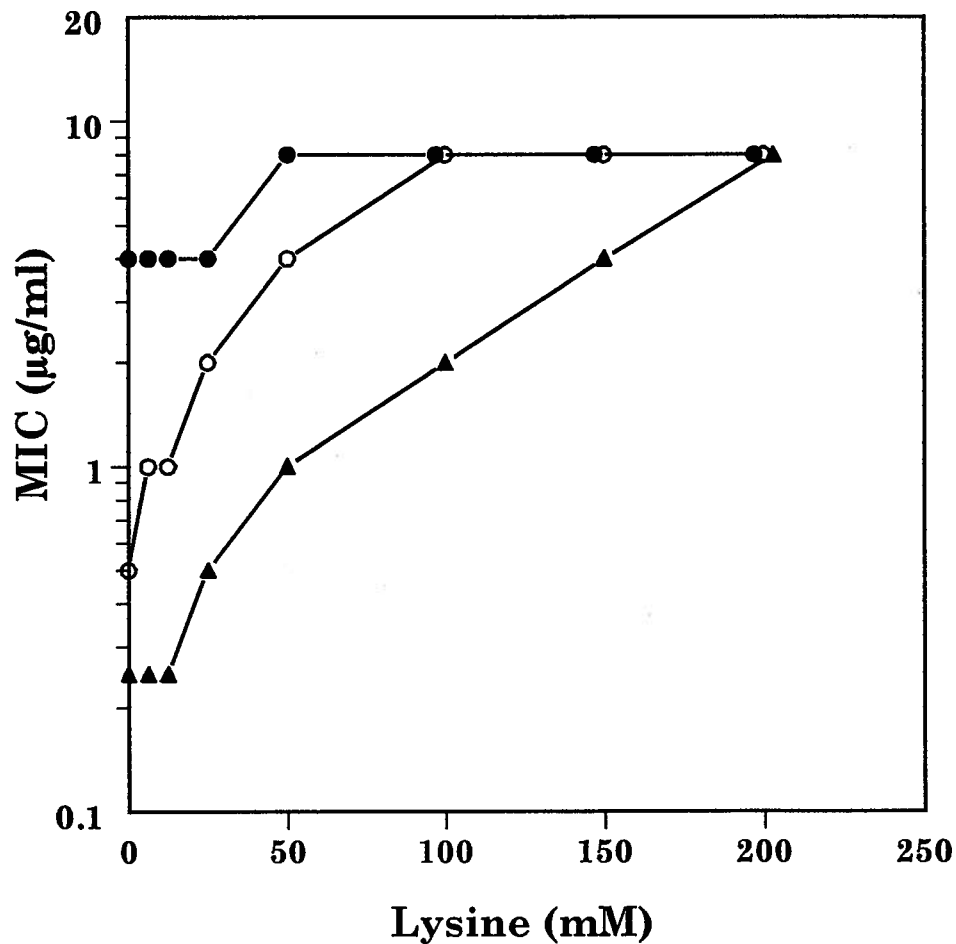


Figure 17: Competition between L-lysine and imipenem for the OprD channel.

Effect of L-lysine concentration in BM2 glucose medium on the susceptibility of H103 (open circle), its OprD-overexpressing strain H103(pXH2) (triangle) and OprD-defective strain H729 (filled circle) to imipenem.

H103(pXH2) were not affected by the presence of gluconate or glucose (the 2 fold increase in the presence of gluconate was also observed for the negative control H729), indicating that no common OprD binding sites were involved for gluconate and imipenem.

G. Purification of OprD.

OprD was purified from both *E. coli* and *P. aeruginosa* following the procedures described in Materials and Methods. For the purification of OprD from *E. coli*, the porin deficient strain CE1248 containing plasmid pBK19R was grown in the presence of glucose and IPTG to repress the expression of LamB and induce the high levels of expression of OprD. Similarly, to purify OprD from *P. aeruginosa*, H636(XH2) overexpressing OprD and lacking major porin OprF was used. Cells were grown in glucose to avoid the contamination of OprB (=D1). Different combinations of salt and detergent concentrations were tested to optimize the solubilization conditions. OprD was maximally extracted with 10 mM Tris-HCl, 3% Octyl-POE and 0.1 M NaCl in the presence of 0.5 mM EDTA (Fig. 18, lane 5). When solubilized at room temperature prior to electrophoresis (Fig. 18, lane 6), OprD ran at a lower apparent molecular weight, demonstrating OmpA-like heat modifiability.

When applied to an anion exchange column (Mono Q, Phamacia), the detergent/EDTA soluble protein eluted in two major peaks (Fig. 19A). The first peak was the unbound proteins washed out before applying the salt gradient (Fig.

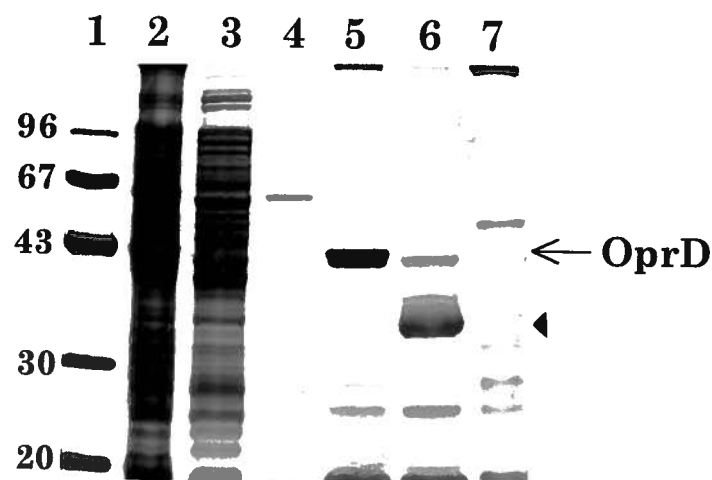


Figure 18: SDS-PAGE of samples from solubilization stages.

Lanes: 1, molecular weight markers; 2, outer membrane; 3, 0.5% octyl-POE soluble fraction; 4, 3% octyl-POE/NaCl soluble fraction; 5 & 6, 3% octyl-POE/NaCl/EDTA soluble fraction; 7, 3% octyl-POE/NaCl/EDTA insoluble fraction. The sample of lane 6 was unheated. Solid triangle indicates the banding position of the heat-modifiable form of OprD.

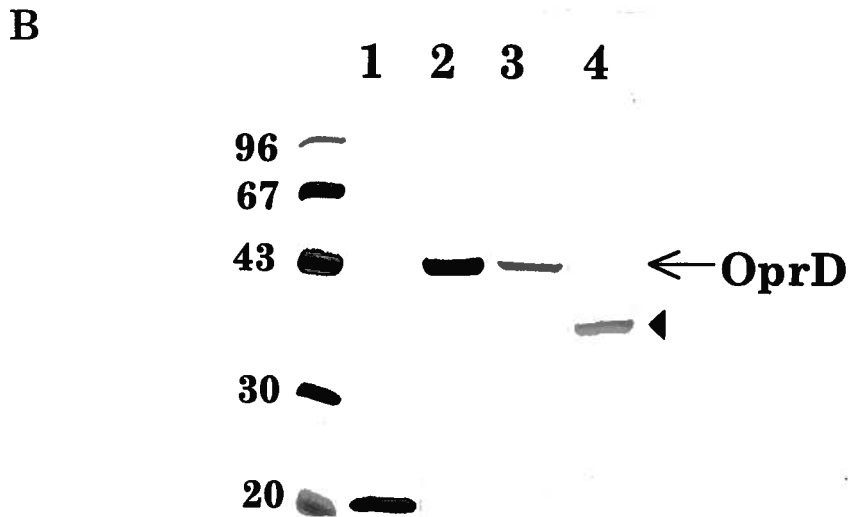
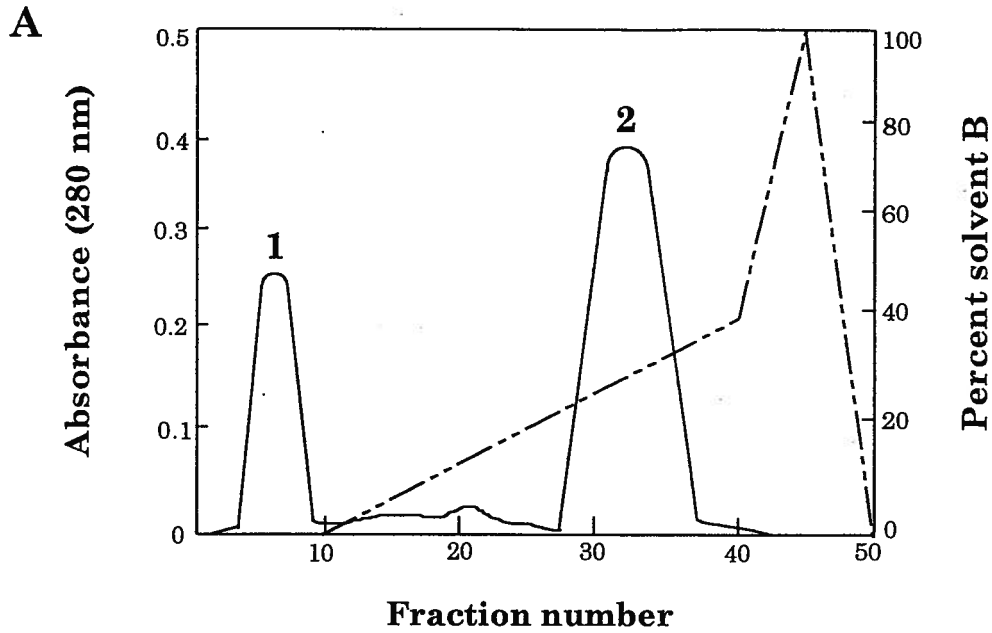


Figure 19: Purification of OprD.

(A) Mono-Q FPLC elution profile. Buffer A: 10 mM Tris-HCl (pH 8.0), 5 mM EDTA, and 0.08% LDAO. Buffer B: buffer A plus 1.0 M NaCl. Broken line indicates the salt gradient and numbers refer to peaks 1 and 2. (B) SDS-PAGE of samples eluted from Mono-Q column. Lanes: 1, peak 1 sample; 2, peak 2 sample; 3, purified OprD (heated); 4, purified OprD (unheated). The solid triangle indicates the banding position of the heat-modifiable form of OprD.

19B, lane 1). OprD was eluted in the second peak along with traces of other proteins of higher molecular weight (Fig. 19B, lane 2). Those fractions were pooled and subjected to a second run with a much flatter salt gradient and lower elution speed, OprD was eluted as a single purified protein (Fig. 19B, lane 3). The purified OprD still retained its heat-modifiability characteristic (Fig. 19B, lane 4) and could form functional channels in the black lipid bilayer system (see below).

H. Black Lipid Bilayer Analysis.

The purified OprD protein was added at nanomolar concentrations to the aqueous solution bathing a black lipid bilayer membrane. Membrane conductance increased in a stepwise fashion (Fig. 20A), presumably due to the incorporation of individual porin units into the membrane as suggested for other porins (Benz and Hancock, 1981). For 170 measured single-channel events, the average single channel conductance in 1 M KCl was 20 pS, which was at least 10 times smaller than those of most other porins studied to date. The only exception was the *E. coli* nucleotide-specific porin Tsx, with the average single channel conductance of 10 pS. The purified OprD from *E. coli* and *P. aeruginosa* did not show any differences in single channel conductance, indicating that OprD expressed from the cloned gene was properly folded in the *E. coli* outer membrane. Ishii and Nakae (1993) demonstrated occasional "open" channels of OprD with a much higher conductivity (400 pS), especially in the presence of LPS. However, I did not observe any of such

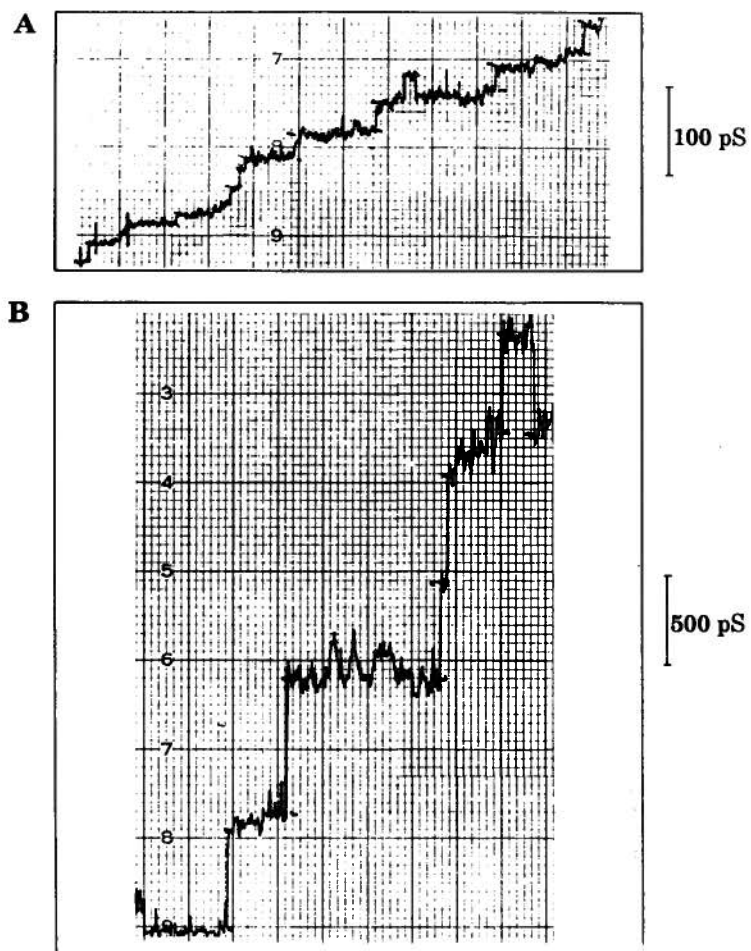


Figure 20: Chart recording of stepwise increase of the membrane current formed by 1% oxidized cholesterol in n-decane in the presence of purified proteins.

(A) Native OprD. (B) OprD Δ L5. The aqueous phase contained 1 M KCl, PH7.0, the temperature was 20°C and the applied voltage was 20 mV. Note that the resolution of the instrument was higher in (A) than in (B).

events and one possibility for such large channels might be the contamination of other porins in their preparation.

To examine the ion-selectivity of the OprD channel, single channel conductance was measured in salts of varying cation or anion sizes (Table X). Increasing the size of cations from K^+ to Cs^+ to Li^+ (the last being highly hydrated) while keeping Cl^- as the anion resulted in a steady decrease in the average single channel conductance (Table X). In contrast, the single channel conductance was little affected by changing the size of anion from Cl^- to $MOPS^-$ (Table X). The results suggested that OprD channel was cation selective. Consistent with this, zero current membrane potential measurements confirmed that OprD channel exhibited 2.6-fold preference for cations over anions (Table XI). The weak cation selectivity of OprD channel was in good agreement with its preference for basic amino acids. Increasing the salt concentration (3.0 M KCl) did not result in a linear increase in conductance (Table X). A similar result for *E. coli* hemolysin (Benz et al., 1989) has been interpreted as due to the surface charges at the pore mouth which caused a substantial surface potential. For OprD, these charges would be assumed to be due to anionic (acidic) amino acids that would tend to attract cations and repel anions.

To demonstrate that the OprD channel possessed specific binding site(s) for imipenem, a macroscopic conductance inhibition experiment was performed. Large bilayer membranes (2 mm^2) were formed in 1 M KCl. A small amount of purified OprD was added to one side of the membrane, and the conductance started to rise

rapidly for 10~40 min, and thereafter continued to rise at a decreasing rate. At this time, membrane conductance had increased 2~3 orders of magnitude and more than 1,000 channels were present in the membrane. Aliquots (60 μ l) of imipenem solution (20 μ M) were added to the aqueous solution at both sides of the membrane, and the conductance decreased to a new level over a period of about 2 min (see Chapter 4, Fig. 31). The ability of imipenem to block KCl movement provided direct evidence that OprD contained imipenem binding site(s). In addition, by plotting the data as % inhibition of conductance as a function of imipenem concentration, it was possible to derive an I_{50} value (i.e., a concentration of imipenem resulting in 50% inhibition of the original conductance) of 1.4 μ M.

I. Summary.

A set of *P. aeruginosa* isogenic strains with genetically defined levels of OprD were constructed and utilized to characterize the *in vivo* substrate selectivity of this porin. To determine the role of OprD in antibiotic uptake, nine strains representing different levels of OprD and OprF were used to determine the MICs of different antibiotics. The results clearly demonstrated that OprD could be utilized by imipenem and meropenem but, even when substantially overexpressed, could not be significantly utilized by other β -lactams, quinolones or aminoglycosides. To test the function of OprD in the transport of carbon sources, strains were grown in minimal medium with limiting concentrations of the carbon sources, glucose,

gluconate or pyruvate. The results indicated that OprD selectively facilitated the diffusion of gluconate under growth-rate limiting conditions. In contrast, it did not function as the predominant channel for the transport of glucose or pyruvate. Competition experiments confirmed that imipenem shared common binding sites with basic amino acids in the OprD channel, but not with gluconate or glucose. In addition, OprD was purified and was able to reconstitute channels in black lipid bilayer model membranes. OprD formed very small pores with an average single channel conductance in 1.0 M KCl of 20 pS, and the channel was weakly cation selective. When large numbers of OprD channels were incorporated into lipid bilayer membranes, addition of imipenem resulted in progressive decrease in membrane conductance, indicating the presence of specific binding site(s) for imipenem in the OprD channel. This allowed the calculation of an I_{50} value of 1.4 μ M.

CHAPTER THREE Structural Characterization of OprD: Membrane Topology Model

A. Introduction.

The crystal structures of 5 porins was a milestone in our understanding of porin functions. To fully understand the molecular mechanism involved in the facilitated uptake of basic amino acids and imipenem, a detailed knowledge of the molecular structure of OprD is required. The amino acid sequence of OprD (Fig. 12; Yoneyama et al., 1992) was typical of porins: charged residues were distributed almost uniformly along the primary sequence and as a consequence there were no clear hydrophobic stretches which would be predicted to span the membrane as an alpha helix. Therefore it is very likely that the structured transmembrane segments are essentially composed of β -strands. In this chapter, the first OprD topology model was constructed by multiple alignments together with secondary structure predictions. PCR-mediated site-directed mutagenesis was then employed to separately delete the predicted external loops and to verify the accuracy of the model.

B. Prediction of an OprD Topology Model.

In a previous paper (Jeanteur et al., 1994a), the alignments of 30 non-specific porins from 5 distant families were reported. Alignment of OprD was not

considered in detail. However attempts to match the OprD sequence with other *P. aeruginosa* porins and the *E. coli* porins OmpF and TolC showed that OprD had the highest homology to OmpF with an alignment score using the Needleman and Wunsch method (1970) of 2.6, which was close to 3.0, the minimal score required for an alignment to be considered significant. Based on the sequence alignment between OmpF and OprD, sixteen β -strands were predicted (Fig. 21). Alignment was very clear for the N and C terminal β -strands, but the homology was weaker in the middle part of the sequence, similar to that reported for other porins (Jeanteur et al., 1991). The 16 transmembrane segments had the typical amphipathic features of porin β -strands in that they were composed of alternating polar and non-polar residues exposed to the aqueous channel and hydrophobic membrane interior respectively (Fig. 22). The sizes of the predicted β -strands (10~21 residues) were in agreement with the lengths of β -strands observed for the solved porin structures, and the ends of these β -strands were often composed of aromatic residues, which may function as one of the stabilizing forces for the barrel structure (Cowan et al., 1992).

The β -strands were connected by short turns at the periplasmic side and by long loops at the cell surface. Consistent with the larger number of amino acids in OprD than in the other members of the porin superfamily, the 8 external loops were often slightly longer than the ones observed for the known porin structures. The predicted loop L3 (Q₁₃₅ to T₁₆₅) was a long loop (Fig. 22). It was the longest external loop observed in the *E. coli* porin OmpF and PhoE, *R. capsulatus* and

```

OprD      DAFVSDQAEAKGFIEDSSLDLLLRNYFNRDGKSGSGDRVDWTQG 45
:          :: | : : : | | : |
OmpF      AEIYNKDGKVDLYGKAVGLHYFSKNGENSYGGN      GDMTYARLG 44
          ~~~~~~

OprD      FLTTYESGFTQGTVGFVDAFGYLGLKLDGTSDKTGTGNLPVMNDGKP 93
:          | :: : : | : : : | | |
OmpF      FKGETQINS      DLTGYGQWEYNFQGNSEGADAQTGNKTR      82
          ~~~~~~

OprD      RDDYSRAGGAVKVRISKTMLKWGEMQPTAPVFAAGGSRLFPQTATGFQ 141
:          : : | | : : | : | : |
OmpF      LAFAGLKYADV      GSFDYGRNYGVVYDALGYT 112
          ~~~~~~

OprD      LOSSEFEGLDLEAGHFTEGKEPTTVKSRGELYATYAGETAKSADFIGG 189
:          | | | | : : | : : : |
OmpF      DMLPEFGGDTAYSDDFFVGRVGGVATYRNSNFFGLVDGLNFAVQYLK 160
          ~~~~~~

OprD      RYAITDNL SASLYGAELEDIYRQYYLNSNYTIPLASDQSLGDFDNIY 236
:          | | : : | : : : | : :
OmpF      NERDTARRSNGDGVGGSISYEYEGFGIVGAYGAADRNTNLQEAQPLGNG 208
          ~~~~~~

OprD      RTNDEGKAKAGDISNTTWSLAAAYTLDAHTFTLAYQKVHGDQPFDYIG 284
:          | : : | : : : : | : : : |
OmpF      KK      AEQWATGLKYDANNIYLAANYGETRNATPITNKF 244
          ~~~~~~

OprD      FGRNGSGAGGDSIFLANSVQYSDFNGPGEKSWQARYDLNLASYGVVPG 332
:          | : : : | : : | : |
OmpF      TNTSGFANKTQDVLVAQYQFDF      GL 269
          ~~~~~~

OprD      TFMVRYINGKDIDGTKMSDNNVGYKNYGYGEDGKHHE TNLEAKYVVQS 380
:          : | : | | | | : : | : |
OmpF      RPSIAYTKSKAKDVEGIGDVDL      VNYFEVGATYYFNK 305
          ~~~~~~

OprD      GPAKDL SFRIRQAWHRANADQEGDQNEFRLIVDYPLSIL 420
:          : : : : | : | | : : | : :
OmpF      NMSTYVDYIINQIDSDNKLGVGSDD      TVAVGIVYQF 340
          ~~~~~~

```

Figure 21: Sequence alignment between OprD and OmpF.

Dashed lines indicate identical amino acids and ':' indicates conservative substitutions. The known β -strands of OmpF are marked by ~~~~ and the predicted β -strands of OprD are marked by ____.

Figure 22: Membrane topology model of OprD.

The sixteen predicted transmembrane β -strands are boxed, and the 8 external loops are labelled as L1 to L8. The deleted amino acid residues are presented as unfilled letters.

L1 N R D G K S G S G D R V⁴⁰ D W T Q G F L T T Y⁵⁰ E S G F T Q G
 F Y Y N R L L L D²⁰ L S S D E I F G K A¹⁰ E A Q D S V A F
L2 V M N D⁹⁰ G K P R D D Y S R A¹⁰⁰ G G A V K V R I S K¹¹⁰ T M L K W G E M Q
 P L N G T G T⁸⁰ K D S T G D L K L G⁷⁰ L Y G F A D V G F G⁶⁰ V T
L3 E G L¹⁵⁰ L E A G H F T E G¹⁶⁰ K E P T T V K S R R G¹⁷⁰ E L Y A T Y A G E T¹⁸⁰
 F E S S Q L Q F¹⁴⁰ G T A T Q P F L R S¹³⁰ G G A A F V P A T P¹²⁰
L4 L S A S²⁰⁰ L Y G A E L E D I Y²¹⁰ R N
 N D T I A Y R¹⁹⁰ G G I F D A S K A
L5 K A K A G D I S²⁵⁰ N T T W S L A A A Y²⁶⁰ T L D A H T F T
 G E D²⁴⁰ N T R Y I N F D F G²³⁰ L S Q D S A L P I T²²⁰ Y N S N L Y Y
L6 S G A G G D S I F L A³⁰⁰ N S V Q Y S D F N G³¹⁰ P G E K S W Q A R
 G N R G F G I Y D F²⁸⁰ P Q D G H V K Q Y L A²⁷⁰
L7 S³⁵⁰ D N N V G Y K N Y G Y³⁶⁰ G E D G K H H E T³⁷⁰ N L E A K Y V V Q S³⁸⁰
 M I K T G D I D K G N³⁴⁰ I Y R V M F T L G P³³⁰ V G Y S A L N L D Y³²⁰
L8 Q G E G D Q N E F R⁴¹⁰ L I V D Y P L S I L⁴²⁰
 D⁴⁰⁰ A N A R H W A Q R I³⁹⁰ R F S L D K A P G

Rhodopseudomonas blastica porin crystal structures, in which it completely folded inside the pore forming the constriction zone for general porins and part of the constriction zone for the specific porin LamB (Cowan et al., 1992; Weiss and Schulz, 1992; Kreuzsch et al., 1994; Schirmer et al., 1995).

C. PCR-Based Site Directed Deletion Mutagenesis.

To test the validity of the predicted external loops, site-specific deletion mutagenesis was performed to separately delete short stretches of amino acids (4-8) from each of the predicted loop to see if these deletions were tolerated. The deletions were made around the middle of the predicted loops, as shown by the unfilled letters in Fig. 22. For the shorter loops, L4 and L6, only 4 amino acids were deleted, and for the remaining six longer loops, 8 amino acids were deleted. The rationale was that the external loops can undergo substantial variation without affecting the configuration of the protein. In contrast, β -strands buried in the membrane are more conserved and more sensitive to deletions or insertions (Jeanteur et al., 1991). If the predicted loops were correct, the consequent deletion mutant protein would retain the native conformation and assemble correctly in the outer membrane. Otherwise, if the deletion happened in the transmembrane regions, the protein would lack one of the major stabilizing forces of the structure and the mutant protein could not assemble properly in the outer membrane.

Early methods for site-directed mutagenesis using single stranded DNA gave

low efficiencies of obtaining the desired mutation. The development of PCR (Saiki et al., 1985), however, provided a new approach (Vallette et al., 1989). These methods use primers bearing the mutations, which, after PCR, were then incorporated into the PCR products. By using an appropriate strategy, the mutation frequency could reach 100%. In this work, 2 PCR strategies, direct extension and overlap extension were used as described in Material and Methods (Fig. 6, Table III).

Since all of the restriction enzyme sites used in the PCR/cloning procedures had to be unique, plasmid pBK19R was modified to eliminate the unnecessary restriction sites. Plasmid pMBK19R was constructed to eliminate the restriction site *Pst*I in the multiple cloning site (Fig. 7), which would interfere with the mutagenesis of the predicted loops L3, L4 and L5. Plasmid pMBE19R, containing only the N-terminus of the *oprD* coding region, was constructed to eliminate one *Sal*I site in the multiple cloning site, and another *Sal*I site and one *Eco*RI site in the C-terminus of the *oprD* gene (Fig. 8). After PCR-mutagenesis of the predicted loops L1 and L2 using pMBE19R as the template, the 1.2-kb *Eco*RI fragment encoding the C-terminus of OprD was then cloned back in the correct orientation to complete the *oprD* coding region. *E. coli* CE1248 containing pMBK19R expressed OprD at the same level as *E. coli* CE1248(pBK19R), whereas *E. coli* CE1248(pMBE19R), containing only part of the *oprD* gene, did not express OprD (data not shown).

The major limitations of PCR were the unspecific products and the

unexpected mutations ("errors") generated by the DNA polymerase. To obtain a good yield of the desired PCR products, and to minimize the error and unspecific products, I optimized the conditions with respect to DNA polymerase, template amount and thermal cycling conditions. First, instead of Taq DNA polymerase, the high-fidelity thermophilic Vent DNA polymerase was utilized. The fidelity of the Vent DNA polymerase was 5 to 15 fold higher than that of Taq DNA polymerase, due in part to an integral 3'-5' proofreading exonuclease activity. Second, different amounts of DNA template ranging from 1 pg to 100 ng were tested. Ten ng turned out to be the optimal amount, since insufficient yield was obtained when less than 10 ng of template DNA was used and unspecific product was present when too much template was used. Finally, I varied the annealing temperature (50-60°C), used a short extension time (1~1.5 min instead of 3 min) and fewer cycles of PCR (20 cycles instead of 30) to minimize errors.

After inserting the mutagenic PCR products back into the parental plasmid, a simple and rapid primary screening was utilized to identify the desired deletion mutants. Plasmids were isolated from the transformants and digested with the same pair of restriction enzymes used in the PCR/cloning procedure to generate the fragments of interest. The digestion mix was analyzed on 1.5~2.0 % agarose gels, small but readily observable differences were noted between the corresponding fragments containing the desired deletion (12~24 bp) and the original gene (data not shown). From the mutagenesis of each predicted loop, 5 mutant plasmids containing the deletions were selected and the whole PCR-amplified regions were

sequenced. The exact amino acid positions of deletion and the identities of the deleted amino acids from 8 deletion mutants are summarized in Table VII.

D. Characterization of the Deletion Mutants

The expression of deletion mutant OprD derivatives was examined in the porin deficient strain *E. coli* CE1248. The outer membranes containing the deletion mutations were isolated and examined by SDS-PAGE (Fig. 23A), and on Western-immunoblot using an anti-OprD polyclonal antiserum (Fig. 23B). The mutant polypeptides from the deletion mutagenesis of six predicted loops, L1, L2, L5, L6, L7 and L8, co-fractionated with the outer membranes, were typically heat modifiable, and were expressed at similar levels compared to cells expressing wild type OprD (Fig. 23A, lanes 4, 5, 8-11). They also showed a slightly increased electrophoretic mobility as compared to wild type OprD, consistent with the deletion of a few amino acid residues. These results indicated that deletions of short stretches of amino acids in these six predicted loops did not substantially change the native conformation of OprD, such that the consequent mutant proteins were assembled into the outer membrane, a result suggesting that these loops were accurately predicted. The deletion of the predicted loop L3 caused diminished but observable expression (Fig. 23A, lane 6), as confirmed by Western-immunoblot results (Fig. 23B, lane 6), indicating that this deletion was tolerated. However, since the deleted stretch had 4 negatively charged residues (Fig. 22), which could

Table VII: Deletion mutagenesis of the predicted loops.

Plasmids		Deletion sites ^a	Amino acids deleted	Mutagenesis efficiency
<i>E. coli</i>	<i>P. aeruginosa</i>			
pHE1	pHP1	Tyr-26	TyrTyrPheAsnArgAspGlyLys	60%
pHE2	pHP2	Asn-84	AsnLeuProValMetAsnAspGly	80%
pHE3	pHP3	Glu-146	GluPheGluGlyLeuAspLeuGlu	100%
pHE4	pHE4	Asn-196	AsnLeuSerAla	90%
pHE5	pHE5	Asp-240	AspGluGlyLysAlaLysAlaGly	100%
pHE6	pHP6	Asn-288	AsnGlySerGly	100%
pHE7	pHP7	Met-349	MetSerAspAsnAsnValGlyTyr	100%
pHE8	pHP8	Asn-398	AsnAlaAspGlnGlyGluGlyAsp	100%

a. Position 1 is the start site of the mature OprD, see Figure 22 for actual amino acid deleted.

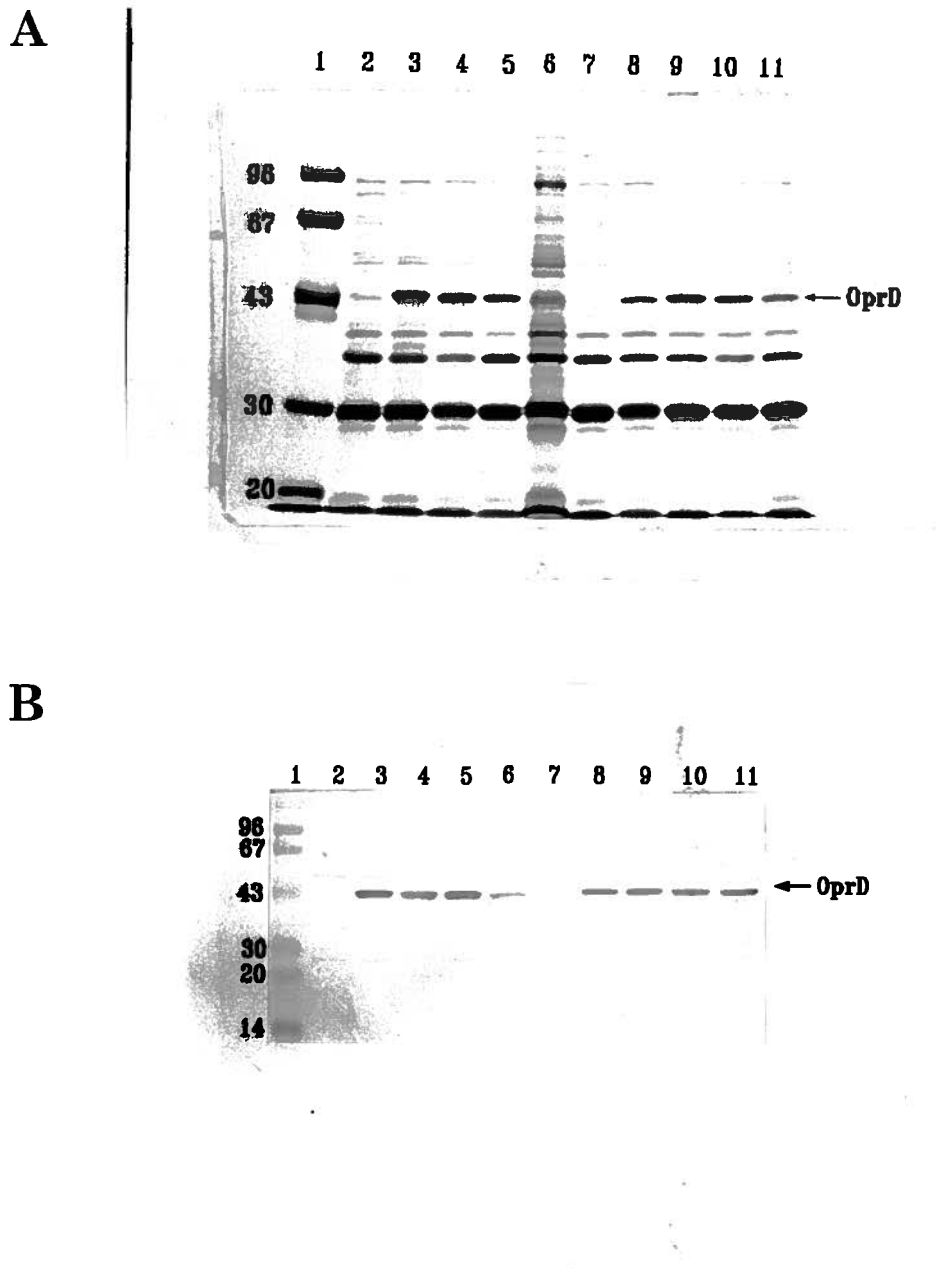


Figure 23: Expression of OprD derivatives in the outer membrane of *E. coli*.

(A) SDS-PAGE and (B) Western-immunoblot. The banding position of OprD is indicated by an arrow on the right. Lane 1 contained molecular weight markers. Lanes 2~11 contained outer membranes from CE1248 cells containing the following plasmids: lane 2, pMTZ19R; 3, pMBK19R; 4, pHE1; 5, pHE2; 6, pHE3; 7, pHE4; 8, pHE5; 9, pHE6; 10, pHE7; 11, pHE8. For each lane, 20 μ g of outer membrane protein was loaded.

be important for protein folding, the deletion may have perturbed the OprD structure sufficiently to lead to reduced protein production or unstable products. The deletion of the originally predicted loop L4 did not permit stable expression of an OprD protein (Fig. 23, lane 7). The deletion may have involved a transmembrane segment or a much less flexible turn. This and the potential for alternative positioning of β -strands 7 and 8 led to a modification of the model (Appendix, Fig. 34).

To confirm the above conclusions based on the deletion mutagenesis, the expression of these OprD derivatives was examined in the native host *P. aeruginosa*. All of the mutant *oprD* genes were subcloned in the same orientation as the *lac* promoter into the shuttle plasmid pUCP19 (Schweizer, 1991). The recombinant plasmids were then transformed into the *P. aeruginosa* OprD-defective strain H729. Examination of plasmid-encoded β -lactamase levels indicated no significant difference ($p > 0.5$) in β -lactamase levels for any of the transformants (Table VIII), suggesting that the plasmids were present in similar copy numbers. SDS-PAGE (Fig. 24A) as confirmed by Western-immunoblot (Fig. 24B) analysis showed the same profile as observed in *E. coli*, with the exception of the mutant deleting 8 residues of predicted loop L3 for which no expression was observed (Fig. 24, lane 8), further confirming that six of the predicted loops were accurate. The loop L3 mutant grew much slower than the remaining mutants.

To exclude the possibility that lack of expression of the OprD derivatives with deletions in the predicted loops L3 and L4 was due to the blocked transport

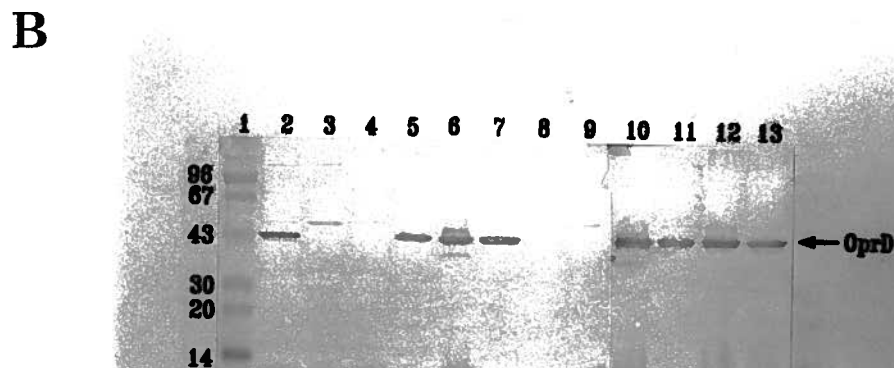
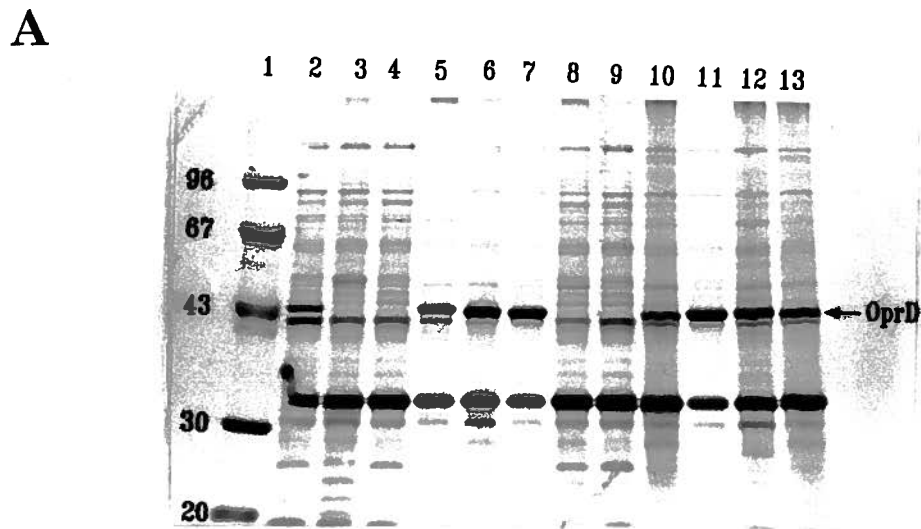


Figure 24: Expression of the OprD derivatives in the outer membrane of *P. aeruginosa* OprD-defective strain H729.

(A) SDS-PAGE and (B) Western-immunoblot. The banding position of OprD is indicated by an arrow on the right. Lanes: 1, molecular weight markers; 2, H103; 3, H729. Lanes 4~11 contained outer membranes from H729 containing the following plasmids: lane 4, pUCP19, 5, pXH2; 6, pHP1; 7, pHP2; 8, pHP3; 9, pHP4; 10, pHP5; 11, pHP6; 12, pHP7; 13, pHP8. For each lane, 20 μ g of outer membrane protein was loaded.

of the mutant peptides to the outer membrane, whole cell lysates were made and assessed by Western-immunoblotting using anti-OprD antibody. There were no detectable bands corresponding to OprD Δ L3 or OprD Δ L4 in the whole cell lysate (Fig. 25, lane 6 & 7), confirming the complete degradation of those two mutant proteins.

E. Trypsin Susceptibility of the Deletion Variants

The above results indicated that the OprD derivatives were properly located and assembled in the outer membrane. To probe the configuration of these OprD derivatives in *P. aeruginosa*, trypsin susceptibility assays were performed.

Outer membrane proteins tend to be protease resistant because of their possession of extensive β -structures with the linking surface loops tightly packed and folded in towards the porin channel (Cowan et al., 1992). In our studies, trypsin treatment of the outer membrane from H729 containing wild type OprD protein resulted in substantial retention of full sized OprD with a small amount of degradation to two protected fragments of apparent molecular masses of 32 kD and 16 kD (Fig. 26, lane 3). Similar results were obtained for *P. aeruginosa* strain H729 expressing OprD derivatives with deletions in loops L7 and L8 (Fig. 26, lanes 8, 9). Derivatives with deletions in loops L1, L2, L5 and L6 also were substantially trypsin resistant, although one or two additional fragments of mass 25 kD and 40 kD, were generated by trypsin treatment (Fig. 26, lanes 4 to 7). This is in

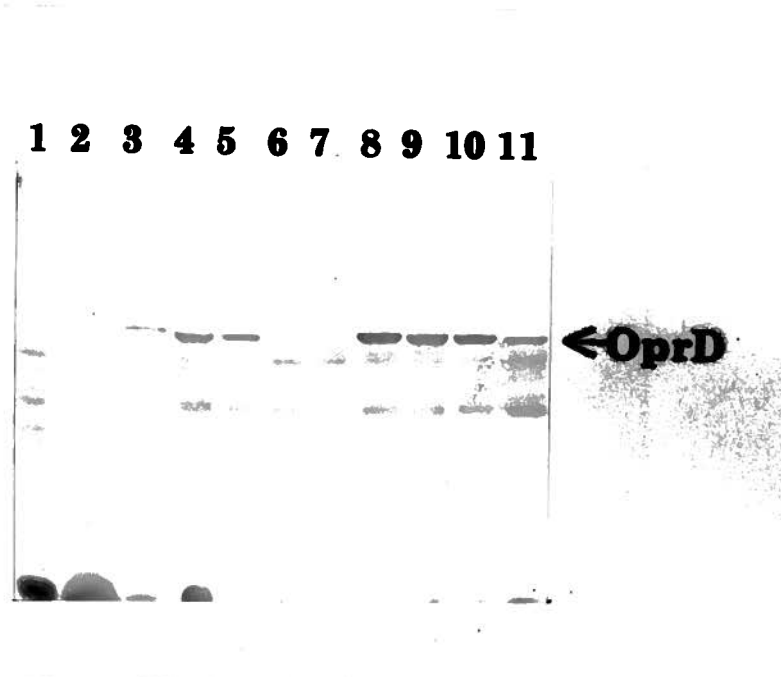


Figure 25: Western-immunoblot demonstrating expression of OprD derivatives in *P. aeruginosa* whole cell lysates.

Lanes: 1, H729; lanes 2~11 contained whole cell lysates from H729 containing the following plasmids: lane 2, pUCP19; 3, pXH2; 4, pHP1; 5, pHP2; 6, pHP3; 7, pHP4; 8, pHP5; 9, pHP6; 10, pHP7; 11, pHP8.

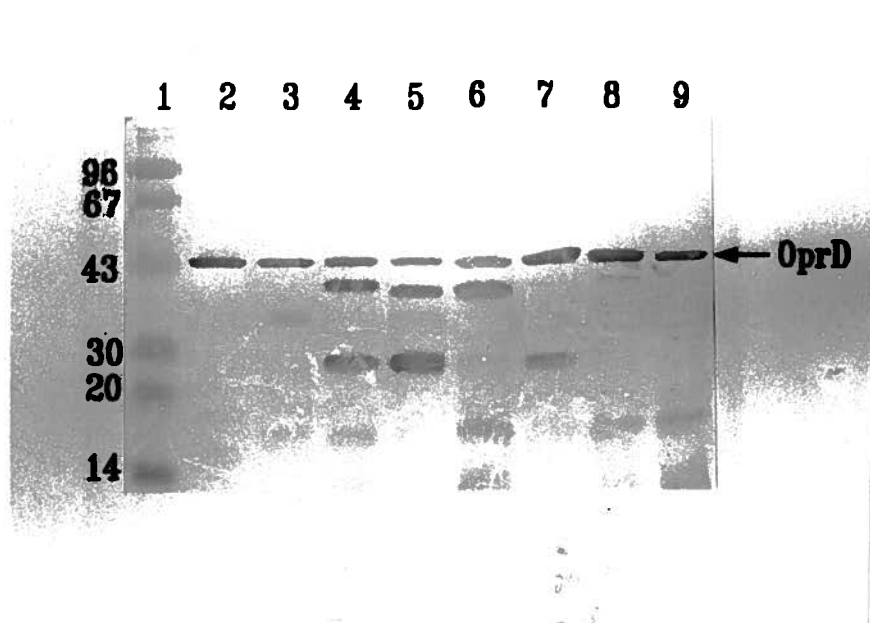


Figure 26: Trypsinization studies of OprD derivatives.

Western-immunoblot of trypsinized outer membrane samples of *P. aeruginosa* strain H729 containing OprD derivatives. Lane 1 is molecular weight marker and lane 2 is the untreated wild type OprD control. Lanes 3-9 contained trypsin-treated outer membranes from H729 with the following plasmids: lane 3, pXH2; 4, pHP1; 5, pHP2; 6, pHP5; 7, pHP6; 8, pHP7; 9, pHP8.

agreement with the proposal that deletions of these predicted loops could have caused local modifications of OprD configuration, leading to the exposure of certain trypsin susceptible sites. Nevertheless these data were generally consistent with the correct folding of the OprD derivatives. Increasing the amounts of trypsin and/or incubation time resulted in the generation of more fragments for both wild type and mutant OprD.

F. Revised OprD Model.

Based on the above data, the OprD model was refined in collaboration with Dr. Denis Jeanteur. By combining multiple alignments with amphipathicity calculations, it was demonstrated that, although OprD was a specific porin for basic amino acids and imipenem, in contrast to other members of the non-specific porin superfamily, it could be aligned almost as well to OmpF as was OmpF to the structurally-related porin from *Rhodobacter capsulatus* (Appendix, Table XII). Detailed examination indicated that the alignment was stronger in the predicted membrane spanning regions and on this basis, OprD was the first specific porin that could be included in the porin superfamily alignment (Appendix, Fig. 33). In contrast, neither OprD nor other members of the porin superfamily could be successfully aligned with other specific porins such as *E. coli* porin LamB or Tsx (Jeanteur et al., 1994a).

From the multiple alignments and amphipathicity calculations, sixteen β -

strands were predicted and could be aligned to those of other members of the porin superfamily. Four other segments, according to our membrane criteria, could also be predicted as transmembrane segments, but were rejected in the alignment procedure. In addition, the placement of β -strands 7 and 8 relied on the fact that deletion of the predicted L4 in the original model, did not result in expression. The predicted loop 3 (S₁₃₀ to R₁₆₉) was as long or longer than any other loops (Appendix, Fig. 34). Four periplasmic turns, T1, T4, T5 and T6 were clearly predicted by turn propensity analysis (Appendix, Fig. 33). Most of these turns were short (2 to 9 residues) and of about the same length as those determined from the known structures. A revised OprD membrane topology model was proposed (Appendix, Fig. 34), which was in general agreement with the previous model.

G. Summary.

The first OprD topology model was proposed based on the sequence alignment with *E. coli* porin OmpF and structural predictions. Sixteen β -strands were predicted, connected by short turns at the periplasmic side, whereas the eight external loops were of variable length but tended to be much longer. PCR-based site directed mutagenesis was performed to separately delete short stretches (4-8) of amino acid residues from each of the predicted external loops. These mutants were characterized by DNA sequencing, expression of the mutant OprD derivatives, and assessments of trypsin susceptibility. The deletion mutants from the predicted

external loops L1, L2, L5, L6, L7, and L8 were tolerated in both *E. coli* and *P. aeruginosa*, whereas the L3 mutant was only expressed in *E. coli* and the L4 mutant was not expressed in either bacterium. In addition, expressed mutant proteins maintained substantial resistance to trypsin treatment in the context of outer membranes. Based on this model, Denis Jeanteur performed multiple sequence alignments between OprD and seven representatives from the porin superfamily. OprD was the first specific porin that could be aligned with members of the so-called porin superfamily. Utilizing this alignment in conjunction with amphipathicity calculations, a revised OprD model was proposed.

CHAPTER FOUR Structure/Function Relationships: Functional Alterations of Deletion Mutants.

A. Introduction.

The OprD topology model predicted 8 external loops, including 3 long loops, L2, L3 and L7. At least one of them might fold inside the channel to form the 'eyelet' region, and the specific binding site for imipenem would be anticipated to be located in that region. To elucidate the organization of the channel and to locate the specific binding site for imipenem, the deletion mutants were examined regarding their function in antibiotic and sugar transport. In addition, two interesting OprD derivatives, OprD Δ L2 and OprD Δ L5 were purified and analyzed in the black lipid bilayer system. As shown below, the results are used to propose a molecular architecture for the OprD channel and to explore the transport mechanism of imipenem through the specific porin.

B. Effects of Deletion on Imipenem/Meropenem Susceptibilities.

To determine if any of the deletions influenced the function of OprD as a channel for imipenem and the related carbapenem antibiotic meropenem, MICs were assessed for those two antibiotics in the OprD-defective strain H729 background. As described earlier (Chapter 2), strain H729 expressing excess OprD from plasmid pXH2 had an MIC that was 16 to 32 fold lower than those observed

for strain H729 and H729 carrying the vector pUCP19 (Table VIII). Similarly there was a 16 to 32 fold reduction in MIC for strain H729 expressing the mutant OprDs with deletions in loops L1, L5, L6, L7 or L8. In contrast, the loop L2 deletion expressed from plasmid pHP2 resulted in only a 2 to 4 fold reduction in MIC to imipenem and meropenem (Table VIII).

To demonstrate the differences in MICs were only due to the deletions performed on the predicted loops, the following control experiments were performed. Three control antibiotics were used, including two polycationic antibiotics (gentamicin and polymyxin) and trimethoprim which diffuse cross the outer membrane through the self-promoted pathway and the hydrophobic pathway respectively. There were no significant differences in MIC for any of the strains studied (n.b. a 2 fold difference in MIC is considered by convention to be within experimental variability), indicating that the mutant proteins did not grossly disrupt the outer membrane since it had retained its barrier property (Table VIII). To exclude the possibility that the differences in MICs resulted from the different copy numbers of the plasmids encoding OprD derivatives, we measured the plasmid-encoded β -lactamase levels in all the strains. The results indicated that the plasmid copy numbers were similar (Table VIII). In addition, there were no significant differences in growth rates for all the strains, indicating that the deletions did not cause metabolic disturbances.

It has been previously demonstrated that lysine will compete with imipenem for uptake through OprD (Fukuoka et al., 1993), resulting in an increasing MIC as

Table VIII: Effects of deletions on imipenem/meropenem susceptibilities of *P. aeruginosa* strains.

Strains	β -lactamase activity (nmol nitrocefin/mg of cell per min)	MICs ($\mu\text{g/ml}$) ^a				
		Imipenem	Meropenem	Gentamicin	Polymyxin B Trimethoprim	
H729	5.4 ± 0.6	16.0	2.0	2.0	4.0	100
H729(pUCP19)	166 ± 15	16.0	2.0	1.0	4.0	100
H729(pXH2)	194 ± 53	0.5	0.125	2.0	4.0	100
H729(pHP1)	129 ± 44	1.0	0.125	1.0	4.0	100
H729(pHP2)^b	128 ± 26	4.0^c	1.0^c	2.0	2.0	100
H729(pHP5)	122 ± 21	1.0	0.125	1.0	4.0	100
H729(pHP6)	188 ± 56	1.0	0.06	2.0	2.0	100
H729(pHP7)	135 ± 26	0.5	0.06	2.0	4.0	100
H729(pHP8)	131 ± 35	0.5	0.06	2.0	4.0	100

- a. MICs were determined by the agar dilution method on Mueller-Hinton plates. Each MIC was determined three times independently.
- b. The bold letters indicate the strain which showed significant difference in susceptibilities of imipenem/meropenem.
- c. The bold numbers indicate the MICs of imipenem/meropenem which were significantly different from the controls.

a function of lysine concentration. In contrast, lysine had no significant effect on imipenem MICs measured using the L2 deletion mutant OprD strain H729(pHP2) (Fig. 27). These data suggested that this deletion substantially influenced the passage of both imipenem and lysine through OprD.

C. Effects of Deletions on Other Antibiotic Susceptibilities.

MICs of other antibiotics for strain H729 expressing the OprD deletion derivatives were also assessed. It was interesting to note that the deletion in L5 led to the enhancement of susceptibilities to different kinds of antibiotics, including β -lactams (cefpirome, cefotaxime and aztreonam), quinolones (ciprofloxacin and fleroxacin), chloramphenicol and tetracycline (Table IX). For chloramphenicol, the susceptibility increased 32-fold. Similar results were obtained for the deletions in L7 and L8, except that there were no differences in susceptibility to tetracycline (Table IX). The results indicated that the deletions may have resulted in a more open channel leading to a significant increase in the permeability of the channel to antibiotics that were normally excluded. This could be explained by the deletions either changing OprD from a specific porin to a general porin, or converting OprD to a specific channel with high general permeability as observed for the *E. coli* sucrose porin ScrY (Schülein et al., 1991).

To determine if the deletions in loops L5, L7 and L8 also affected the passage of imipenem and lysine through OprD (i.e. from specific to non-specific

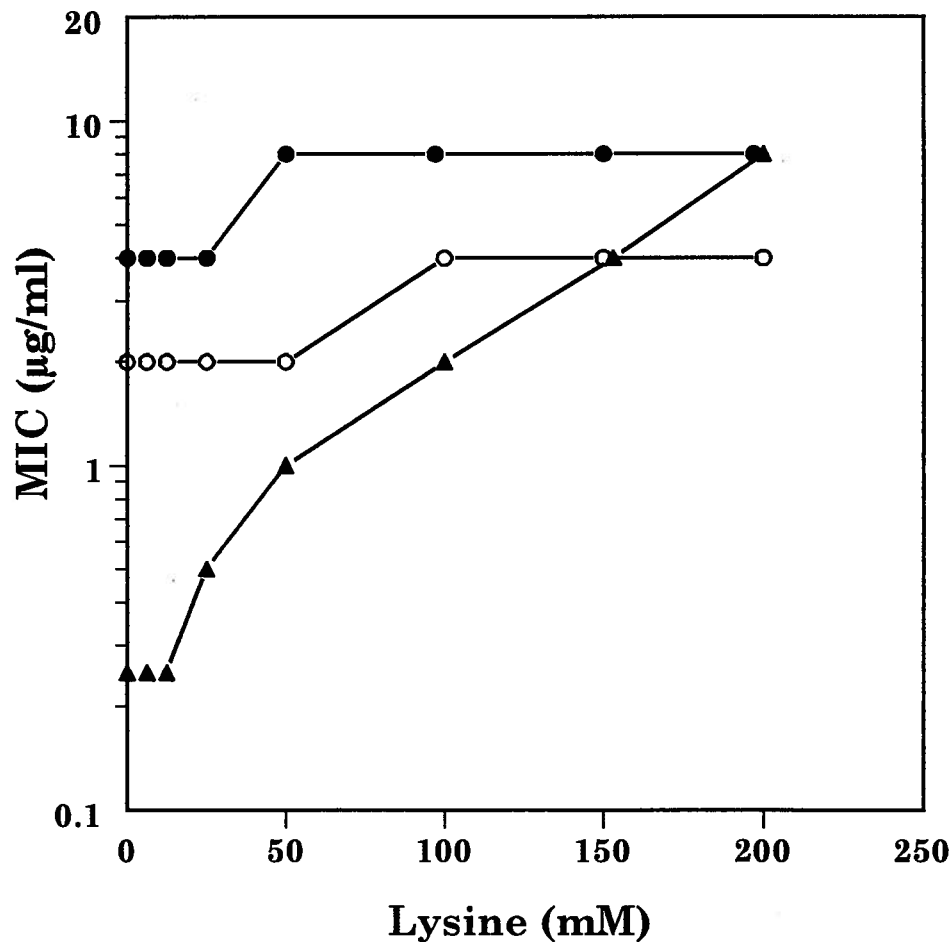


Figure 27: Competition between L-lysine and imipenem for OprD Δ L2.

Effect of L-lysine concentration in BM2 glucose medium on the susceptibility of OprD-defective strain H729 (filled circle), H729 expressing OprD with deletion in the predicted loop 2, H729(pHP2) (open circle) and H729 expressing native OprD, H729 (pXH2) (triangle) to imipenem.

Table IX: Effects of deletions on other antibiotic susceptibilities of *P. aeruginosa* strains.

Strains	MICs ($\mu\text{g/ml}$) ^a							
	Cefpirome	Cefotaxime	Aztreonam	Ciprofloxacin	Floxacin	Tetracycline	Chloramphenicol	
H729	1.0	4.0	1.0	0.125	0.5	6.25	25	
H729(pUCP19)	4.0	8.0	1.0	0.125	0.5	12.5	50	
H729(pXH2)	4.0	8.0	2.0	0.125	0.5	6.25	25	
H729(pHP1)	2.0	4.0	2.0	0.06	0.25	6.25	25	
H729(pHP2)	4.0	8.0	1.0	0.125	0.5	6.25	25	
H729(pHP5)^b	0.5^c	2.0^c	0.5^c	0.0156^c	0.06^c	0.78^c	0.78^c	
H729(pHP6)	8.0	8.0	2.0	0.25	1.0	12.5	50	
H729(pHP7)^b	0.5^c	2.0^c	0.5^c	0.0312^c	0.125^c	6.25	3.12^c	
H729(pHP8)^b	0.5^c	2.0^c	0.5^c	0.0312^c	0.125^c	6.25	3.12^c	

a. MICs were determined by the agar dilution method on Mueller-Hinton plates. Each MIC was determined three times independently.

b. The bold letters indicate the strains which showed differences in antibiotic susceptibilities.

c. The bold numbers indicate the MICs of antibiotics which were different from the controls.

uptake), competition experiments were performed. Figure 28 demonstrated that those deletions did not influence the binding of imipenem or lysine in the OprD channel.

D. Effects of Deletion on Sugar Transport.

To determine if the deletions in L2, L5, L7 and L8 affected the function of OprD as a channel for the transport of gluconate, strain H729 expressing those OprD derivatives were grown in BM2 minimal medium with gluconate as the carbon source at concentrations ranging from 0.5 to 10 mM. Except H729(pHP2), the growth rates of all the strains did not show significant differences from that of strain H729 expressing native OprD, suggesting that those deletions did not affect the passage of gluconate through OprD channel. For some unknown reason, H729(pHP2) did not grow in BM2 with gluconate as the carbon source.

E. Purification of the Mutant OprDs.

To investigate the *in vitro* functions altered by the deletion mutagenesis, OprD Δ L2 and OprD Δ L5 were purified (Fig. 29, lane 4 & 6) following similar procedures described for wild type OprD. The purified OprD Δ L2 retained OmpA-like heat modifiability, as observed for native OprD (Fig. 29, lane 5). However, OprD Δ L5 did not change banding position when solubilized at low temperature

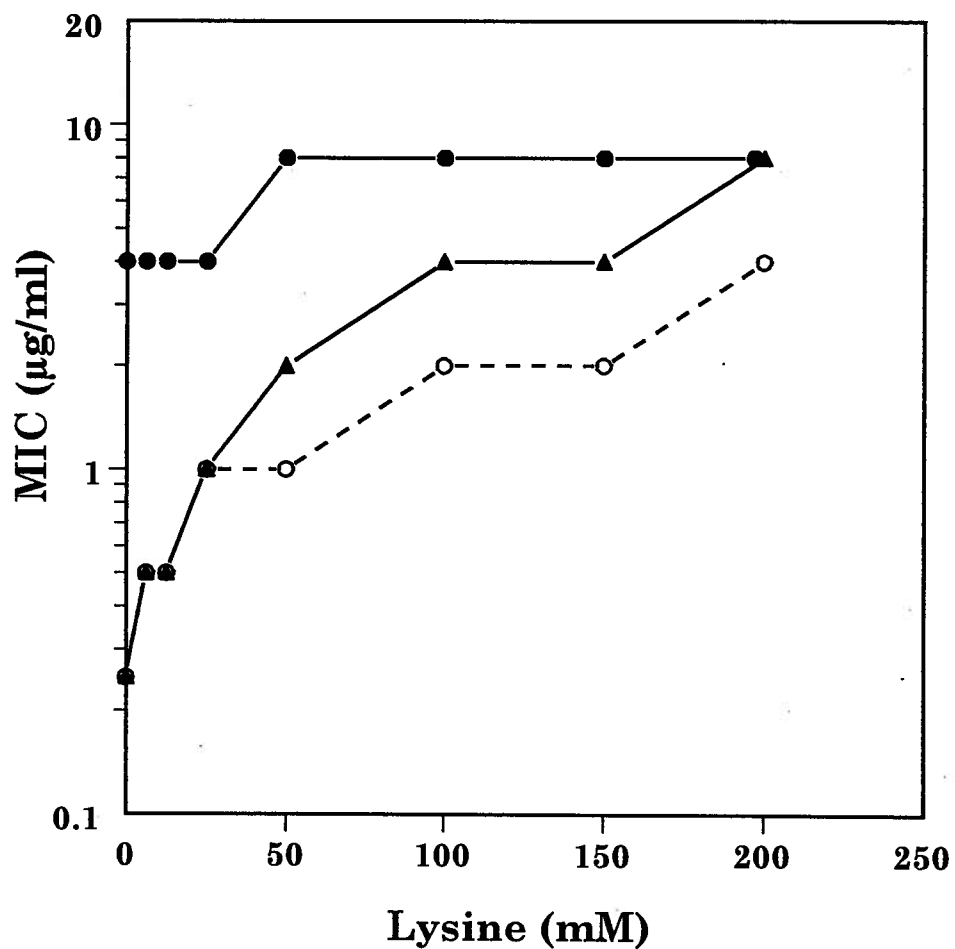


Figure 28: Competition between L-lysine and imipenem for OprD Δ L5/7/8.

Effect of L-lysine concentration in BM2 glucose medium on the susceptibility of OprD-defective strain H729 (filled circle), H729 expressing OprD with deletion in the predicted loop 5, H729(pHP5) (open circle, broken line) and H729 expressing native OprD, H792(pXH2) (triangle) to imipenem. The same results were obtained for strain H729(HP7) and H729(HP8) as that observed for H729(HP5).

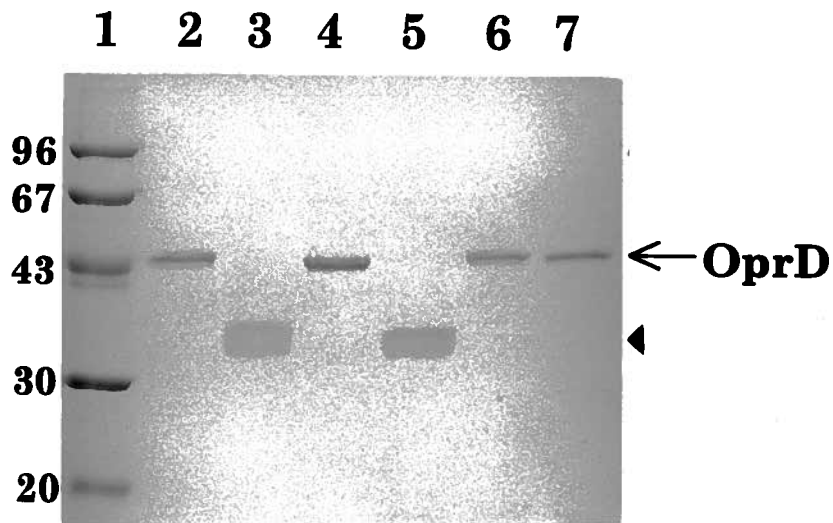


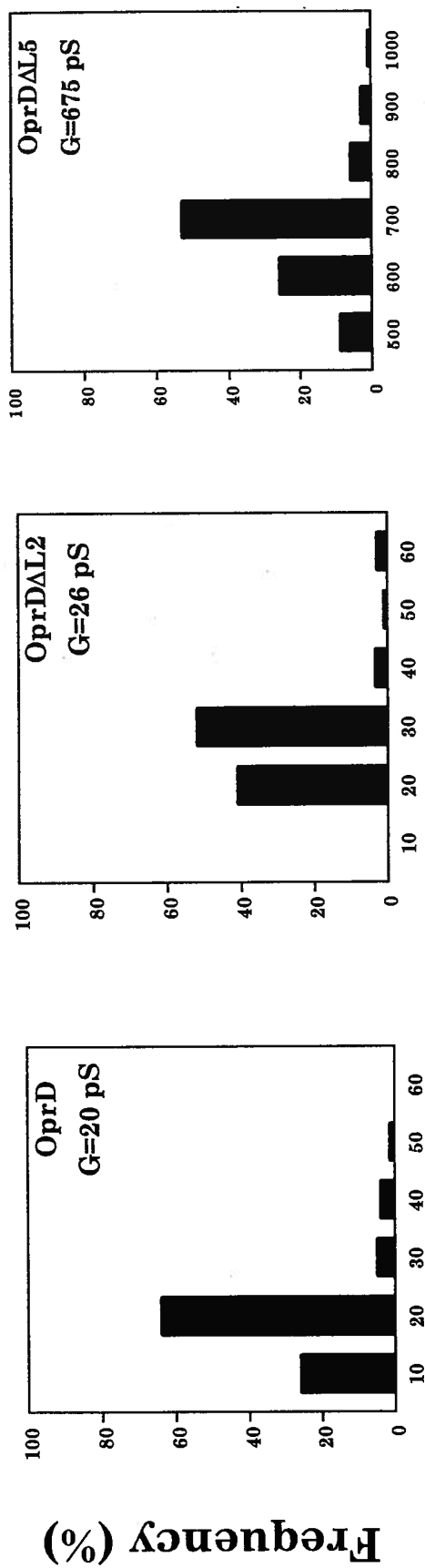
Figure 29: Comparison of heat-modifiabilities of the purified native OprD and mutant OprDs.

Lanes: 1, molecular weight markers; 2 & 3, native OprD; 4 & 5, OprD Δ L2; 6 & 7, OprD Δ L5. Lanes 2, 4, and 6 are heated samples, while lanes 3, 5 and 7 are the corresponding unheated samples.

prior to electrophoresis (Fig. 29, lane 7). The results suggested that the deletion may have affected the structural stability in such way that SDS could completely denature the protein at room temperature. Nevertheless, the purified OprD Δ L5 was still active, which was confirmed by being able to reconstitute channels in the black lipid bilayer model membrane (see below).

F. Effects of Deletion on the Physical Properties of the Channel.

The pore characteristics of OprD Δ L2 and OprD Δ L5 were further studied *in vitro* in black lipid bilayer experiments. At nanomolar concentrations, both porins were able to increase the specific conductance of the lipid bilayer by several orders of magnitude. The time-course of the increase was similar to that of OprD. After a rapid increase during 10~40 min, the membrane conductance increased at a much slower rate. The addition of the porins at much lower concentrations to the aqueous phases bathing lipid bilayer membranes allowed the resolution of stepwise increase in conductance. For OprD Δ L2, the average single channel conductance (26 pS in 1.0 M KCl) was slightly bigger than that of OprD (Fig. 30). However, mutant OprD with deletion in the predicted Loop L5 showed more than 30-fold increase in the average single channel conductance (675 pS in 1.0 M KCl) compared with that of the wild type OprD (Fig. 20B; Fig. 30). Measuring the average single channel conductance of the loop L5 deletion variant in KCl solutions ranging in concentration from 0.3 to 3.0 M showed a linear relationship between the salt



Conductance (pS)

Figure 30: Comparison of single channel conductance between native and mutant OprDs.

Histogram of the conductances observed with membranes formed by 1% oxidized cholesterol in n-decane upon addition to the aqueous phase of purified OprD, OprDAL2 and OprDAL5. G is the average single channel conductance of more than 100 events recorded.

concentration and single channel conductance (Table X). The much bigger single channel conductance confirmed the previous hypothesis that the deletion increased the general permeability of the channel, which in turn, increased the susceptibilities of H729(HP5) to different antibiotics (Table IX).

Earlier results showed that OprD was a weakly cation-selective channel. For both OprD Δ L2 and OprD Δ L5, increasing the size of cation caused a steady decrease in the average single channel conductance, while it was little affected by changing the size of anion (Table X), indicating they were still cation selective channels. Zero current membrane potential measurements confirmed that they had similar cation preferences to that of the wild type OprD (Table XI).

As described earlier (Chapter 2), macroscopic conductance due to native OprD, in 1.0 M KCl, could be inhibited by imipenem with an I_{50} value of 1.4 μ M (Fig. 31). In contrast, for OprD Δ L2, no decrease in conductance was observed up to the tenth addition of imipenem (Fig. 31, 0.2 μ M each addition). These results indicated that OprD Δ L2 had a much lower affinity for imipenem, which further suggested the deleted stretch was involved in the specific binding of imipenem. This *in vitro* property was also in agreement with the *in vivo* functional data for H729(HP2). In case of OprD Δ L5, the progressive decrease in conductance upon the addition of imipenem solution was still observed (Fig. 31), suggesting that the deletion did not affect the specific binding for imipenem. Therefore OprD Δ L5 was still a specific porin but with much higher general permeability, like the *E. coli* sucrose porin ScrY (Schülein et al., 1991).

Table X: Average single-channel conductance of the native and mutant OprD pores in different salt solutions.

Aqueous salt solutions	Conductance (pS)		
	WT OprD	OprD Δ L2	OprD Δ L5
0.3 M KCl	- ^a	- ^a	229
1.0 M KCl	20	26	675
3.0 M KCl	26	31	1711
1.0 M CsCl	15	<10	557
1.0 M LiCl	<10	- ^a	272
1.0 M KMOPS	19	25 ^b	640

- a. The single channel conductance was too small for the resolution of the equipment to detect.
- b. 1.0 M KMOPS was replaced by 1.0 M KNO₃, since the membrane was too noisy in 1.0 M KMOPS in the presence of OprD Δ L2.

Table XI: Zero-current membrane potentials.

Porins	Pc/Pa
WT OprD	2.60 ± 0.39
OprD Δ L2	2.90 ± 1.30
OprD Δ L5	2.61 ± 0.27

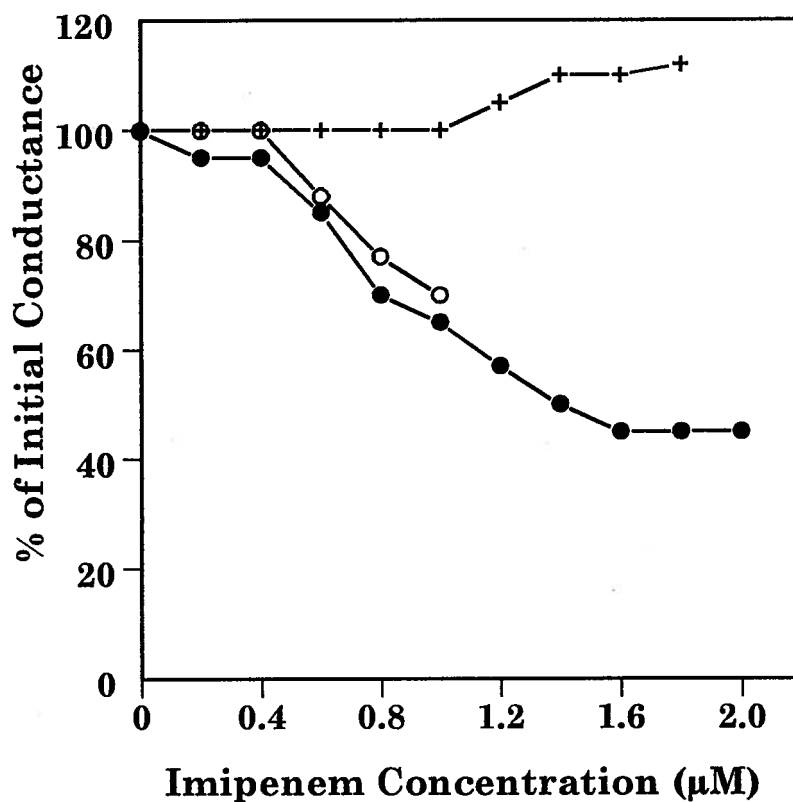


Figure 31: Macroscopic conductance inhibition experiments.

Macroscopic conductance inhibition experiments using native OprD (filled circle), OprD Δ L2 (plus) and OprD Δ L5 (open circle). Purified protein was added to the salt solution (1.0 M KCl) and the increase in membrane conductance due to insertion of porin pores was followed until the rate of increase had slowed (1~2 hours). At this time, aliquots of imipenem solution were added to the bathing salt solutions (volume 6 ml) in both compartments of the lipid bilayer chamber (i.e., to each side of the membrane) to increase the concentration in steps of 0.2 μM and stirred until the conductance stabilized (about 2 min). After a stable conductance level was achieved additional aliquots were added to each side of the membrane.

G. Summary.

In Chapter 3, an OprD topology model was proposed and 8 deletion mutants were made, one from each of the predicted external loops. Six of these deletion mutants could be expressed in the *P. aeruginosa* outer membrane. The effects of deletions on the *in vivo* and *in vitro* functions of OprD were examined in this chapter. OprD derivatives with deletions in loops, L1, L5, L6, L7 and L8 reconstituted similar imipenem supersusceptibility in the *P. aeruginosa* OprD-defective background. In contrast, L2 deletion mutant only partially reconstituted the supersusceptibility. Consistent with this, competition experiments showed that lysine had no significantly antagonistic effect on imipenem MICs for H729(HP2). Furthermore, purified OprD Δ L2 showed much lower affinity to imipenem in macroscopic conductance inhibition experiments. These data indicated that L2 was involved in imipenem binding. Another interesting mutant, L5 deletion mutant, resulted in supersusceptibility to many antibiotics, Further analysis confirmed that this deletion had changed OprD to a ScrY-like porin, a specific porin with high general permeability.

DISCUSSION

OprD is an interesting porin from the *P. aeruginosa* outer membrane since it facilitates the diffusion of basic amino acids and imipenem, a potent antibiotic that has been used for the therapy of *P. aeruginosa* infections. In this study, the *oprD* gene was cloned, nucleotide-sequenced and overexpressed in both *E. coli* and *P. aeruginosa*. These and other genetic manipulations provided effective approaches to investigating structure-function relationships in OprD, in an attempt to address the mechanism by which imipenem and nutrients diffuse through this specific porin.

A. Function of OprD in Antibiotic Uptake.

In this study, the genetic approach was employed to define the *in vivo* role of OprD in antibiotic uptake. Previous studies using clinical isolates had indicated a role for OprD in uptake of zwitterionic carbapenems, including imipenem. However, these clinical isolates had different genetic backgrounds and there was no convincing evidence presented that they were isogenic, differing only in their ability to produce OprD. Also, it was known that there were at least one regulatory locus (*opdE*) and one poorly understood multiple-antibiotic resistance locus (*nfxC*) (Fukuda et al., 1990) that could influence OprD expression and imipenem susceptibility. Furthermore, the potential for obtaining double mutants when using clinical strains or when selecting directly with antibiotics was reported (Zhou et al.,

1993). All these indicated the importance of utilizing truly isogenic strains obtained without direct antibiotic selection.

The strains constructed had identical genetic backgrounds except for their OprD levels (Table IV), as confirmed by their outer membrane protein profiles (Fig. 15). In addition, there were no significant differences in the growth rates of any of the strains in either rich medium or minimal medium. Therefore, the differences in MICs were only due to differing OprD levels. OprD was only moderately expressed in wild type strains like H103 in most growth media (Fig. 15). Nevertheless this level of expression was sufficient to enhance the uptake of imipenem and meropenem, since the OprD deficient mutant H729 was four fold more resistant to these antibiotics than the parent strain H103 (Table IV). However the level of OprD in strain H103 was insufficient to permit maximal uptake, and outer membrane permeability to imipenem and meropenem was still rate-limiting, since overexpression of OprD led to enhanced susceptibility to both antibiotics. These data confirmed OprD could facilitate the diffusion of imipenem/meropenem across *P. aeruginosa* outer membrane.

The MIC of imipenem for the OprD-defective strain H729 was 16 µg/ml, a concentration at which an isolate is considered resistant from a clinical perspective (Barza, 1985). It indicated a very slow diffusion of imipenem through non-specific porins and possibly non-porin pathways. The rate of such nonspecific diffusion processes is essentially proportional to the external concentration of imipenem (Trias et al., 1989). At an external concentration of 16 µg/ml, the diffusion rate of

imipenem through OprD would be predicted to be at least ten times higher than that through non-specific porins, and more than 95% of the imipenem molecules would diffuse through the saturable, specific channel formed by OprD (Trias and Nikaido, 1990b).

From a structural perspective, the facilitated diffusion of imipenem was due to the presence of a specific binding site(s) in the OprD channel, as confirmed by model membrane studies. The first crystal structure of a specific porin LamB revealed that a series of residues, located at the most constricted portion of and along the channel, interacted with maltose in a highly stereospecific fashion. Therefore, it might be anticipated that the high affinity of imipenem for the OprD channel resulted from similar binding process. Evidence for this included that some other carbapenems, for example, meropenem (Livermore and Yang, 1989), bipanem (Catchpole et al., 1992) and panipenem (Fukuoka et al., 1993), with similar structures to imipenem, could also utilize the OprD channel for the facilitated diffusion. All of these carbapenems have a single basic group at position 2 of a carbapenem. However, carbapenems lacking a basic residue (Trias and Nikaido, 1990a) or with one more basic group at position 1 or 6 (Fung-Tomc et al., 1995) could not use the OprD channel, reflecting the critical requirement for certain substrate structures by the channel. On the other hand, deletion of the binding sites located in L2 caused loss of the ability of imipenem to inhibit macroscopic conductance (Fig. 31).

Some authors have also suggested a role for OprD in uptake of quinolones

(Michea-Hamzhepour et al, 1991) or other antibiotics (Satake et al., 1990) in spite of their different chemical structures from imipenem. These conclusions were based in part on poorly defined clinical or experimental animal isolates, or on *in vitro* model liposome swelling experiments that have been criticized on other grounds (Bellido et al., 1992; Trias et al., 1989). The *in vivo* experiments described here, utilizing genetically defined isogenic variants, were more definitive. If OprD were to be involved in uptake of quinolones and other antibiotics, one would expect that the substantial overexpression of OprD in H103(pXH2) and H729(pXH2) would increase the normal low outer membrane permeability of *P. aeruginosa* and thus decrease MICs of these antibiotics. In contrast no significant alteration in susceptibility was observed. Therefore, OprD could only facilitate the diffusion of imipenem and those carbapenems with only one positive group at position 2.

B. Function of OprD in Nutrient Uptake: Is Lysine the Best Substrate?

There is no doubt that the original purpose of having OprD in the *P. aeruginosa* outer membrane was not for transport of imipenem, which would tend to result in cell death, but for the facilitated uptake of essential nutrients. Previous work demonstrated that basic amino acids and small peptides containing these amino acids were the natural substrates of the OprD channel (Trias and Nikaido, 1990b; Fukuoka et al., 1991). In this study, competition experiments using isogenic mutants confirmed that basic amino acids shared common binding sites with

imipenem in the OprD channel.

The function of OprD in transport of carbon sources was not examined in detail in the literature although other authors suggested a role for uptake of small sugars, based on results from liposome swelling experiments (Yoshihara and Nakae, 1989; Yoshihara et al., 1991). In this thesis, three isogenic strains including OprD-defective strain H729, wild type strain H103 and OprD-overexpressing strain H103(pXH2) were utilized to investigate the role of OprD in transport of three commonly used carbon sources for *P. aeruginosa*: gluconate, glucose and pyruvate. Previous work demonstrated that OprF was the major porin for uptake of di-, tri- and tetrasaccharides (Bellido et al., 1992). However OprF levels did not influence growth on gluconate. Consistent with this, it was demonstrated here that OprD was the major porin for gluconate in that its absence (in strain H729 *oprD*:: Ω) led to a nearly three fold decrease in growth rate on 0.5~1.0 mM gluconate (compared with the parent strain H103), whereas its overexpression resulted in a 70% increase in growth rate (Fig. 16A). As expected for an outer membrane diffusion-limited process, these differences disappeared at high concentrations, at which concentrations other porins including OprF might be expected to function adequately. In addition, no significant differences in the rates of growth on glucose or pyruvate or on rich media were observed regardless of OprD expression levels (Fig. 16), indicating that the results for gluconate were not due to metabolic disturbances caused by the loss or overexpression of OprD. The result obtained for glucose did not indicate that OprD is unable to permit the passage of glucose since

these studies were performed in strains capable of being induced for the glucose specific porin OprB. However, given the approximately 5 fold higher level of OprD than OprB in strain H103(pXH2) grown on glucose, it seems likely that OprD has at best a minor role in glucose uptake, as confirmed in part by the data in Table VI.

To see if gluconate might be an analog of basic amino acids and imipenem, we compared their three-dimensional structures by using the computer program HyperChem. Except for the common possession of a carboxyl group, gluconate was not structurally related to the basic amino acids or imipenem. This was also confirmed by competition experiments (Table VI), which suggested that common binding sites were not involved in imipenem and gluconate passage through OprD. Three possibilities were proposed to explain how the OprD channel might facilitate the transport of gluconate. First, since both basic amino acids and imipenem contain carboxyl groups and since the only difference between gluconate and glucose is that the former has a carboxyl group, the carboxyl group might function in directing the molecules to the channel and in binding to sites within the channel. Second, there might be two functional domains in the OprD channel, one for the binding of basic amino acids and the other one for gluconate. Third, given the low outer membrane permeability of *P. aeruginosa*, gluconate may pass through the channel in a nonspecific fashion. This latter suggestion would make the OprD channel analogous to the sucrose porin ScrY which has the properties of both substrate-specific and general porins (Schülein et al., 1991).

Despite the fact that basic amino acids could diffuse efficiently through the

OprD channel, there were a few pieces of evidence which suggested that basic amino acids may not be the best natural substrate of this channel. First, the affinity of the channel toward basic amino acids was much lower than its affinity toward the presumably "unnatural" analog, imipenem. A competition experiment showed that the concentration of lysine (100 to 200 mM) required to completely block the transport of imipenem was 2,000 to 4,000 times higher than the corresponding imipenem concentration (0.05 mM) (Fig. 17). Consistent with this, I did not observe the inhibition of the macroscopic conductance when titrated with lysine solution in model membrane system, possibly because the small volume of the testing chamber (6 ml) could not build up high enough concentration of lysine to block the transport of KCl. Second, the channel clearly preferred the D-isomers of lysine and arginine over their L-isomers (Trias and Nikaido, 1990b). Third, the OprD channel could also facilitate the diffusion of a wide variety of peptides, including di-, tri- and tetrapeptides with basic amino acids at the COOH-terminal position, or dipeptides with basic amino acids at the NH₂-terminal position followed by a small amino acid residue at the COOH-terminal position (Trias and Nikaido, 1990b). These suggested that imipenem is really a dipeptide analogue, a suggestion that matches with its unique susceptibility to hydrolysis by renal dipeptidase. Thus the fit of basic amino acids into the binding site may be rather poor.

C. Prediction of an OprD Membrane Topology Model.

Functional studies have indicated that OprD could facilitate the uptake of basic amino acids and imipenem by virtue of possessing specific binding sites, but no previous work had been done to identify the structural characteristics of this porin or the specific binding sites which are involved in antibiotic and nutrient uptake through this specific channel. In the absence of crystallographic data, this thesis presented a prediction of the topology model of OprD and an approach to assess the accuracy of this model.

The published crystal structures of the general porins and specific porins reveal consensus structures. They all form trimers of identical subunits, each monomer subunit consisted of 16 or 18 anti-parallel β -strands forming a barrel surrounding a pore. These strands are connected by very short loops on the periplasmic face of the porin whereas the loops on the outside of the bacteria are of variable length but in general are longer (Cowan et al., 1992; Weiss and Schulz, 1992; Kreuzsch et al., 1994; Schirmer et al., 1995). Analysis of the structures of a family of bacterial general porins by sequence alignment and structure predictions suggested similar structures for all of the general porins in the porin superfamily (Jeanteur et al., 1991). *P. aeruginosa* OprD, like other specific porins, was considered unlikely to align with the porin superfamily. However, the transmembrane segments of OprD showed good homology with the known β -strands of OmpF (Fig. 21). A more detailed study by Dr. Denis Jeanteur subsequently indicated that OprD was the first specific porin which could be aligned with the porin superfamily (Appendix, Fig. 33)

To verify the accuracy of the model, an efficient site-directed deletion mutagenesis technique was developed in this study. The utilization of PCR resulted in a high ratio of mutant to wild type fragments. The two strategies used here, direct extension and overlap extension, are of general applicability. The rapid screening step allowed us to sequence only those clones with the desired deletions. By using Vent DNA polymerase and optimizing the PCR conditions, the average error frequency was lowered to 1 in 2,000 base pairs. Given the substantial saving in time, general feasibility for obtaining the deletion, and low rate of undesired mutations, these techniques can be applied to any membrane protein.

The OprD model provided a prediction of the flexible segments (loops) of OprD. Generally speaking, insertions or deletions in porins should be non-disruptive of overall structures only if they occur in the surface loops. Comparison between the crystal structures of OmpF and PhoE demonstrated that all the evolutionary insertions or deletions were restricted to the loop regions and a single short turn (Cowan et al., 1992). Consistent with this, sequence comparisons of porins from distant families showed that the loop regions often varied substantially in length, in contrast to the highly conserved β -strands (Jeanteur et al., 1994a). One reason is that selective pressure from the environment, eg. antibiotics or phages may play a role in allowing certain regions to evolve at rates higher than others. Another possible explanation is that the external loops simply have more freedom to change without altering porin secretion, folding or the ability to form a transmembrane channel. For example, deletions of certain PhoE cell surface-

exposed regions did not interfere with the translocation across the inner membrane or the incorporation into the outer membrane (Agterberg et al., 1989). Moreover, spontaneous deletions located in the OmpF or OmpC external loops could produce mutant OmpF or OmpC proteins which were not only active but also allowed the passage of large maltodextrins (Benson et al., 1988; Misra and Benson, 1988). In contrast, the membrane spanning segments contribute especially to the conformation required for stability, folding or outer membrane localization, since studies involving deletion mutagenesis of PhoE, removing either the first (Bosch et al., 1988) or the last (Bosch et al., 1989) transmembrane segment, drastically affected or completely inhibited incorporation into the outer membrane.

Three criteria were used to evaluate whether the mutant proteins folded into near-native configurations. First, the polypeptides encoded by mutant OprD alleles in *E. coli* and the native host *P. aeruginosa* were identified (Fig. 23 & 24). The high levels of expression and correct location in the outer membrane of OprD derivatives containing deletions of the presumed loops L1, L2 and L5 to L8, were consistent with our model. The deletion of the predicted L3 was tolerated in *E. coli*, but resulted in reduced expression. The same phenomenon was observed for certain deletion mutants of PhoE (Agterberg et al., 1989). We anticipated that, as for other members of the porin superfamily, L3 may be involved in forming the 'eyelet' region. In *E. coli* porins, the individual residues involved in the eyelet are highly conserved, and mutations in this region could affect the size, conductivity and specificity of the channel (Jeanteur et al., 1994b). In addition, such mutations also

destabilized the trimer in many cases (Lakey et al., 1991). These may account for the diminished expression. The L3 deletion mutant did not direct the production of any OprD in the outer membrane of *P. aeruginosa*. This may reflect an innate and more efficient ability of *P. aeruginosa* to proteolyse unstable products, compared to *E. coli*. A second criterion used to assess configuration was trypsin susceptibility (Fig. 26). All of the OprD derivatives were resistant to digestion to some extent, indicating that the deletions did not cause extensive alterations in configuration. The third criterion was functional activity (Table VIII). All of the tolerated deletion mutant OprDs could form functional channels and did not grossly disrupt the outer membrane since it retained its barrier properties against polymyxin, gentamicin and trimethoprim (Table VIII). Five of the deletion mutants could reconstitute full imipenem and meropenem susceptibility. Only one, the loop L2 deletion mutant, lost the ability to reconstitute full susceptibility, suggesting a possible role for loop L2 in imipenem binding.

D. Molecular Architecture of the OprD Channel.

Structural and functional studies allowed construction of a molecular architecture for the interior of the OprD channel (Fig. 32). In the crystal structure of specific porin LamB, more than one loop folds inside the channel, including L3, which was entirely folded into the barrel to form the eyelet, whereas L1 and L6 from the same monomer and L2 from the adjacent monomer were folded inward to

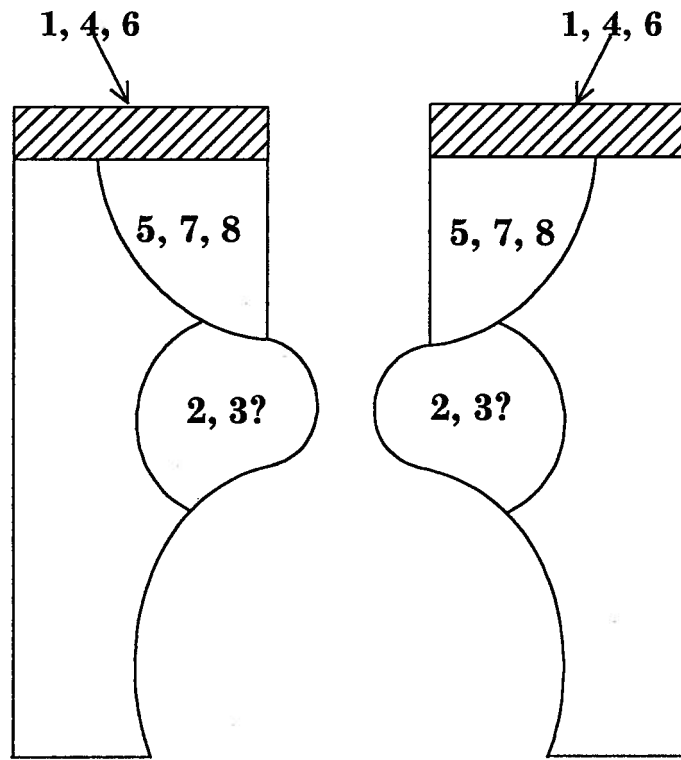


Figure 32: Schematic representation of the predicted interior architecture of the OprD channel.

different extents. Similarly, I predict that five loops may fold inside the OprD channel. L2 and possibly L3 are proposed to completely fold into the barrel, and together with some residues from the barrel walls, form the constriction zone toward the middle of the channel. In addition, L5, L7 and L8 would be partially or completely folded into the channel to further restrict the lumen at the channel entrance (especially L5). The other loops, L1, L6 and possibly L4, together with the surface-exposed portion of the partially inward folded loops would be arrayed on the surface of OprD. One of these loops might reach into the neighbouring monomer and be involved in stabilizing the trimer. This model is consistent with all the functional data presented in this thesis.

Several pieces of evidence supported the involvement of L2 in the eyelet region. First, the L2 mutant only partially reconstituted the supersusceptibility to imipenem in the OprD-defective background H729. For meropenem, the difference in MICs between H729 and H729(pHP2) was only 2-fold, which by convention, could be considered insignificant (Table VIII). The results indicated that the uptake of imipenem and meropenem was seriously affected by this deletion. In addition, competition experiments demonstrated that the deletion substantially influenced the uptake of lysine, since lysine lost its antagonistic effects on imipenem MIC for H729(pHP2) (Fig. 27). Consistent with this, imipenem was unable to inhibit the macroscopic conductance of KCl through channels formed by OprD Δ L2 (Fig. 31). All of these data indicated that the deleted stretch was critical for the efficient binding of imipenem and basic amino acids. From the crystal structure of LamB,

all the residues identified to be responsible for the binding of maltodextrin were located in the eyelet region (Hofnung, 1995). Therefore, L2 was very likely located in the eyelet region of the OprD channel. However, our data did not preclude the co-involvement of loop L3 which, in all of the structurally defined porins, folds into the center of the channel to form the 'eyelet' region determining channel diameter and selectivity.

The placements of L5, L7 and L8 were based on the fact that the deletions performed on these predicted loops led to the enhancement in susceptibilities to those antibiotics which cross outer membrane through the hydrophilic pathway (Table IX). The antibiotics included β -lactams, quinolones, chloramphenicol and tetracycline (the latter for the L5 deletion mutant only). Control experiments indicated that the deletions did not disrupt the integrity of the outer membrane, or substantially affect the growth rates of the mutants. Therefore, the supersusceptibilities were only due to the deletions resulting in more open channels with higher permeability. In good agreement with this, the single channel conductance of OprD Δ L5 (675 pS) was more than 30 times higher than that of native OprD (20 pS). Interestingly, these deletions did not affect the specific binding site(s), as confirmed by the antagonistic effects of lysine concentration on imipenem MICs for the mutants (Fig. 28), and the retention of the ability of imipenem to inhibit macroscopic conductance for the OprD Δ L5 channels (Fig. 31). Therefore, these 3 loops were not involved in the eyelet region. Instead, they were similar to L1, L2 and L6 of LamB, which folded inward and restricted the size of

the entrance to this channel. The MICs of chloramphenicol and tetracycline for H729(pHP7) and H729(pHP8) were 4-fold and 8-fold higher than the MICs for H729(pHP5), respectively (Table IX). The chemical structures of these two antibiotics are quite bulky, and the four-ring-structured tetracycline is even bulkier than chloramphenicol. In order to allow the maximum passage of these two antibiotics, I propose that the channel has to be more open. Therefore the differences in MICs could be explained if the deletion of the predicted L7 and L8 did not open the channel as widely as did the deletion of L5. Based on this, I assumed that L5 contributed the most to restricting the channel size, whereas L7 and L8 only partially restricted the channel size.

Regarding other loops such as L1 and L6, the deletions did not significantly affect susceptibilities to imipenem or the other antibiotics tested (Table VIII & IX), suggesting that these two loops were not as important in determining the channel size or selectivity. Therefore, L1, L6 and possibly L4 are proposed to be completely exposed at the cell surface, and with surface-exposed parts of L7 and L8, they cover most of the outer surface of OprD.

The modelling of channel architecture supported the assumption that outer membrane permeability is important for antibiotic susceptibility. The single channel conductances of the channels could be ordered as OprD (20 pS) < OprD Δ L2 (26 pS) < OprD Δ L5 (675 pS). The small size of the native OprD channel presumably served to maintain the low intrinsic permeability of the *P. aeruginosa* outer membrane (Nicas and Hancock, 1983a). Deletion of the predicted loop L2

slightly opened the channel, so it did not enhance the susceptibilities to the antibiotics tested, except imipenem and meropenem. The L7 and L8 deletion derivatives, presumably opened the channel significantly, resulting in increased susceptibilities to β -lactams, quinolones, and chloramphenicol. However these two mutant channels were still not as large as the L5 deletion mutant channel since they were not able to increase the susceptibility to tetracycline (Table IX). The only difference between H729(pXH2) and H729(pHP5) was that the latter one contained a deletion of 8 amino acids from OprD, resulting in the presence of a large channel in *P. aeruginosa* outer membrane. The supersusceptibility of H729(pHP5) thus supported the important role of the outer membrane of *P. aeruginosa* as a barrier to antibiotics (Nikaido and Hancock, 1986).

E. The Journey of Imipenem Through the OprD Channel.

The molecular architecture of OprD is helpful in understanding the process of imipenem uptake. The journey of imipenem and basic amino acids through the OprD channel may be depicted as follows. The initial prescreening regarding size and charge might be done by the loops exposed at the cell surface. These could function as a primary filter, concentrating the substrates such as imipenem and basic amino acids, especially when they were in low concentrations in the medium. The substrate molecule would then enter the mouth of the channel which would be constricted by L5, L7 and L8. Similar to the maltose transport system, small

peptides and imipenem are long molecules, which exceeded, in their long axis, the exclusion limit of the OprD channel. Therefore, the residues located at the mouth would orient imipenem and peptides so that they would be aligned to the pore axis. It is unknown whether the same "greasy slide" could be applied to the OprD channel, but for the efficient transport of such extended molecules, there must be residues located along the channel to guide their diffusion. The substrate molecules would then encounter the constriction zone about half way through the channel, at which position side chains, largely comprising charged residues from L2, possibly L3, and the barrel wall would bind to the substrates in a highly stereospecific manner influenced by the size, geometry and charge of the substrate molecule. This would presumably account for the specificity of the channel. After the passage through the narrow constriction zone, the imipenem molecule would be effectively released into the bulk solvent. In spite of the structural similarity in side chains between imipenem and basic amino acid containing dipeptides, it is obvious that imipenem has a carbapenem nucleus which is quite different from the peptide backbone (Fig. 3), and this might be the reason for the different affinities between imipenem and basic amino acids as described before. The higher affinity of imipenem suggested that imipenem could fit in the specific binding site(s) better than basic amino acids. On the other hand, it is possible that the specific binding site(s) might be located in such a way that they could have good but not very high affinity for various nutrients of similar structures, such as basic amino acids and small peptides containing these amino acids. The carbapenems with one additional

positive group at position 1 or 6 might be excluded from the mouth due to their bulkiness or they might not be able to fit into the specific binding site(s). Regarding the uptake of gluconate, certain positive charged residues located at the filter or mouth might attract its carboxyl group. After gluconate entered the channel, its small size might permit the diffusion at a reasonable speed.

F. General Porins and Specific Porins.

Porins have been subdivided into 2 classes, specific porins and general porins (Hancock, 1987). *R. capsulatus* porin has been classified as a general porin. However, in the crystal structure, a solute binding site was observed within the pore at the external side of the eyelet, with an unknown solute co-crystallized in it (Weiss and Schulz, 1992). Furthermore, this porin has been reported to bind efficiently to tetrapyrrolo (Bollivar and Bauer, 1992). Therefore, the *R. capsulatus* porin that had been previously suggested to belong to a class of general porins can behave as both specific and non-specific porins, depending on the solute. Based on this observation, Schulz (1993) first proposed that all porins might have specific substrates, but that these specific substrates have been detected in only few porins. The first supporting data were from crystal structures of general porins and specific porin. Although there is no detectable sequence homology and a different number of β -strands, the resemblance of the maltoporin folding to that of the general porins is obvious. In addition, general porins also generate a local electrostatic field near

the channel constriction zone, sufficient to orient small hydrophilic molecules and repel hydrophobic ones (Schulz, 1993), suggesting that there is only a quantitative difference between the filtering and binding. The alignment of the OprD sequence with the porin superfamily provided further strong evidence to support Schulz's proposal about the dual nature of porins.

From the crystal structure of LamB, the entrance of the pore was highly covered by surface-exposed loops. In addition, several loops folded inside to further restrict the entrance. Therefore it was not surprising that LamB has a low single channel conductance (0.15 nS) (Benz et al., 1986). Consistently, it has been found that many specific porins have pore sizes which are about one order of magnitude smaller than those of the general diffusion pores, such as OmpF of *E. coli* (1.8 nS). For example, *P. aeruginosa* OprD (0.02 nS), OprP (0.25 nS) (Hancock and Benz, 1986), and *E. coli* Tsx (0.01 nS) (Benz et al., 1988), all demonstrated very low single channel conductances in model membrane studies. However, there are also specific porins with high conductivity, almost equivalent to that of OmpF, for example, *E. coli* ScrY (1.4 nS) and *P. aeruginosa* OprD Δ L5 (0.67 nS). From a structural perspective, all porins have an analogous β -barrel structure, with at least one internal loop defining the selectivity. "Specific" porins have more loops folded into the channel to prefilter molecules by further restricting the entrance of molecules based on their size and charge. Therefore they would have a decreased exclusion limit for molecules other than the given substrates, which in turn, would make the uptake of those specific substrates as their predominant functions. "General"

porins, in contrast, would have less loops (only one) folded inside, and thus offer more open channels which would allow the non-specific diffusion of many other molecules at a significant rate. Despite these differences, it seems possible that many porins are both specific and general in nature.

REFERENCES

- Albers-Schönberg G., B.H. Arison, O.D. Hensens, J. Hirschfield, K. Hoogsteen, E.A. Kaczka, R.E. Rhodes, J.S. Kahan, F.M. Kahan, R.W. Ratcliffe, E. Walton, L.J. Ruswinkle, R.B. Morin, and B.G. Christensen. 1978. Structure and absolute configuration of thienamycin. *J. American Chemical Society*. **100**: 6491-6499.
- Angus, B.L., A.M. Carey, D.A. Caron, A.M.B. Kropinski, and R.E.W. Hancock. 1982. Outer membrane permeability in *Pseudomonas aeruginosa*: comparison of a wild-type with an antibiotic-supersusceptible mutant. *Antimicrob. Agents Chemother.* **12**: 299-309.
- Agterberg, M., H. Adriaanse, E. Tijhaar, A. Resink, and J. Tommassen. 1989. Role of the cell surface-exposed regions of outer membrane protein PhoE of *Escherichia coli* K12 in the biogenesis of the protein. *Eur. J. Biochem.* **185**: 365-370.
- Atkinson, T. and M. Smith. 1984. Purification of oligonucleotides obtained by small scale (0.2 μ mol) automated synthesis by gel electrophoresis. In "Oligonucleotide Synthesis: A practical Approach", M.J. Gait (ed.). IRL Press, Oxford, 35-81.
- Barza, M. 1985. Imipenem: first of a new class of beta-lactam antibiotics. *Annals of Internal Medicine*. **103**: 552-560.
- Bauer, K., M. Struyvé, D. Bosch, R. Benz, and J. Tommassen. 1989. One single residue is responsible for the special interaction between polyphosphate and the outer membrane porin PhoE of *Escherichia coli*. *J. Biol. Chem.* **264**: 16393-16398.
- Bellido, F., N.L. Martin, R.J. Siehnel, and R.E.W. Hancock. 1992. Reevaluation, using intact cells, of the exclusion limit and role of porin OprF in *Pseudomonas aeruginosa* outer membrane permeability. *J. Bacteriol.* **174**: 5196-5203.
- Benson, S.A., J.L.L. Occi, and B.A. Sampson. 1989. Mutations that alter the pore function of the OmpF porin of *Escherichia coli* K12. *J. Mol. Biol.* **203**: 961-970.
- Benz, R., K. Janko, and P. Lauger. 1978. Formation of large ion-permeable membrane channels by the matrix protein (porin) of *Escherichia coli*. *Biochim. Biophys. Acta* **511**: 238-247.
- Benz, R., and R.E.W. Hancock. 1981. Properties of the large ion-permeable pores formed from protein F of *Pseudomonas aeruginosa* in lipid bilayer membranes. *Biochim. Biophys. Acta* **646**: 298-308.
- Benz, R., A. Schmid, and R.E.W. Hancock. 1985. Ion selectivity of gram-negative bacterial porins. *J. Bacteriol.* **162**: 722-727.

Benz, R.A., A. Schmid, T. Nakae, and G.H. Vos-Scheperkeuter. 1986. Pore formation by LamB of *Escherichia coli* in lipid bilayer membranes. *J. Bacteriol.* **165**: 978-986.

Benz, R., A. Schmid, and G.H. Vos-Scheperkeuter. 1987. Mechanism of sugar transport through the sugar-specific LamB channel of *Escherichia coli* outer membrane. *J. Membr. Biol.* **100**: 21-29.

Benz, R.A., A. Schmid, T. Nakae, C. Maier, and E. Bremer. 1988. Characterization of the nucleotide-binding site inside the Tsx channel of *Escherichia coli* outer membrane reconstituted experiments with lipid bilayer membranes. *Eur. J. Biochem.* **176**: 699-705.

Benz, F., A. Schmid, W. Wagner, and W. Doebel. 1989. Pore formation by the *Escherichia coli* hemolysin: evidence for an association-dissociation equilibrium of pore-forming aggregates. *Infect. Immun.* **57**: 887-895.

Bollivar, D.W., and C.E. Bauer. 1992. Association of tetrapyrrole intermediates in the bacteriochlorophyll a biosynthetic pathway with the major outer-membrane porin protein of *Rhodobacter capsulatus*. *Biochem. J.* **282**: 471-476.

Bosch, D., and J. Tommassen. 1987. Effects of linker insertion on the biogenesis and functioning of the *Escherichia coli* outer membrane pore protein PhoE. *Mol. Gen. Genet.* **208**: 485-489.

Bosch, D., W. Voorhout, and J. Tommassen. 1988. Export and localization of N-terminally truncated derivatives of *Escherichia coli* K-12 outer membrane protein PhoE. *J. Biol. Chem.* **263**: 9952-9957.

Bosch, D., M. Scholten, C. Verhagen, and J. Tommassen. 1989. The role of carboxy-terminal membrane-spanning fragment in the biogenesis of *Escherichia coli* K-12 outer membrane protein PhoE. *Mol. Gen. Genet.* **216**: 144-148.

Boulain, J.C., A. Charbit, and M. Hofnung. 1986. Mutagenesis by random linker insertion into the *lamB* gene of *Escherichia coli* K-12. *Mol. Gen. Genet.* **205**: 339-348.

Brown, M.R.W. The role of the cell envelope in resistance. In "Resistance of *Pseudomonas aeruginosa*", M.R.W. Brown (Ed.), printed in Great Britain by J. W. Arrowsmith Ltd, Bristol, 71-107.

Bryan, L.E. 1979. Resistance to antimicrobial agents: The general nature of the problem and the basis of resistance. In "*Pseudomonas aeruginosa*: Clinical Manifestations of Infection and Current Therapy", R.G. Doggett (Ed.), Academic

Press, New York, 219-270.

Büscher, K.H., W. Cullmann, W. Dick, and W. Opferkuch. 1987. Imipenem resistance in *Pseudomonas aeruginosa* resulting from diminished expression of an outer membrane protein. *Antimicrob. Agents Chemother.* **31**: 703-708.

Catchpole, C.R., R. Wise, D. Thornber, and J.M. Andrews. 1992. In vitro activity of L-627, a new carbapenem. *Antimicrob. Agents Chemother.* **36**: 1928-1934.

Cornette, J.L., K.B. Cease, H. Margalit, J.L. Spouge, J.A. Berzofsky, and C. Delisi. 1987. Hydrophobicity scales and computational techniques for detecting amphipathic structures in proteins. *J. Mol. Biol.* **195**: 659-685.

Cowan, S.W., T. Schirmer, G. Rummel, M. Steiert, R. Ghosh, R.A. Pauptit, J. Jansonius, and J.P. Rosenbush. 1992. Crystal structures explain functional properties of two *E. coli* porins. *Nature* **358**: 727-733.

Cronan, J.E., R.B. Gennes, and S.R. Maloy. 1987. Cytoplasmic membrane. In "*Escherichia coli* and *Salmonella typhimurium*: Cellular and Molecular Biology", F.C. Neidhardt (ed.) ASM Publications, Washington, D.C., 31-55.

Devereux, J., P. Haeblerli, and O. Simthies. 1984. A comprehensive set of sequence analysis programs for the VAX. *Nucl. Acids Res.* **12**: 387-395.

Ditta, G., T. Schmidhauser, E. Yakobson, P. Lu, X.W. Liang, D.R. Finlay, D. Guiney, and D.R. Helinski. 1985. Plasmids related to the broad host range vector, pRK290, useful for gene cloning and for monitoring gene expression. *Plasmid* **13**: 149-153.

Drewry, D.T., K.C. Symes, G.W. Gray, and S.G. Wilkinson. 1975. Studies of polysaccharide fractions from the lipopolysaccharide of *Pseudomonas aeruginosa* NCTC 1999. *Biochem. J.* **149**: 93-106.

Eisenberg, D., R.M. Weiss, and T.C. Terwilliger. 1982. The helical hydrophobic moment: a measure of the amphiphilicity of a helix. *Nature* **299**: 371-374.

Ferenci, T., and K.S. Lee. 1982. Direct evolution of the lambda receptor of *Escherichia coli* through affinity chromatographic selection. *J. Mol. Biol.* **160**: 431-444.

Foulds, J. 1976. *tolF* Locus in *Escherichia coli*: chromosomal location and relationship to loci *cmlB* and *tolD*. *J. Bacteriol.* **128**: 604-608.

Freundlieb, S., U. Ehmann, and W. Boos. 1988. Facilitated diffusion of *p*-

nitrophenyl- α -D-maltohexaoside through the outer membrane of *Escherichia coli*. J. Biol. Chem. **263**: 314-320.

Fukuda, H., M. Hosaka, K. Hirai, and S. Iyobe. 1990. New norfloxacin resistance gene in *Pseudomonas aeruginosa* PAO. Antimicrob. Agents Chemother. **34**: 1757-1761.

Fukuoka, T., N. Masuda, T. Takenouchi, N. Sekine, M. Iijima, and S. Ohya. 1991. Increase in susceptibility of *Pseudomonas aeruginosa* to carbapenem antibiotics in low-amino-acid media. Antimicrob. Agents Chemother. **35**: 529-532.

Fukuoka, T., S. Ohya, T. Narita, M. Katsuta, M. Iijima, N. Masuda, H. Yasuda, J. Trias, and H. Nikaido. 1993. Activity of carbapenem panipenem and role of the OprD (D2) protein in its diffusion through the *Pseudomonas aeruginosa* outer membrane. Antimicrob. Agents Chemother. **37**: 322-327.

Fung-Tomc, J. C., E. Huczko, J. Banville, M. Menard, B. Kolek, E. Gradelski, R. E. Kessler and D. P. Bonner. 1995. Structure-activity relationships of carbapenems that determine their dependence on porin protein D2 for activity against *Pseudomonas aeruginosa*. Antimicrob. Agents Chemother. **39**: 386-393.

Gehering, K., C.H. Cheng, H. Nikaido, and B.K. Jap. 1991. Stoichiometry of maltodextrin-binding sites in LamB, an outer membrane protein from *Escherichia coli*. **173**: 1873-1878.

Gotoh, N., H. Wakebe, E. Yoshihara, T. Nakae, T. Nishino, 1989. Role of protein F in maintaining structural integrity of the *Pseudomonas aeruginosa* outer membrane. J. Bacteriol. **171**: 983-990.

Hanahan, D. 1983. Studies on the transformation of *Escherichia coli* with plasmids. J. Mol. Biol. **166**: 557-580.

Hancock, R.E.W. and A.M. Carey. 1979. Outer membrane of *Pseudomonas aeruginosa*. Heat- and 2-mercaptoethanol-modifiable proteins. J. Bacteriol. **140**: 902-910.

Hancock, R.E.W. and A.M. Carey. 1980. Protein D1-a glucose-inducible, pore-forming protein from the outer membrane of *Pseudomonas aeruginosa*. FEMS Microbiol. Lett. **8**: 105-109.

Hancock, R.E.W. 1981. Aminoglycoside uptake and mode of action-with special reference to streptomycin and gentamicin. J. Antimicrob. Chemother. **1981**: 249-276.

Hancock, R.E.W., R.T. Irvin, J.W. Costerton, and A.M. Carey. 1981a. *Pseudomonas aeruginosa* outer membrane: peptidoglycan-associated proteins. *J. Bacteriol.* **145**: 628-631.

Hancock, R.E.W., V.J. Raffle, and T.I. Nicas. 1981b. Involvement of the outer membrane in gentamicin and streptomycin uptake and killing in *Pseudomonas aeruginosa*. *Antimicrob. Agents Chemother.* **19**: 777-785.

Hancock, R.E.W., K. Poole, and R. Benz. 1982. Outer membrane protein P of *Pseudomonas aeruginosa*: regulation by phosphate deficiency and formation of small anion-specific channels in lipid bilayer membranes. *J. Bacteriol.* **150**: 730-738.

Hancock, R.E.W. 1984. Alteration in outer membrane permeability. *Ann. Rev. Microbiol.* **38**: 237-264.

Hancock, R.E.W., and R. Benz. 1986. Demonstration and chemical modification of a specific phosphate binding site in the phosphate-starvation-inducible outer membrane porin protein P of *Pseudomonas aeruginosa*. *Biochim. Biophys. Acta* **860**: 669-707.

Hancock, R.E.W. 1987. Role of porins in outer membrane permeability. *J. Bacteriol.* **169**: 929-933.

Hancock, R.E.W., and A. Bell. 1988. Antibiotic uptake into gram-negative bacteria. *Eur. J. Clin. Microbiol.* **7**: 713-720.

Hancock, R.E.W., R. Siehnel, and N. Martin. 1990. Outer membrane proteins of *Pseudomonas*. *Mol. Microbiol.* **4**: 1069-1075.

Hancock, R.E.W., C. Egli, R. Benz, and R.J. Siehnel. 1992. Overexpression in *Escherichia coli* and functional analysis of a novel PPi-selective porin, OprO, from *Pseudomonas aeruginosa*. *J. Bacteriol.* **174**: 471-476.

Hancock, R.E.W., D.N. Karunaratne, and C.B. Egli. 1994. Molecular organization and structural role of outer membrane macromolecules. In "Bacterial Cell Wall", J.M. Ghuysen and R. Hakenbeck (Eds.) Elsevier Science B.V., 263-279.

Hashizume, T., F. Ishino, J.I. Nakagawa, S. Tamaki, and M. Matsuhashi. 1984. Studies on the mechanism of action of imipenem (N-formimidoyl thienamycin) *in vitro*: binding to the penicillin-binding proteins (PBPs) in *Escherichia coli* and *Pseudomonas aeruginosa*, and inhibition of enzyme activities due to the PBPs in *E. coli*. *J. Antibiotics.* **37**: 394-400.

- Hellinger, W.C., and N.C. Brewer. 1991. Imipenem. *Mayo Clin. Proc.* **66**: 1074-1081.
- Ho. S.N., H.D. Hunt, R.M. Horton, J.K. Pullen, and L.R. Pease. 1989. Site-directed mutagenesis by overlap extension using polymerase chain reaction. *Gene* **77**: 51-59.
- Hofnung, M. 1995. An intelligent channel (and more). *Science* **267**: 473-474.
- Huang, H. and R.E.W. Hancock. 1993. Genetic definition of the substrate selectivity of outer membrane porin protein OprD of *Pseudomonas aeruginosa*. *J. Bacteriol.* **175**: 7793-7800
- Huang, H., R. Siehnel, F. Bellido, E. Rawling, and R.E.W. Hancock. 1992. Analysis of two gene regions involved in the expression of the imipenem-specific, outer membrane porin protein OprD of *Pseudomonas aeruginosa*. *FEMS Microbiol. Lett.* **97**: 267-274.
- Ishii, J., and T. Nakae. 1993. Lipopolysaccharide promoted opening of the porin channel. *FEBS Lett.* **3**: 251-255.
- Jeanteur, D., J.H. Lakey, and F. Pattus. 1991. The bacterial porin superfamily: sequence alignment and structure prediction. *Mol. Microbiol.* **5**: 2153-2164.
- Jeanteur, D., J.H. Lakey, and F. Pattus. 1994a. The porin superfamily: diversity and common features. In "Bacterial Cell Wall". Ghuysen, J.M., and Hakenbeck, R. (Eds), Amsterdam: Elsevier Science, 363-380.
- Jeanteur, D., T. Schirmer, D. Fourel, V. Simonet, G. Rummel, C. Widmer, J.P. Rosenbush, F. Pattus, and J.M. Pages. 1994b. Structural and functional alterations of a colicin-resistant mutant of OmpF porin from *Escherichia coli*. *Proc. Natl. Acad. Sci. USA.* **91**: 10675-10679.
- Kahan, J. S., F.M. Kahan, R. Goegelman, S.A. Currie, M. Jackson, E.O. Stapley, T.W. Miller, A.K. Miller, D. Hendlin, S. Mochales, S. Hernandez, H.B. Woodruff, and J. Birnbaum. 1979. Thienamycin, a new β -lactam antibiotic. I. Discovery, taxonomy, isolation and physical properties. *J. Antibiot.* **32**: 1-12.
- Kahan, F.M., H. Kropp, J.G. Sundelof, and J. Birnbaum. 1983. Thienamycin: development of imipenem-cilastatin. *J. Antimicrob. Chemother.* **12**(suppl): S1-S35.
- Karunaratne, D.N., J.C. Richards, and R.E.W. Hancock. 1992. Characterization of lipid A from *Pseudomonas aeruginosa* O-antigen B band lipopolysaccharide by 1D and 2D NMR and mass spectral analysis. *Arch. Biochem. Biophys.* **299**: 368-376.
- Kleffel, B., R.M. Garavito, W. Baumeister, and J.P. Rosenbush. 1985. Secondary

structure of a channel-forming protein from *E. coli* outer membrane. *EMBO. J.* 4: 1589-1592.

Kreusch, A., A. Neubüser, E. Schiltz, J. Weckesser, and G.E. Schulz. 1994. Structure of the membrane channel porin from *Rhodopseudomonas blastica* at 2.0 Å resolution. *Protein Sci.* 3: 58-63.

Kropinski, A.M., L.C. Chan, and F.H. Milazzo. 1979. The extraction and analysis of lipopolysaccharide from *Pseudomonas aeruginosa* strain PAO, and three rough mutants. *Can. J. Microbiol.* 25: 390-398.

Kropinski, A.M., B. Jewell, J. Kuzio, F. Milazzo, and D. Berry. 1985. Structure and functions of *Pseudomonas aeruginosa* lipopolysaccharide. In "*Pseudomonas aeruginosa*: New Therapeutic Approaches from Basic Research", D.P. Speert and R.E.W. Hancock (Eds.) Karger, Basel, Switzerland, 58-73.

Kropp, H., J.G. Sundelof, J.S. Kahan, F.M. Kahan, and J. Birnbaum. 1980. MKO787 (*N*-formimidoyl thienamycin): evaluation of in vivo and in vitro activities. *Antimicrob. Agents Chemother.* 1980. 17: 993-1000.

Kropp, H., J.G. Sundelof, R. Hajdu, and F.M. Kahan. 1982. Metabolism of thienamycin and related carbapenem antibiotics by the renal dipeptidase, dehydropeptidase-I. *Antimicrob. Agents Chemother.* 22: 62-70.

Kropp H., L. Gerckens, J.G. Sundelof, and F.M. Kahan. 1985. Antibacterial activity of imipenem: the first thienamycin antibiotic. *Rev. Infec. Dis.* 7 (Suppl 3): S389-S410.

Kyte, J. and R.F. Doolittle. 1982. A simple method for displaying the hydropathic character of a protein. *J. Mol. Biol.* 157: 105-132.

Lakey, J.H., E.J.A. Lea, and F. Pattus. 1991. OmpC mutants which allow growth on maltodextrins show increased channel size and greater voltage sensitivity. *FEBS Lett.* 278: 31-34.

Leanza W.J., K.J. Wildonger, T.W. Miller, and B.G. Christensen. 1979. *N*-acetimidoyl- and *N*-formimidoylthienamycin derivatives: antipseudomonal β -lactam antibiotics (letter). *J. Med. Chem.* 22: 1435-1436.

Lee, E.H., M.H. Nicolas, M.D. Kitzis, G. Pialoux, E. Collatz, and L. Gutmann. 1991. Association of two resistance mechanism in a clinical isolate of *Enterobacter cloacae* with high-level resistance to imipenem. *Antimicrob. Agents Chemother.* 35: 1093-1098.

Lipman B., and H.C. Neu. 1988. Imipenem: a new carbapenem antibiotic. *Med. Clin. North. Am.* **72**: 567-579.

Liu, P.V. 1974. Extracellular toxins of *Pseudomonas aeruginosa*. *J. Infect. Dis.* **130** (suppl): S94-S99.

Livermore, D.M., and Y.J. Yang. 1987. β -lactamase lability and inducer power of newer β -lactam antibiotics in relation to their activity against β -lactamase-inducibility mutants of *Pseudomonas aeruginosa*. *J. Infect. Dis.* **155**: 775-782.

Livermore, D.M., and Y. Yang. 1989. Comparative activity of meropenem against *Pseudomonas aeruginosa* strains with well-characterized resistance mechanism. *J. Antimicrob. Chemother.* **24**: S149-S159.

Livermore, D.M. 1992. Interplay of impermeability and chromosomal beta-lactamase activity in imipenem-resistant *Pseudomonas aeruginosa*. *Antimicrob. Agents. Chemother.* **36**: 2046-2048.

Lugtenberg, B. and L. van Alphen. 1983. Molecular architecture and functioning of the outer membrane of *Escherichia coli* and other gram-negative bacteria. *Biochim. Biophys. Acta* **737**: 51-115.

Lynch, M.J., G.L. Drusano, and H.L.T. Mobley. 1987. Emergence of resistance to imipenem in *Pseudomonas aeruginosa*. *Antimicrob. Agents. Chemother.* **31**: 1892-1896.

Manoil, C., and J. Beckwith. 1986. A genetic approach in analyzing membrane protein topology. *Science* **233**: 1403-1408.

Marchal, C., and M. Hofnung. 1983. Negative dominance in gene *lamB*: random assembly of secreted subunits issued from different polysomes. *EMBO J.* **2**: 81-86.

Massidda, O., G.M. Rossolini, and G. Satta. 1991. The *Aeromonas hydrophila cphA* gene: molecular heterogeneity among class B metallo- β -lactamases. *J. Bacteriol.* **173**: 4611-4617.

Michea-Hamzhehpour, M., Y.X. Furet, and J.C. Pechere. 1991a. Role of protein D2 and lipopolysaccharide in diffusion of quinolones through the outer membrane of *Pseudomonas aeruginosa*. *Antimicrob. Agents Chemother.* **35**: 2091-2097.

Michea-Hamzhehpour, M., C. Lucain, and J.C. Pechere. 1991b Resistance to pefloxacin in *Pseudomonas aeruginosa*. *Antimicrob. Agents Chemother.* **35**: 512-518.

Misra, R., and S.A. Benson. 1988. Genetic identification of the pore domain of the OmpC porin of *Escherichia coli* K12. *J. Bacteriol.* **170**: 3611-3617.

Mizuno, T. 1979. A novel peptidoglycan-associated lipoprotein found in the cell envelope of *Pseudomonas aeruginosa* and *Escherichia coli*. *J. Biochem.* **86**: 991-1000.

Morrison, D.C. 1985. Nonspecific interaction of bacterial lipopolysaccharides with membranes and membrane components. In "Handbook of Endotoxin", L.J. Berry (Ed.) Elsevier, Amsterdam, Vol 3: 25-55.

Mutharia, L.M., and R.E.W. Hancock. 1983. Surface localization of *Pseudomonas aeruginosa* outer membrane porin protein F using monoclonal antibodies. *Infect. Immun.* **42**: 1027-1033.

Needleman, S.B., and C.D. Wunsch. 1970. A general method applicable to the research for similarities in the amino acid sequence of two proteins. *J. Mol. Biol.* **48**: 443-453.

Nicas, T.I. 1983. Ph.D thesis "Role of the outer membrane of *Pseudomonas aeruginosa* in antibiotic resistance". Univ. British Columbia, Canada.

Nicas, T.I., and R.E.W. Hancock. 1983a. *Pseudomonas aeruginosa* outer membrane permeability: isolation of a porin protein F-deficient mutant. *J. Bacteriol.* **153**: 281-285.

Nicas, T.I., and R.E.W. Hancock. 1983b. Alterations of susceptibility to EDTA, Polymyxin B and Gentamicin in *Pseudomonas aeruginosa* by divalent cation regulation of outer membrane protein H1. *J. Gen. Microbiol.* **129**: 509-517.

Nikaido, H. and T. Nakae. 1979. The outer membrane of Gram-negative bacteria. *Adv. Microbiol. Physiol.* **20**: 163-250.

Nikaido, H., and E.Y. Rosenberg. 1981. Effect of solute on diffusion rates through the transmembrane pore of the outer membrane of *E. coli*. *J. Gen. Physiol.* **77**: 121-?

Nikaido, H., E.Y. Rosenberg, and J. Foulds. 1983. Porin channels in *Escherichia coli*: studies with β -lactams in intact cell. *J. Bacteriol.* **153**: 232-240.

Nikaido, H. and R.E.W. Hancock. 1986. Outer membrane permeability of *Pseudomonas aeruginosa*. In "The Bacterial", J.R. Sokatch (ed.). Academic Press, New York, Vol X: 145-193.

Nikaido, H., and M. Vaara. 1985. Molecular basis of bacterial outer membrane

permeability. *Microbiol. Rev.* **49**: 1-32.

Oliver, D.B. 1987. Periplasm and protein secretion. In "*Escherichia coli* and *Salmonella typhimurium*: Cellular and Molecular Biology", F.C. Neidhardt (Ed.) ASM Publications, Washington, D.C., 56-69.

Olsen, R.H., W. DeBusscher, and W.R. McCombie. 1982. Development of broad host range vectors and gene banks: self-cloning of the *Pseudomonas aeruginosa* PAO chromosome. *J. Bacteriol.* **150**: 60-69.

Osano, E., Y. Arakawa, R.W. Yankun, M. Ohta, T. Horri, H. Ito, F. Yoshimura, and N. Kato. 1994. Molecular characterization of the enterobacterial metallo β -lactamase found in a clinical isolate of *Serratia marcescens* that shows imipenem resistance. *Antimicrob. Agents Chemother.* **38**: 71-78.

Paul, C. and J. Rosenbush. 1985. Folding patterns of porin and bacteriorhodopsin. *EMBO. J.* **4**: 1593-1597.

Pollack, M. 1990. *Pseudomonas aeruginosa*. In "Principles and Practice of Infectious Diseases", G.L. Mandell, R.G. Douglas and J.E. Bennett (Eds). Churchill Livingstone, New York, 1673-1691.

Poole. K. and R.E.W. Hancock. 1986. Isolation of a Tn501 insertion mutant lacking porin protein P of *Pseudomonas aeruginosa*. *Mol. Gen. Genet.* **202**: 403-409.

Quinn, J.P., E.J. Dudek, C.A. DiVincenzo, D.A. Lucks and S.A. Lerner. 1986. Emergence of resistance to imipenem during therapy for *Pseudomonas aeruginosa*. *J. Infect. Dis.* **154**: 289-294.

Rietschel, E.T., H. Mayer, H.W. Wollenweber, U. Zahringer, O. Luderitz, O. Westphal, and H. Brade. 1984. Bacterial lipopolysaccharides and their lipid A component. In "Bacterial Endotoxin: Chemical, Biological and Clinical Aspects", J.Y. Homma, S. Kanegasaki, O. Luderitz, T. Shiba, and O. Westphal (Eds.) Verlag Chemie, Weinheim, pp. 11-22.

Rolinson, G.N. 1986. β -lactam antibiotics. *J. Antimicrob. Chemother.* **17**: 5-36.

Rottem, S., and L. Leive. 1977. Effect of variations in lipopolysaccharides on the fluidity of the outer membrane of *Escherichia coli*. *J. Biol. Chem.* **252**: 2077-2081.

Saiki, R.K., S. Scharf, F. Faloona, K.B. Mullis, G.T. Horn, H.A. Erlich, and N. Arnheim. 1985. Enzymatic amplification of β -globin genomic sequences and restriction site analysis for diagnosis of sickle cell anemia. *Science.* **230**: 1350-1354.

Saino, Y., F. Kobayashi, M. Inoue, S. Mitsuhashi. 1982. Purification and properties of inducible penicillin β -lactamase isolated from *Pseudomonas maltophilia*. *Antimicrob. Agents Chemother.* **22**: 564-570.

Sambrook, J., E.F. Fritsch, and T. Maniatis. 1989. *Molecular Cloning. A Laboratory Manual*. Cold Spring Harbour Laboratory Press, Cold Spring Harbour, New York.

Sandermann and Strominger. 1972. Purification and properties of C₅₅-isoprenoid alcohol phosphokinase from *Staphylococcus aureus*. *J. Biol. Chem.* **247**: 5123-5131.

Satake, S., E. Yoshihara, and T. Nakae. 1990. Diffusion of β -lactam antibiotics through liposome membranes reconstituted from purified porins of the outer membrane of *Pseudomonas aeruginosa*. *Antimicrob. Agents Chemother.* **34**: 685-690.

Schimpff, S.C., M. Moody, V.M. Young. 1970. Relationship of colonization with *Pseudomonas aeruginosa* to develop of *Pseudomonas* bacteremia in cancer patients. *Antimicrob. Agents Chemother.* **10**: 240-244.

Schirmer, T., T.A. Keller, Y.F. Wang, and J.P. Rosenbush. 1995. Structural basis for sugar translocation through maltoporin channels at 3.1 Å resolution. *Science* **267**: 512-514.

Schülein, K., R. Ebner, K. Jaheris, J.W. Lengeler, and F. Titgemeyer. 1991. A sugar-specific porin, ScrY, is involved in sucrose uptake in enteric bacteria. *Mol. Microbiol.* **5**: 941-950.

Schulz, G.E. 1993. Bacterial porins: structure and function. *Current Opinion in Cell Biology* **5**: 701-707.

Schweizer, H.P. 1991. *Escherichia-Pseudomonas* shuttle vectors derived from pUC18/19. *Gene* **97**: 109-112.

Schweizer, H.P. 1992. Allelic exchange in *Pseudomonas aeruginosa* using novel ColE1-type vectors and a family of cassettes containing a portable *oriT* and the counter-selectable *Bacillus subtilis sacB* marker. *Mol. Microbiol.* **6**: 1195-1204.

Sekar, V. 1987. A rapid screening procedure for the identification of recombinant bacterial clones. **5**: 11-13

Sherbert, G.V., M.S. Lakshmi. 1973. Characterization of *Escherichia coli* cell surface by isoelectric equilibrium analysis. *Biochim. Biophys. Acta* **298**: 50-58.

- Siehnell, R.J., N.L. Matin, and R.E.W. Hancock. 1990. Sequence and relatedness in other bacteria of the *Pseudomonas aeruginosa oprP* gene coding for the phosphate-specific porin P. *Mol. Microbiol.* **4**: 831-838.
- Siehnell, R.J., C. Egli, and R.E.W. Hancock. 1992. Mol. Microbiol. Polyphosphate-selective porin OprO of *Pseudomonas aeruginosa*: expression, purification and sequence. *Mol. Microbiol.* **6**: 2319-2326.
- Simon, R., U. Preifer, and A. Pühler. 1983. A broad host range mobilization system for *in vivo* genetic engineering: transposon mutagenesis in Gram negative bacteria. *Bio/Technology* **1**: 784-790.
- Sykes, R.B., and A. Morris. 1975. Resistance of *Pseudomonas aeruginosa* to antimicrobial drugs. *Prog. Med. Chem.* **12**: 333-93.
- Spurlino, J.C., G-Y. Lu, and F.A. Quioco. 1991. The 2.3-Å resolution structure of the maltose or maltodextrin-binding protein, a primary receptor of bacterial active transport and chemotaxis. *J. Biol. Chem.* **266**: 5202-5219.
- Tausk F., M.E. Evans, L.S. Patterson, C.F. Federspiel, and C.W. Stratton. 1985. Imipenem-induced resistance to antipseudomonal β -lactams in *Pseudomonas aeruginosa*. *Antimicrob. Agents Chemother.* **28**: 41-45.
- Thomson, K.S., C.C. Sanders, and H. Chmel. 1993. Imipenem resistance in *Enterobacter*. *Eur. J. Clin. Microb. Infect.* **12**: 610-613.
- Towbin, M., T. Staehlin, and J. Gordon. 1979. Electrophoretic transfer of proteins from polyacrylamide gels to nitrocellulose sheets: procedure and some applications. *Proc. Natl. Acad. Sci. U.S.A.* **76**: 4350-4354.
- Trias, J., E.Y. Rosenberg, and H. Nikaido. 1988. Specificity of the glucose channel formed by protein D1 of *Pseudomonas aeruginosa*. *Biochim. Biophys. Acta* **938**: 493-496.
- Trias, J., J. Dufresne, R.C. Levesque, and H. Nikaido. 1989. Decreased outer membrane permeability in imipenem-resistant mutants of *Pseudomonas aeruginosa*. *Antimicrob. Agents Chemother.* **33**: 1201-1206.
- Trias, J., and H. Nikaido. 1990a. Outer membrane protein D2 catalyzes facilitated diffusion of carbapenems and penems through the outer membrane of *Pseudomonas aeruginosa*. *Antimicrob. Agents Chemother.* **34**: 52-57.
- Trias, J., and H. Nikaido. 1990b. Protein D2 channel of the *Pseudomonas aeruginosa* outer membrane has a binding site for basic amino acids and peptides.

J. Biol. Chem. **265**: 15680-15684.

Vallette, F., E. Mege, A. Reiss, and M. Adesnik. 1989. Construction of mutant and chimeric genes using the polymerase chain reaction. Nucl. Acids Res. **17**: 723-733.

Van der Ley, P., H. Amesz, J. Tommassen, and B. Lugtenberg. 1985. Monoclonal antibodies directed against the cell surface-exposed part of PhoE pore protein of the *Escherichia coli* K-12 outer membrane. Eur. J. Biochem. **147**: 401-407.

Vogel, H. and D.M. Bonner. 1956. Acetylornithase of *E. coli*: partial purification and properties. J. Biol. Chem. **218**: 97-106.

Vogel, H., and F. Jahnig. 1986. Models for the structure of outer membrane proteins of *Escherichia coli* derived from Raman spectroscopy and prediction methods. J. Mol. Biol. **190**: 191-199.

Weiss, M.S., U. Abele, J. Weckesser, W. Welte, E. Schiltz, and G.E. Schulz. 1991. Molecular architecture and electrostatic properties of a bacterial porin. Science **254**: 1627-1630.

Weiss, M.S. and G.E. Schulz. 1992. Structure of porin refined at 1.8 Å resolution. J. Mol. Biol. **207**: 493-509.

Winberg, G. and M.L. Hammarskjöld. 1980. Isolation of DNA from agarose gels using DEAE paper. Application to restriction site mapping of adenovirus type 16 DNA. Nucl. Acids Res. **8**: 253-264.

Wong, S.Y., H. Jost, and R.E.W. Hancock. 1993. Linker-insertion mutagenesis of *Pseudomonas aeruginosa* outer membrane protein OprF. Mol. Microbiol. **10**: 283-292.

Woodruff, W.A., T.R. Parr, R.E.W. Hancock, L.F. Hanne, T.I. Nicas, and B.H. Iglewski. 1986. Expression in *Escherichia coli* and function of *Pseudomonas aeruginosa* outer membrane porin protein F. J. Bacteriol. **167**: 473-479.

Woodruff, W.A. and R.E.W. Hancock. 1988. Construction and characterization of *Pseudomonas aeruginosa* protein F-deficient mutants after *in vitro* and *in vivo* insertion mutagenesis of the cloned gene. J. Bacteriol. **170**: 2592-2598.

Woodruff, W.A. and R.E.W. Hancock. 1989. *Pseudomonas aeruginosa* outer membrane protein F: structural role and relationship to the *Escherichia coli* OmpA protein. J. Bacteriol. **171**: 3304-3309.

Yoneyama, H., E. Yoshihara, and T. Nakae. 1992. Nucleotide sequence of the

protein D2 gene of *Pseudomonas aeruginosa*. *Antimicrob. Agents Chemother.* **36**: 1791-1793.

Yoneyama, H., and T. Nakae. 1993. Mechanism of efficient elimination of protein D2 in outer membrane of imipenem-resistant *Pseudomonas aeruginosa*. *Antimicrob. Agents Chemother.* **37**: 2385-2390.

Yoshishara, E., and T. Nakae. 1989. Identification of porins in outer membrane of *Pseudomonas aeruginosa* that form small diffusion pores. *J. Biol. Chem.* **264**: 6297-6301.

Yoshishara, E., H. Yoneyama, and T. Nakae. 1991. *In vitro* assembly of the functional porin trimer from dissociated monomers in *Pseudomonas aeruginosa*. *J. Biol. Chem.* **266**: 952-957.

Yoshimura, F., and H. Nikaido. 1982. Permeability of *Pseudomonas aeruginosa* outer membrane to hydrophilic solutes. *J. Bacteriol.* **152**: 636-642

Yoshimura, F., and H. Nikaido. 1985. Diffusion of β -lactam antibiotics through the porin channels of *Escherichia coli* K-12. *Antimicrob. Agents Chemother.* **27**: 84-92.

Yoshinori, Y., T. Nishikawa, and Y. Komatsu. 1993. Cloning and nucleotide sequence of anaerobically induced porin protein E1 (OprE) of *Pseudomonas aeruginosa* PAO1. *Mol. Microbiol.* **8**: 993-1004.

Yotsuji, A., S. Minami, M. Inoue, and S. Mitsuhashi. 1983. Properties of novel β -lactamase produced by *Bacteroides fragilis*. *Antimicrob. Agents Chemother.* **24**: 925-929.

Young, L.S. 1984. The clinical challenge of infections due to *Pseudomonas aeruginosa*. *Rev. Infec. Dis.* **6**: S603-607.

Zhou, X.Y., M. Kitzis, and L. Gutmann. 1993. Role of cephalosporinase in carbapenem resistance of clinical isolates of *Pseudomonas aeruginosa*. *Antimicrob. Agents Chemother.* **37**: 1387-1389.

APPENDIX

A. Revised OprD Model by Multiple Alignments and Amphipathicity Calculations.

(a) MULTIPLE ALIGNMENTS. Alignments of closely related sequences were performed using classical alignment tools such as those available in the GCG package (Devereux et al., 1984). For distant sequences such tools are not very accurate, mainly because they tend to introduce gaps which incur the same penalty all along the sequence. For porins, it is clear that the loop regions are much more variable and even very long gaps may be easily introduced without problem. Conversely, insertion of gaps in the transmembrane regions should be heavily penalized. Therefore that was taken into account manually in the final alignment predictions

(b) MEMBRANE CRITERIA. The hydrophobicity 'H' of a segment was defined as usual (Kyte and Doolittle, 1982). The hydrophobicity of each residue was taken from the PRIFT table (Cornette et al., 1987). The hydrophobic moment $\langle\mu\rangle$ was introduced by Eisenberg et al. (1982) to describe the amphipathicity of the protein segments. The membrane criteria value, using a linear combination of hydrophobicity and hydrophobic moment, $H + \langle\mu\rangle$, determined the transmembrane segments quite precisely (Jeanteur et al., 1991).

(c) TURN PREDICTIONS. According to Paul and Rosenbush (1985), a turn could be defined as a segment consisting of 3 or more residues containing at least one turn promoter and no turn blockers. We refined this criteria by computing a

frequency matrix of residue occurrence within short periplasmic turns, external loops and transmembrane strands from those porins with known structures (Cowan et al., 1992; Weiss and Schulz, 1992) and from a set of very closely related porins. Using this linear matrix of turn frequencies, we predicted turns by identifying them as segments of 3 residues with a 'turn promoter' propensity that was 3 times higher than the 'turn blocker' propensity.

In general, a β -strand was defined as a segment with high value of the membrane criteria, no gaps, no turn predictions and sequence conservation. In contrast, a loop was defined by its low value of membrane criteria, the presence of gaps, turn predictions and sequence variability.

Table XII: Homologies and identities among the porin superfamily.

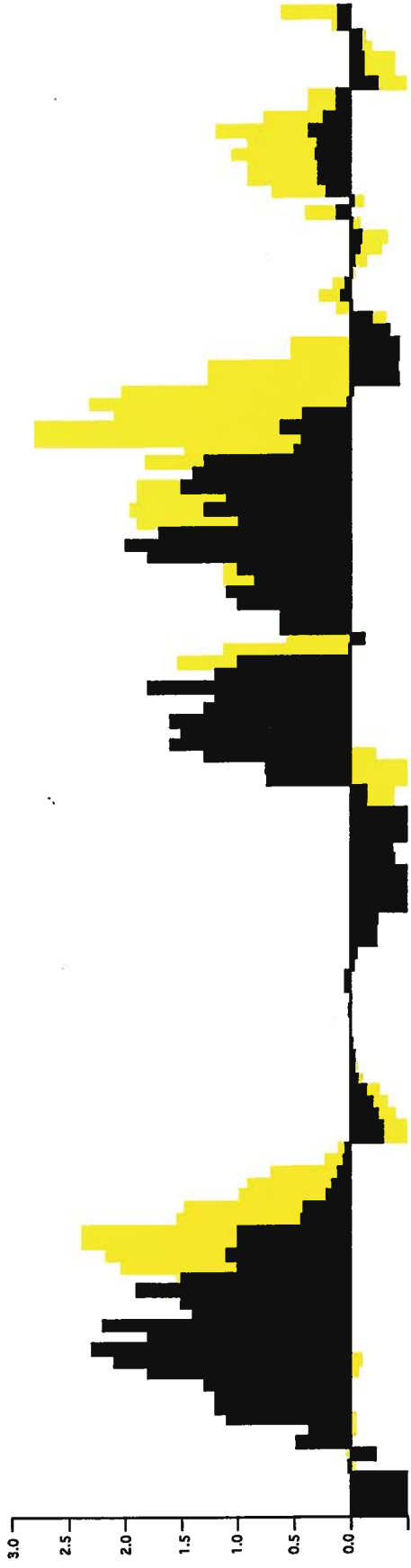
Identities	HIOMPPA	ECOOMP	OPRD	OPRE	NMPORA	NSPOR	RHODO	RBLASTICA
	<i>H. influenza</i>	<i>E. coli</i>	<i>P. aeruginosa</i>	<i>P. aeruginosa</i>	<i>N. meningitidis</i>	<i>N. scca</i>	<i>R. capsulatus</i>	<i>R. blastica</i>
	P2	OmpF	OprD	OprE	PorA1	Por		
Homologies	M93268	M74489	Z14065	P32722	X52995	X65461	P312443	
HIOMPPA	21%	21%	9%	8%	17%	15%	14%	15%
ECOOMP	30%		15%	12%	16%	21%	18%	16%
OPRD	18%	23%		39%	13%	11%	11%	11%
OPRE	15%	20%	51%		11%	11%	11%	10%
NMPORA	27%	26%	22%	22%		47%	16%	13%
NSPOR	26%	32%	21%	21%	58%		15%	13%
RHODO	26%	28%	19%	18%	27%	26%		28%
RBLASTICA	25%	26%	18%	17%	24%	25%	40%	

Aligned sequences were analyzed with DISTANCE (Devereux et al., 1984) using a threshold of 1.0 for identities and 0.6 for homologies. Identities between sequences are shown on the top part of the table while homologies are in the bottom. The column headings give the name used in Fig. 33, the species, gene name and accession number. Accession numbers beginning with the letter P are from the Swissport database, others are from the Genebank/EMBL database. Where the accession number is provided, the sequence and gene name correspond to that entry.

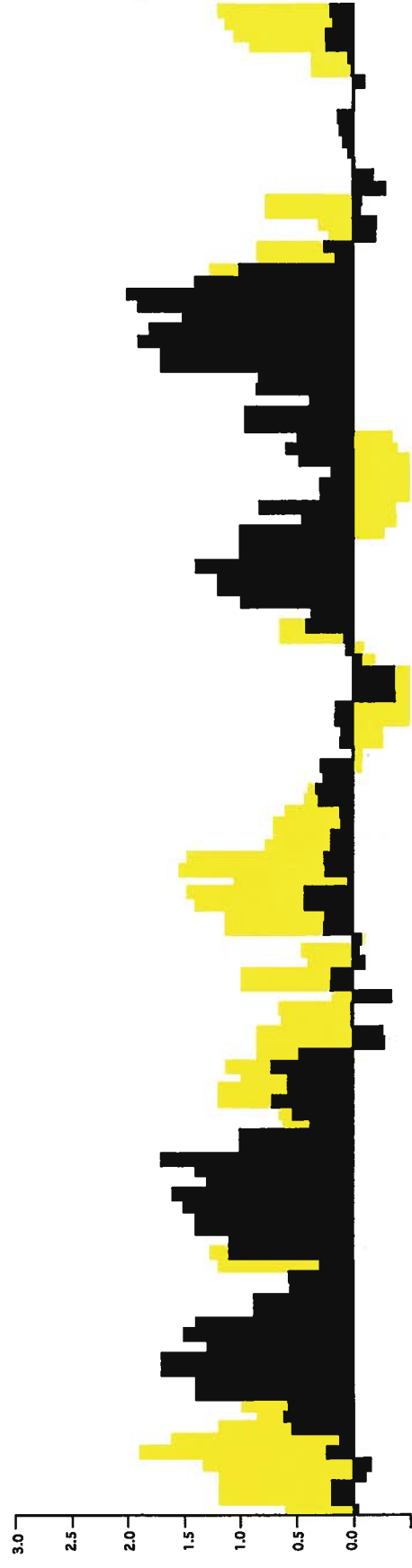
Figure 33: Multiple sequence alignments between OprD and representatives of porin superfamily.

Membrane spanning strands are boxed in solved structures. The lines and numbers under the alignment represent the predicted β -strands. The residues which were predicted to face the hydrophobic core of the membrane are shaded, some of them presenting certain polar properties are in yellow. Aromatic residues are shown in bold, charged residues involved in the eyelet are bold and in bigger size. Major turn predictions are indicated by *.

The hydrophobicity plus hydrophobic moment ($H + \langle m \rangle$) was calculated from 32 sequences (Jeanteur *et al.*, 1994) and is shown in black. The hydrophobic moment was calculated using a periodicity of 1/2 and 1/2.5 in order to take into account untwisted and twisted β -strands. Each column represents a ($H + \langle m \rangle$) calculated with a window of 9 residues centred at the current position. In yellow the calculation is displayed for OprD sequence alone.



H10MPFA AVVYNNEGTKVETGRRLSILAEQSSSTE.....DNQEQHGALRNQGSRRHMTIHNFGD.GIYVQGGYETRRVSKASKEKA.....
 ECOQMPF AEIYNKDGKVDLQKAVLXVYFSKNGGE.....MSYGGNDMTYRGGIKLEYEINS.DIHYGQGMVNFQGMNNSSEGA.....
 OPRD DAFVSDQAEA KGHLEDSLQILIRMYFINDGKS.....GSDRNVDTQGLTYEYEGFTDQYVGGDAFGLYGLKLDGTS.....
 OPIREAGHLEDSLQILIRMYFINDGKS.....GSDRNVDTQGLTYEYEGFTDQYVGGDAFGLYGLKLDGTS.....
 INPORADVSRYGELKSGVEGRMYLQTEAQAANDGASQVKVTKAKSRIRTKISDFISGEGGGLIMYQQGFTQGVVGGDAFGLYGLKLDGTS.....
 NSPORDVTYGGVKKSGVEGRMYLQTEAQAANDGASQVKVTKAKSRIRTKISDFISGEGGGLIMYQQGFTQGVVGGDAFGLYGLKLDGTS.....
 RHOODEIKSISGDAKSGVEGRMYLQTEAQAANDGASQVKVTKAKSRIRTKISDFISGEGGGLIMYQQGFTQGVVGGDAFGLYGLKLDGTS.....
 RELASTICAEISLQDQIRGQVAVDGVLE.....DITLSSRIRIRIVYTIYDDEQQ.GITFGALRATGWDGODES.....



H10MPFA DQFADIVNKVYVILTEIGNNT.....FEEVKILGAKTIADKTIADKTYGGLL.....NSKKYIPTGNTVIGTINQ.....
 ECOQMPF DAQTGKTRLQAFAGLKYAD.....RSGSPDYBMY.GVYDAGYTDLPEFFGDT.....AYSDFFVGRVGGVAVNENSN.FGL.....
 OPRD RAGGAVKVRISKTHIKWGEQPTALVYVAFRGSRR.LPQTAIGFQLSSSEFFGLDLE.....ASHFTGKGRSTVKSRELYVAVAGETAKS.....
 OPIRE SLGLTAKAKKSNTEIRYGTLOPKL.....FELVLRAGVANQDASQALDPDSNND.....MVAQLGILKRRDDDMVSDPSPPESSRDSK.....
 INPORAEQWGNRRSFTGALAG.....FELVLRAGVANQDASQALDPDSNND.....MVAQLGILKRRDDDMVSDPSPPESSRDSK.....
 NSPORESWGTRELFVGLGAG.....FELVLRAGVANQDASQALDPDSNND.....MVAQLGILKRRDDDMVSDPSPPESSRDSK.....
 RHOODGTAGRRLQIYVIM.....GNTVEVGGD.TAFDSVALTYSBNGYEASSFDAQSSFFAYNSKYDASGALDRYRIBIATYV.....
 RELASTICAGTAGRRLQIYVIM.....GNTVEVGGD.TAFDSVALTYSBNGYEASSFDAQSSFFAYNSKYDASGALDRYRIBIATYV.....

Figure 34: Revised membrane topology model of OprD.

The sixteen predicted transmembrane β -strands are boxed, and the 8 external loops are labelled as L1 to L8. The deleted amino acid residues are presented as unfilled letters.

L7 T K M S³⁵⁰ D N N V G Y K N Y G Y G E D G K H H E T³⁷⁰ N L E A K Y V V Q S³⁸⁰ G
G D I D K G N³⁴⁰ I Y R V M F T L G P³³⁰ V G Y S A L N L D Y³²⁰ R A Q W S

L8 Q G E G D Q N E F R⁴¹⁰ L I V D Y P L S I L⁴²⁰
D⁴⁰⁰ A N A R H W A Q R I³⁹⁰ R F S L D K A

L6 G S²⁹⁰ G A G G D S I F L A³⁰⁰ N S V Q Y S D F N G³¹⁰ P G E K
N R G F G I Y D F²⁸⁰ P Q D G H V K Q Y A²⁷⁰ L T F T H

L5 K A K A G D I S²⁵⁰ N T T W S L A A A Y²⁶⁰ T L D A
G E D²⁴⁰ N T R Y I N F D F G²³⁰ L S Q D S P L A

L4 A E L E D I Y²¹⁰ R Q Y Y L N S N Y T²²⁰ I P L A
G Y L S²⁰⁰ A S L N D T I A Y R¹⁹⁰ G G I F D A S

L3 G L¹⁵⁰ D L E A G H F T E G¹⁶⁰ K E P T T V K S R G¹⁷⁰ E L Y A T Y A G E T¹⁸⁰ A K
E F E S S Q L Q F¹⁴⁰ G T A T Q P F L R S¹³⁰ G G A A F V P A T P¹²⁰ Q

L2 V M N D⁹⁰ G K P R D D Y S R A¹⁰⁰ G G A V K V R I S K¹¹⁰ T M L K W G E M Q
L N G T G T⁸⁰ K D S T G D L K L G⁷⁰ L Y G F A D V G F G⁶⁰ V T G Q

L1 F N R³⁰ D G K S G S G D R V⁴⁰ D W T Q G F L T T Y⁵⁰ E S S G F T
Y Y N R L L L L D²⁰ L S S D E I F G K A¹⁰ E A Q D S V D A F